THE UNIVERSITY OF CHICAGO

COGNITIVE AND CHEMICAL INFLUENCES ON OLFACTORY SYSTEM NEURODYNAMICS

A DISSERTATION SUBMITTED TO

THE FACULTY OF THE DIVISION OF THE SOCIAL SCIENCES

IN CANDIDACY FOR THE DEGREE OF

DOCTOR OF PHILOSOPHY

DEPARTMENT OF PSYCHOLOGY

BY

HUIBO LI

CHICAGO, ILLINOIS

AUGUST 2025

Abstract

This dissertation investigates several factors that influence the olfactory system from both sensory and cognitive perspectives. I examine how rats smell and perform olfactory tasks on behavioral and neural levels using appetitive tasks and local field potentials (LFPs), respectively. Study 1 (chapters 3, 4 and 5) tests how cognitive demand such as task difficulty interacts with olfactory stimulus similarity to modulate olfactory system dynamics and behavior. Olfactory system neurophysiology is strongly modified by the context in which animals identify odors. Rats and mice rely on enhanced olfactory bulb (OB) gamma oscillation (65-110 Hz) power to effectively perform discrimination of similar odors. However, previous research has shown that the degree to which rats amplify gamma oscillations, a signature of neural firing precision, varies across studies which employ different tasks, training protocols, and response requirements. Particularly concerning gamma band LFP oscillations (65-110 Hz) in the OB, I hypothesize that cognitive demand significantly affects rats' behavior and modulates OB gamma oscillations. I tested this hypothesis by designing a variant of the two-alternative choice (TAC) discrimination task in which rats learn to identify two very similar and two very different odors with or without a visual cue that limits the decision space on each trial. Rats with the informative cue use longer sampling times and show lower power gamma oscillations than rats with a non-informative cue. Several other behavioral and neural differences separate the two groups of rats, including patterns of connectivity among olfactory and hippocampal areas and beta oscillation (15-30 Hz) power. Study 2 (chapter 6) investigates the interactions between the trigeminal system and olfactory system. Given that most odors also activate the trigeminal system to varying degrees, we examine how trigeminal input modulates olfactory perception in binary mixture perception. I find that trigeminal odorants tend to be overshadowed by less or non-trigeminal components in

binary mixtures. Overall, this work serves to unfold the complex story of olfactory processing by showing that the olfactory system dynamically adjusts its state and works closely with systems like the limbic and trigeminal systems differently under different contexts.

Dedication

To my mom, who has overcome challenges unimaginable to people of my current generation and cultural environment. She's the reason why I've pursued everything I've wanted to pursue in my life.

Table of Contents

List of Figures

List of Tables

Acknowledgments

First and foremost, I want to express my deepest gratitude to Dr. Leslie Kay. Working under your mentorship has been one of the most rewarding and transformative experiences of my academic and personal journey. I am not using hyperbole when I say my life would have been completely different without you in it. Your unwavering support, thoughtful guidance, generous encouragement, humour, talent, and most importantly, your "do it right" attitude have shaped me as a scientist and as a person.

You created a lab environment rooted in curiosity, compassion, and integrity—one that inspired me daily and gave me the confidence to pursue difficult questions in science and in life. You provided a real-life role model for finding happiness in a fulfilling career while also being a kind, giving and impactful member of the world.

Thank you for always taking the time to listen, to challenge me, and to celebrate both the small and large milestones along the way. Your mentorship extended far beyond the lab, and your belief in me has had a lasting impact that I will carry with me throughout my career.

I am profoundly grateful to have had you as my advisor.

I also want to thank my mom, whom I dedicate this dissertation to. She has risen above unimaginable challenges to provide the life I have today.

I would also like to express my deepest appreciation for my partner, Zac. I vow in the name of science to not let my closest to get the most turbulent side of me. Through ups and downs, he provides a pillar that is essential to complete my triangle of emotional stableness.

Lastly, I'd also like to thank and hug and kiss my pets, Olivia and Miantiao, a thousand times for the distraction, entertainment, and emotional support they've provided me in this journey.

Chapter 1: Introduction

The olfactory system is implicated in several neurological disorders; it can't be too surprising given the direct connection between the olfactory bulb and the limbic system, that olfaction is related to memory and emotional disorders such as Alzheimer's disease and depression(Djordjevic et al., 2008a, 2008b; Kohli et al., 2016). Moreover, outside the human disorder landscape, in the animal world, olfactory function can be crucial to individual and species survival. Animals rely on olfaction for food foraging, nutrition, procreation, and other social functions. There is even evidence that human emotion-based chemosignals differentially activate the autonomic nervous systems of domesticated animals such as dogs and horses(Semin et al., 2019).

For humans, it's not obvious that the sense of smell plays a large part in daily life. For this reason and others, olfaction has long been understudied and considered unimportant to human health. However, the unfortunate reminder of COVID-19 has brought the importance of olfaction to the forefront of neuroscience research. To begin with, contrary to common impressions, the olfactory system (retronasal olfaction) is what gives rise to the essential, unique flavors of food(Rozin, 1982). The gustatory system senses more fundamental aspects such as sweetness, bitterness, and saltiness. Losing the sense of smell is losing the ability to taste the orangeness in orange and chocolatiness in chocolate. Damage to the central brain areas involved in the sense of smell may also have complex and long-term physiological effects on our brain and immune system, influencing memory, emotional health, and possibly lifespan(Kay, 2022; Watson et al., 2021). Losing the sense of smell is more than an inconvenience; it can be a sign of viral infection of the olfactory system, which may lead to neurodegenerative consequences in the long run(Kay, 2022). Data collected during the first wave of COVID-19 in 2020 marked 85% of

the infected as having olfactory dysfunction. 15 million people worldwide might be influenced by olfactory dysfunction caused by the SARS-CoV-2 virus.

OB neuroanatomy and system circuitry

There has been substantial progress in understanding the OB mechanisms of coordinated neural activity as represented in the LFP. The rat olfactory bulb is a laminar cortical area composed of 3 cell layers or six layers, including intervening synaptic layers, and sits below the ventral surface of the frontal lobe and dorsal to the cribriform plate of the ethmoid bone. The layer division convention may differ from paper to paper. The six layers however are generally referred to with anatomical and functional importance: (1) the external or olfactory nerve layer: axons of the incoming olfactory receptor neurons (ORNs); (2) the glomerular layer: glomeruli formed by axons of ORNs synapse with dendrites of mitral cells, tufted cells, and periglomerular cells; (3) the external plexiform layer: mainly synapses between dendrites of mitral and tufted cells and granule cell dendrites. (4) the mitral cell layer: cell bodies of mitral cells; (5) the internal plexiform layer, thin layer of mitral cell lateral dendrites and some granule cell bodies; and (6) the granule cell layer: soma of the granule cells.

Olfactory Sensory Neurons (OSNs) in the nasal epithelium express olfactory sensory receptors, which are activated by volatile molecules in mammals. OSNs that express the same type of receptors converge onto glomeruli on either side of the OB and form synapses with the apical dendrites of mitral and tufted cells (MCs/TCs). The lateral dendrites of excitatory MCs form reciprocal dendrodendritic synapses with GABAergic granule cells (GCs), which have an inhibitory effect on mitral cell dendrites. GCs release γ-Aminobutyric acid (GABA) onto MC dendrites in a graded fashion dependent on Ca^{2+} flow through NMDA receptors (NMDARs) and other voltage-dependent Ca^{+2} channels (VDCCs) expressed on GC spines(Chen et al., 2000;

Isaacson & Strowbridge, 1998; Schoppa et al., 1998). This negative feedback local circuitry has been shown to be necessary and sufficient for OB gamma oscillations. GCs receive centrifugal input from the Piriform Cortex (PC), the Entorhinal Cortex (EC), and the hippocampus. GC excitability modulates gamma and beta transitions in the OB, such that top-down, neuromodulatory, or strong sensory input causes GCs to enter a hyperexcitable state, and slow decay time constants in this state support beta oscillations (Osinski et al., 2018; Osinski & Kay, 2016). Mitral and tufted cells are the main projection neurons. They were initially bundled together given some of their similarities, but there is now more evidence supporting different roles of mitral and tufted cells in olfactory sensing(Imamura et al., 2020; Manabe & Mori, 2013). Tufted cells project to part of the anterior olfactory nucleus (AON) and the olfactory tubercle (OT) (Igarashi et al., 2012; Nagayama et al., 2014). Mitral cells project to the AON, the OT, the anterior and posterior piriform cortex (aPC and pPC), the lateral entorhinal cortex (LEC), the medial amygdaloid nucleus (MEA), and the anterior and posterolateral cortical amygdaloid nucleus (ACo and PLCo).

The granule cell layer in the OB receives direct centrifugal input from AON, PC, and the Ammon's horn (CA1) area of the ventral hippocampus(Okuyama et al., 2016; Padmanabhan et al., 2019). PC also receives input from the hippocampus and septum, which drives part of the hippocampal theta rhythm. There are multiple pathways through which hippocampal input can influence mitral and tufted cell activities. Beta band coherence between OB and hippocampus increases during odor sampling in a GNG task (Martin et al., 2007). The OB theta rhythm may also be coupled with hippocampal theta when rats engage in olfactory-cue-guided navigation tasks (Sheriff et al., 2021). It is highly likely that the hippocampus can coordinate with the olfactory system in an olfactory discrimination task with context specificity. In fact, there has

been identified a direct input from the CA1 region of the hippocampus and the entorhinal cortex to the GCL in the rat OB(de Olmos et al., 1978; Gulyás et al., 1998; Panhuber et al., 1985).

Local Field Potentials (LFPs)

LFPs are the summed local fields of cell aggregates. When we use LFP as a tool to study the brain, the LFPs we measure can be from various aggregates depending on the research question at hand. Often, these aggregates are identifiable areas in the brain in the traditional sense, but more often, they may be a subset of a specific area that is of a specific type of physiology or distribution. Given its clear cell layer structures, the rat olfactory bulb provides a graceful model for using the LFPs to understand brain activities.

Neurons are the current/voltage sources of LFPs. One given neuron may form up to a few hundred thousand synapses and may show different shapes of activations depending on which synapses are activated. Moreover, currents may not only sum but they may also cancel out. The electric field of a cell assembly, therefore, could take numerous activation shapes depending on which neurons are activated. Although these characteristics of the current sources make it hard to isolate the individual elements of LFPs, the aggregated activities of a cell assembly of an appropriate geometry and other structural characteristics inform us about the state of the cortex during perceptual and cognitive processes. LFP in the olfactory system is especially informative, given its structure and what we know about LFP oscillations in the OB. In the OB, the parallel organization of the bipolar GABAergic granule cells provides a robust electrical field for observation. The radially symmetric mitral cells virtually cancel out their own field. LFP in the OB has been well-studied and used to test many informative hypotheses about the circuitry of the OB over the past 60+ years (Kay, 2015). For instance, in the OB, depending on the synaptic

currents of granule cells, we could observe either beta or gamma(Neville & Haberly, 2003; Osinski & Kay, 2016).

A dendrodendritic negative feedback loop supports gamma and beta oscillations in the OB

Olfactory bulb gamma band LFP is generated by a local negative feedback interaction model (Eeckman & Freeman, 1990; Freeman, n.d., 1972; Mori & Takagi, 1978; Rall & Shepherd, 1968). The principal neurons, mitral cells and granule cell interneurons, form reciprocal dendrodendritic synapses in the OB. Mitral cells are distributed radially in the OB, resulting in a cancellation of their summed field. Hence, olfactory bulb LFP (or referred to as EEG in earlier studies), as observed, is generated by the granule cell field. When OB gamma oscillations are observed, inhibitory neurons (granule cells) fire in phase with gamma frequency, and excitatory neurons (mitral/tufted cells) fire with a ~1/4 cycle lead from the peak of the oscillations(Eeckman & Freeman, 1990). Simultaneous unit activities and LFP recordings in the MC layer and GC layer have confirmed that during OB gamma LFP, mitral cells receive phasic inhibition at gamma frequency from the granule cells, by spiking and subthreshold activities(Lagier et al., 2004).

Furthermore, GC excitability modulates gamma and beta transitions in the OB(Eeckman & Freeman, 1990). GC spines express N-methyl-D-aspartate receptors (NMDARs) and other voltage-dependent Ca2+-dependent channels (VDCCs). GABA released by the GCs is modulated through the activation of these cation channels. Beta emerges in the model in Osinski & Kay (2016) as a result of slowly decaying inhibition by GCs, modulated by both the NMDARs and VDCCs. A change in GC excitability of about 100ms may cause a sudden shift of beta and gamma oscillations in the OB.

This knowledge about the OB circuit and activity dynamics provides the foundation for further investigation into the physiological underpinnings of olfactory-related behaviors.

Another advantage of studying LFP in the olfactory system is that olfactory system similarities are highly conserved in mammals. Most of what we know about the olfactory system was acquired through experiments in rodents, particularly rats, mice, and hamsters. There have also been studies on macrosmatic animals other than rodents, for instance, rabbits and cats. We can infer physiological and anatomical information for human literature based on rodent work; however, direct human knowledge is an area we can work on in the olfactory field. Lane et al. reviews this topic in detail, comparing the source of our knowledge of the human olfactory neuroanatomy. Here we note that so far, evidence suggests the LFP oscillations in humans, particularly in the piriform cortex, in agreement with rodent studies, reflect cognitive functions such as odor learning and attention(Zelano et al., 2005). Direct knowledge on the human olfactory bulb is still limited due to technical difficulties. However, recently, there has been progress in methods to reliably measure human OB activity(Iravani et al., 2020). More comparisons between rodent and human olfactory oscillations would help understand the relevant mechanisms of olfactory-related neurological disorders.

LFP significance

LFP oscillations represent coordinated cell activity and are more than the summed spikes of a cell assembly. Firing rate is only a reduced dimension of the information LFPs carry. For instance, firing rates of mitral cells could remain the same as the power density of the assembly shifts from a higher gamma range to a lower gamma range(Lepousez & Lledo, 2013). In the mammalian olfactory system, OB LFPs are characterized by three main bands: theta (1-12 Hz), beta (15-30 Hz), and gamma (low gamma or gamma2 35- 65 Hz, and high gamma or gamma1

65-100 Hz, with sub bands 65-80 Hz and 85-110 Hz) (Kay, 2003). These neural oscillations have functional and/or behavioral significance in sensory and cognitive processes.

In the OB, beta oscillations can be induced by multiple factors, including repeated presentations of high-volatility odors (Lowry & Kay, 2007) and mastering of discrimination learning tasks (Martin et al., 2004). Gamma oscillations (high gamma) are functionally related to the discrimination of closely related odors (Martin et al., 2007; Nusser et al., 2001). Blocking gamma oscillations in the OB disrupts rats', mice' and honeybees' ability to discriminate finely related odorants (Lepousez & Lledo, 2013; Nunez-Parra et al., 2013; Stopfer et al., 1997). Theta oscillations in the OB track respiratory rhythms (Rojas-Líbano et al., 2014) and can also represent hippocampal theta (Sheriff et al., 2021). And respiratory rhythms modulate gamma oscillations in the OB (Biskamp et al., 2017; Rojas-Líbano et al., 2014).

Molecular features of odors, such as carbon chain length and sorptiveness, have also been shown to influence olfactory perception. Within odors of the same functional group, a subject's ability to tell a pair of odors apart negatively correlates with carbon chain length difference of the pair (Laska & Teubner, 1999). It is harder for rats to detect low sorptiveness odors compared to high ones; they also adjust sniffing dynamics to detect them (longer and more inhalations) (Rojas-Líbano & Kay, 2012).

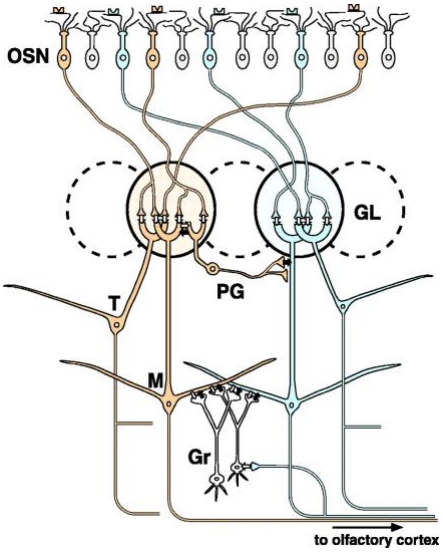

Figure 1.1 schematic of olfactory bulb circuity

(adapted from Mori et al. 1999)

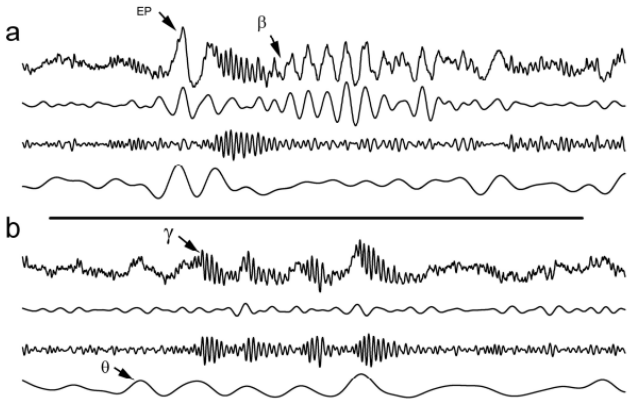

Figure 1.2 Theta, beta and gamma oscillations from the olfactory bulb in waking rats.

Each figure shows from top to bottom: raw data (1-475 Hz), beta band (15-35 Hz), gamma band (35- 115 Hz), and theta band (1-12 Hz). 1.5 seconds of data are shown in each plot, both from the same rat in the same recording session. a) high amplitude beta band oscillation produced in response to odor sensitization. EP- sensory evoked potential; β- approximate beginning of beta oscillation. Note that the beta oscillation is preceded by a brief gamma frequency burst. b) gamma oscillations (marked by γ) associated with the transition from inhalation to exhalation during exploratory behavior. θ- marks respiratory wave in the theta band (inhalation is up). Note the relative absence of beta band activity during this episode. (adapted from Kay 2008)

Gamma is functionally relevant to fine odor discrimination

Gamma oscillations in the olfactory bulb in mice and rats can be characterized into two species: high or gamma 1 (65-110 Hz) and low or gamma 2 (35-65 Hz), which have distinct functional roles in behavior. Gamma 1 is associated with the sniff cycle, with the peak of correlation near the peak of inhalation associated with the OB respiratory rhythm; while gamma 2 occurs between breaths during slow breathing and is inhibited at the onset of sniffing. Gamma

1 is prominent during odor processing in training and novel exploration; gamma 2 is observed during alert motionlessness, waiting periods, and during grooming (Kay, 2003 and laboratory observations).

Manipulations that modify the balance of excitatory and inhibitory circuits within the OB result in changes in gamma oscillations and behavioral performance in fine (similar) odor discrimination. Honeybees' antennal lobe projection neurons (analogous to mitral/tufted cells in mammals) participate in odor-evoked fast oscillations (~30Hz). These oscillations are analogous to olfactory bulb gamma oscillations. Blocking inhibition in the antennal lobe knocks out these oscillations, and the honeybees can discriminate molecularly dissimilar odorants (either 1-hexanol or 1-octanol and the terpene geraniol) but not molecularly similar ones (1-hexanol and 1-octanol)(Stopfer et al., 1997). Blocking GABAergic inhibition from GCs decreases mean gamma frequency in wildtype and a2-subunit knockin(H101R) mice. Mice with blocked GABAergic inhibition show an increased sampling time for normal odor discrimination and fail to discriminate fine odor pairs (combination of enantiomers)(Lepousez & Lledo, 2013). Photoactivation of inhibitory GABAergic neurons in the granule cell layer enhances pattern separation for mixtures, speeds up odor discrimination, and decreases odor discrimination learning pace for mixtures(Gschwend et al., 2015). GABAA-Beta3 knockout mice with increased power and amplitude of gamma oscillations in the OB are better at similar monomolecular odorant discrimination(Nusser et al., 2001).

We know that gamma 1 (65-85 Hz) power in the rat OB is elevated during odor sampling for fine discrimination relative to coarse discrimination(Beshel et al., 2007), but the cognitive elements involved in gamma elevation during odor discrimination tasks, and the underlying mechanisms remain unknown. For the same odors, heptanol and hexanol, two experiments led to

different oscillation characteristics: beta band (15–40 Hz) power increase and no increase in gamma in a Go/No-Go paradigm(Martin et al., 2007) , and enhanced gamma power (65–85 Hz) in a more complex and difficult to learn variant of a TAC task(Beshel et al., 2007). In another experiment, gamma power did not differ significantly by task during the odor period between TAC and GNG when these tasks were matched in difficulty(Frederick et al., 2011, 2016), suggesting that it is not the type of task that elevates gamma oscillation when the difficulty of the tasks is more equal. Our hypothesis is that high gamma in the OB, from now on referred to as gamma oscillations in the OB (while gamma 2 is still referred to as gamma 2), is modulated by cognitive demand. We will explore this further in chapters 3 and 4.

Beta is associated with late odor sampling, learning, and motor planning

Pure odorants with vapor pressures in the high volatility range (1-120 mmHg) induce beta oscillations (~20 Hz) in the OB after repeated passive presentation(Lowry & Kay, 2007). However, this does not happen with odorants with a volatility higher than 120 mmHg. We still don't know why this is the case, but our hypothesis is that very high volatility odors suppress beta in the OB due to strong input.

Beta oscillations in the OB rely on multi-area interactions; blocking centrifugal input (medial part of the olfactory peduncle) to the rat OB reduces the amplitude of odor-induced oscillatory beta responses both in OB and PC(Martin et al., 2006). Beta oscillations in the hippocampus show synchrony with olfactory bulb oscillations and may correlate with memory consolidation and cognitive performance for olfactory tasks(Gourévitch et al., 2010; Leung et al., 2024; Martin et al., 2007).

High volatility odors at 100% concentration provide more molecules for the nose to process than low volatility odors do, which results in a higher perceptual intensity when other

factors are balanced. Results from Lowry and Kay 2007 suggest that beta oscillations in the OB, which were induced after repeated presentation, are not a simple result of correlation to volatility or concentration. Volatility determines the airborne concentration of pure odorants; however, for diluted odorants, airborne concentration is determined by volatility and liquid concentration. Thus, the question remains whether there is something about the physicochemical properties of high volatility odorants or simply a "sweet spot" in airborne concentration that sensitizes the system.

Trigeminal-olfactory interactions

Most odorants also activate the trigeminal nerve, which releases neuromodulators (CGRP and substance P) that can affect the sensitivity of olfactory receptor neurons. It is unknown how the interaction of trigeminal system influences olfactory perception when strong trigeminal odorants are in mixtures with non- or low trigeminal stimulating odorants. Prior attempts at forming theoretical predictions regarding the quality of binary odor mixtures have failed to find any consistent predictor for overshadowing of one component in a binary mixture by the other. We tested the hypothesis that trigeminality contributes to overshadowing effects in binary mixture perception. We tested rats' ability to detect component odorants in four binary odor sets chosen for their relative trigeminality. We predicted that the difference in trigeminal intensity would predict the degree of overshadowing by boosting or suppressing the perceptual intensity of these odorants during learning or during mixture perception. We used a two-alternative choice (TAC) task in which rats were trained to recognize the two components of each mixture and tested on a range of mixtures of the two without reinforcement. We found that even though odorant concentrations were adjusted to balance volatility, all odor sets produced asymmetric psychometric curves. Odor pairs with the greatest difference in trigeminality showed

overshadowing by the odorant with weaker trigeminal properties. Odor sets with more evenly matched trigeminal properties also showed asymmetry that was not predicted by either small differences in volatility or trigeminality. Thus, trigeminal properties may influence overshadowing in odor mixtures, but other factors are also likely involved. These mixed results further support the need to test each odor mixture to determine its odor quality and underscore recent results at the level of olfactory receptor neurons that show massive and unpredictable inhibition among odorants in complex mixtures.

What unites these studies is how the OB responds to different olfactory stimuli under different contexts. The general circuity of the OB has been known since Cajal's hand-drawn graphs of the Olfactory Sensory Neurons (OSNs), glomeruli, mitral and granule cells, but how does this circuitry work internally, and with other parts of the brain, to give rise to behaviors?

Olfactory stimuli and the sensory stimuli available to the brain through other sensory systems make up the external world that the brain senses and reacts to. In singling out olfactory stimuli, we gain more insights into how the brain integrates sensory information to give rise to behaviors. Moreover, this integration process, including the sensory process, may be dynamically different in different contexts to best adapt to the external world and produce appropriate behaviors.

The challenge of an unknown olfactory space makes mapping single-unit activity from the sensory level to higher cortical levels even more challenging than the technical aspect of scientific inquiries. However, a lot of work has been done on olfaction and cognitive processes in the olfactory system, using neural population activity. Especially in circuitry dynamics, we know quite a lot about the relationship between the OB and its next-level cortical connections. There is one gap in our knowledge I'd like to address with my thesis work: how does the olfactory

network change under different contexts? Following my academic ancestors, my thesis work explores how the brain reacts to the ever-changing internal and external world using electrophysiological, behavioral, and computational methods.

Here, I examine context in the broad sense, including non-olfactory profiles of odor stimuli (trigeminality), task type, which manipulates cognitive demand through variations of diverse task elements, including difficulty, and prior experience.

Chapter 2: Methods

Methods for chapters 3 -5 are included in this chapter. Methods for chapter 6 are included in that chapter.

Behavior

Animals

For experiments reported in chapters 3 and 4, we used 8 adult Long Evans rats (4M/4F, purchased from Envigo). Rats were housed individually in a 14/10 h light/dark cycle (lights on at 8AM CST). All experiments were conducted during the light period. Each rat was randomly assigned to a 4-hour time window in the AM (9am-1pm) or PM (1pm-5pm) for training. Same odor set was trained in the same time window. Before experiments, rats were dieted to 85% of their *ad libitum* weight and maintained at this level for the remainder of the experiments. All procedures were done under veterinary supervision and oversight of the University of Chicago Institutional Animal Care and Use Committee in accordance with Association for Assessment and Accreditation of Laboratory Animal Care standards.

Odors

We used binary mixtures as conditioned stimuli. The two choices for rats to discriminate were labeled conditioned stimulus Left (CSLeft) and conditioned stimulus Right (CSRight). Fine pairs are mixes of enantiomers; coarse pairs are mixes of odors of different functional groups and perceptual profiles. Mixture ratios for all pairs except for Odor Set 1 Fine pair (OS1F) was mixed 90-10. To make the fine pairs of OS1 and OS2 of the same level of similarity or difficulty, OS1F was mixed 80-20 to account for carvone enantiomers' relatively different perceptual profiles. Flows of odors were controlled for vapor pressures. For instance, OS2C

component odorants eucalyptol and heptanone as monomolecular stimuli, have a vapor pressure ratio of 1/2. When used as a single component as a CSLeft or CSRight, their respective flows would be controlled to be the inverse of their vapor pressure ratio, 2/1, to produce similar levels of intensities. When mixed as binary mixtures, we dialed the flows of individual monomolecular odorants down to either 90/80 percent or 10/20 percent of the calculated 100 percent flows (based on vapor pressure ratios) and then mixed them to use as a conditional stimulus. Please see details in table 2.1. All rats were trained with a training odor pair (mixtures of amyl acetate and anisole). They were first trained with the task, then trained to learn the coarse and the fine pairs of each odor set. The order of OS1 and OS2 was balanced across rats.

Table 2.1 Odor sets and flows

		CSLeft		CSRight	
		Flow (%|lpm) *adjusted based on vapor pressure			
OS0	-	amyl acetate	anisole	amyl acetate	anisole
		90% 0.18	10%	10%	90%
OS1	Fine	(+)carvone	(-)carvone	(+)carvone	(-)carvone
		80% 0.16 lpm	20% 0.04 lpm	20% 0.04 lpm	80% 0.16 lpm
	Coarse	Citral	PEA	Citral	PEA
		90% 0.11 lpm	10% 0.03 lpm	10% 0.01 lpm	90% 0.33 lpm
OS2	Fine	(+)limonene	(-)limonene	(+)limonene	(-)limonene
		90% 0.18 lpm	10% 0.02 lpm	10% 0.02 lpm	90% 0.18 lpm
	Coarse	Eucalyptol	Heptanone	Eucalyptol	Heptanone
		90% 0.18 lpm	10% 0.009 lpm	10% 0.02 lpm	90% 0.09 lpm

Table 2.2 Odor sets and Vapor pressures				
		VP@25C (pa)		VP@25C (pa)
OS0	amyl acetate	-	anisole	-
OS1F	(+)carvone	70	(-)carvone	67
OS1C	citral	12.17	PEA	11.57
OS2F	(+)limonene	205.5	(-)limonene	200
OS2C	eucalyptol	253.31	heptanone	187

Apparatus

The odorant delivery system and behavioral apparatus were constructed in-house using standard laboratory materials and parts from Med Associates (St Alban, VT). All tubing connections were located outside of the operant chamber. The olfactometer is a positive-pressure, air-dilution system constructed with C-flex and MasterFlex tubing, glass test tubes for odorants, acrylic flowmeters, and solenoid-operated valves controlled by a computer running Med Associates MedPC IV software.

The olfactometer's air is obtained from the building's central line and passes through a carbon filter (Whatman InLine Carbon Filter, Kent, UK) with C-flex tubing (1/8", Cole-Parmer, Vernon Hills, IL) carrying the clean air, unless otherwise specified. Downstream of the filter, air passes through the same length of tubing for each stimulus to reach the vicinity of the operant boxes. For each behavioral box, the air stream is separated into two parallel streams: the clean air stream and the odor input stream. The odor input stream is separated into two parallel odor channels: two streams deliver air into two multi-channel solenoids. Each multi-channel solenoid has six output channels, controlled by the MedPC program and controller to open and close as

needed. Each channel (four out of six used) is connected to a designated flow meter (50mLPM to 2 LPM, Cole-Parmer) to control air flow. The air coming from each flow meter is delivered into a designated liquid pure odorant test tube. The small bubbles produced by the small-gauge teflon tubing at the bottom of the tube maintain the saturated headspace above the odorant in the glass tube. The odorized air stream drawn from this saturated headspace mixes with another odorized air stream (the other component of the binary mixture, connected in the same way described above, except it is from the other multi-channel solenoid) with a T connector. This set of binary mixtures is then mixed with air streams, mixed in the same way, but from different test tubes. The mixed air streams then all mix with the initial diversion air stream, where the final tube is united with a vacuum line controlled by a solenoid, and together they reach the odor port through a T connector. Streams into and out of solenoid channels, into and out of flow meters, are carried by MasterFlex PTFE tubes (1/16'' Cole-Parmer). The final odorized air stream is thus composed of a dilution air stream (1LPM) and an odorized air stream, the flow of which is controlled to range from 0.34 LPM to 50 mLPM according to the volatility of the specific odor. Check valves are inserted into the lines at many locations to eliminate backflow and equalize pressure in the system. The check valves are spaced equally in the two sets of lines for each of the odors.

Solenoid valves for the odorants and the vacuum line, as well as session events, are controlled via custom-written code within Med Associates Med-PC IV software. Airflow through the clean air stream is never interrupted during the session. Two seconds prior to trial start, a solenoid valve opens to allow airflow to one odorant tube, in order to charge the tubing with odorized air. During this period, the vacuum is on, which prevents the odorized air from reaching the odor port. At the end of the 2 seconds, one panel of the traffic light is illuminated, which signals to the rat that the trial has begun, and they can sample the odors in 500ms. The

500ms mandatory wait was instilled to encourage rats to pay attention to the light. For all rats, during initial task training, the middle light was used to cue the trial start. After the 500ms delay from light on, a nose-poke by the rat triggers the closing of the vacuum valve, which allows the odorized stream to flow into the odor port. The vacuum siphons off the odor right outside the nose port, so when the IR detector in the odor port is triggered by nose entry, the delay from the close of the vacuum solenoid to reach the odor port is less than 100 msec. While the rat keeps its nose in the odor port (i.e., while the photobeam is interrupted) the vacuum valve remains closed. Withdrawal of the nose from the odor port opens the vacuum solenoid and closes the odorant solenoid, thereby stopping any additional odorant from entering the odor port. Because the vacuum flow is greater than the odor stream flow, there is a slight negative flow from the odor port and the behavioral chamber into the vacuum. This helps to clear the port of residual odorant between trials.

All training and testing occurred in Med Associates chambers. Two opposing walls of the chamber are made of clear polycarbonate. The front and back walls are made of aluminum and contain three panels where the different devices (i.e., odor and response ports, traffic light panel with three lights, and reward dish) are located. The light panel sits at the top and center of one of center front aluminum panels. Below the light panel at the center, the odor port is the odor port, with the reward dish below the odor port. The response ports are on one (phase 2 only) or both sides, depending on the training phase. The floor of the chamber consists of a stainless-steel grid floor attached to the walls and a piece of Plexiglas on top of it. The odor-port houses the photobeam detector to detect nose entry, with odor delivery from a hole behind the IR beam.

Training

We used a variation of the Two-Alternative Choice (TAC) olfactory discrimination task. The variation largely follows a similar scheme for the training period of a traditional TAC task but differs in the testing phase (referred to as phase 4, as training was composed of three phases). The only difference in the training scheme is the timing of the light. We changed the timing of the light to push rats to use the light as a cue, as the informative condition requires. Both the informative and non-informative rats were trained the same way during task training with the training pair (mixtures of amyl acetate and anisole). For OS1 and OS2, half of the rats were trained with informative lights; the other half were trained with just the middle/yellow light as a control, with the order of OS1 and OS2 balanced within each group. For the informative group, after they learned the task with the training pair, when they started learning the first odor pair they were tested on, they were introduced to the different lights that predicted the odor stimulus type (coarse or fine) of the upcoming trial. For all informative rats, the light on the left side of the traffic panel signifies that the odor that will come is part of the coarse pair, while the light on the right side of the traffic panel signifies an odor from the fine pair. The non-informative group only saw the light in the middle of the panel throughout the experiment.

Two-Alternative Choice paradigm

All rats were trained to perform a Two-Alternative Choice (TAC) behavior protocol once they reached their respective 85% ad lib weights after arrival at the lab. The TAC protocol requires the rat to associate each of two odors or odor mixtures with either the left or the right response port (nose poke port). Training involved progression through three consecutive Phases, which are designated as Phases 1, 2, and 3. Depending on the Phase, an experimental session (hereafter, session) consisted of between 100 and 400 total trials. Each rat was run only one

session per day, on consecutive days. Therefore, a rat never progressed through the Phases within the same day. Performance criteria to move from one Phase to the next are described below. All sessions for each rat for one OS were performed in the same window of the day (AM/PM). AM/PM windows that rats were trained in span at most 4 hours (9a-1p/1p-5p). AM/PM order was randomized across subjects.

A trial is defined as the period between the light on (start of trial) and the light off (end of trial), regardless of whether the rat engaged in the expected task behavior. After the light is on for 500ms, a rat had 5.5 seconds to initiate a trial. The 500ms mandatory wait was instituted to encourage rats to pay attention to a cue light (described below in "task specifics"). For both informative and non-informative groups, the middle light of the traffic light panel was used during all phases of training the task. The first time the informative group of rats were introduced to different lights on the panel, with the position indicating the odor stimulus type, was when they were learning the coarse pair of the first set of odors they would be tested on. The order of OS1 and OS2 was balanced. During the 5.5s period after the mandatory wait, a nose-poke in the odor port caused the vacuum's solenoid to close, which then allowed the free flow of an odorant stream into the odor port only while the rat kept its nose in the odor port. The light remained on until the end of the trial. A trial's duration depended on the phase and performance.

Within a session, a trial could have two results: either be attempted (i.e., the rat nose-poked in the odor port) or not. An attempt is a trial during which a rat poked its nose into the central port to sample the odors. The time between the light off and the next light on for all phases, was 7 seconds (not including penalty for incorrect trials). The number of trials per session within a Phase was as follows: Phase 1, 100 total trials; Phase 2, 200 total trials; Phase 3, either 400 total trials or 320 attempted trials. Sessions ended when these trial criteria were met.

All task parameters were controlled using Med Associates' hardware and the MEDPC IV software interface. Individual trial types were pseudo-randomly selected with replacement using MEDPC IV's RANDI method (phases 1-3) or without replacement using RANDD method (phase 4). This keeps the ratio of CSLeft trial and CSRight trial relatively equal during phase 3, while the order is random. In phase 4, use of randomization without replacement keeps the number of trials for specific odor stimulus types equal across stimuli but the order of appearance random. Within the text, I label these trials as being randomly selected to conform to the conventions of the literature. Flows of CSLeft and CSRight remain the same through Phases 1, 2, and 3.

Phase 1— In Phase 1, rats learned to associate a nose-poke into the odor port during the trial (6 seconds after light on, including 0.5s mandatory wait plus 5.5s) period with a reward (40 mg dustless sucrose precision pellets BioServ) delivered in the reward dish as soon as the nose was withdrawn from the odor port. Rats were given an additional 5 seconds of light on to eat the reward. Odor was on in the port during the nose poke and turned off and evacuated after nose withdrawal. After the first nose-poke, repeated attempts (i.e., multiple nose-pokes at the odor port) within the same trial did not result in additional odorant delivery or reward. To encourage learning, a rat received two 'free' sugar pellets once every 20 trials, but only if the rat had not correctly performed 15 attempts. Rats were run for 100 total trials per session. In order for a rat to complete Phase 1, it had to complete at least 80 attempts in two consecutive days.

Phase 2—In Phase 2, rats learned to pair the initial nose-poke in the odor port and stimulus sampling with a second nose-poke into a response port. We label this positive operant behavior a response. As in Phase 1, rats had 5.5 seconds to initiate a trial by nose-poking in the central odor port, after 0.5s of mandatory wait post light on. The response port was introduced on

the first day of Phase 2 and was located to the left of the odor port. If the rat nose-poked in the odor port during a trial, it had 5 seconds after retracting its nose from the odor port to nose-poke at the response port (termed a response), which resulted in receiving a reward. To keep rats motivated during learning (i.e., while they discovered there was a response port and learned the correct response), 'free' rewards were randomly (1/3 probability) delivered for Phase 1 type behavior (nose poke without response). Also, during the first 5 attempts, if a rat did not make a response after 4 seconds, it received a 'free' reward.

As in Phase 1, only a single conditioned stimulus was delivered. Rats were run for 200 total trials per session. After achieving session performance (correct attempts / total attempts) greater than 70%, the rat progressed to a variation of Phase 2 that decreased the free reward probability from 1/3 to 1/20. In order for a rat to complete Phase 2, it had to achieve session performance greater than 70% for two consecutive days.

Phase 3 —In Phase 3, rats learned to perform an odor discrimination. This was the first Phase in which two different conditioned stimuli were used in the same session. Just as in Phases 1 and 2, rats had 6 seconds in which to attempt a trial (i.e., to nose-poke in the odor port) after light on. In phase 3, an additional response port was introduced and placed to the right side of the odor port. On each trial, one of two conditioned stimuli (CSLeft, used in Phases 1 and 2; CSRight, new) was randomly selected (uniform probability). A correct trial was one in which rats delivered the response in the left response port if CSLeft was presented and delivered the response in the right response port if CSRight was presented. If a response was delivered in the wrong response port, the light was immediately extinguished, and a 7-second penalty delay was used and added to the normal intertrial interval (ITI) of 7s. During the penalty delay, the light remained off, and a nose poke did not initiate any action. If the rat refrained from delivering a

response during the 5 seconds following nose withdrawal, the light was turned off, and a new trial was initiated following the regular ITI.

To move on to Phase 4, learning one of the two test odor sets, rats were required to achieve two days above 70% performance for both the fine and coarse odor pairs, trained in Phase 3 described above. All rats for each OS learned the coarse pair first. When they reached the performance criterion, they moved on to learning the fine odor pair for that odor set. Rats don't go back to previous phases once they learn the task. When they reach the 70% criterion for the fine pair, we retest on the coarse pair for one day. If rats remained above criterion for the coarse pair, they were moved on to testing (phase 4). If their performance dropped below 70%, they were retrained on the coarse pair and retested on fine before moving to testing in the same manner. This means that, on the day before the testing day, and the second day before the testing day, rats performed above 70% accuracy alternately for the fine and coarse sets.

Testing

After learning the two pairs of conditioned stimuli (coarse and fine) in an OS, the rats performed a 4-stimulus discrimination task (phase 4). For a given OS, on a testing day, rats need to assign the correct port response to both the CSLeft and CSRight for both the fine and coarse pair. Before the first testing day, they had not discriminated the four stimuli from both fine and coarse pairs in the same session.

We designed two kinds of tests and asked rats to perform 2 sessions of each, in 4 consecutive days, one session per day. During these four test sessions, rats discriminated the four stimuli, two fine and two coarse odors that they had learned to associate with either right or left responses. There were a total four odor stimuli, 2 learned CSLeft and 2 learned CSRight. Rats

were rewarded every time they went to the correct port in response to the conditioned stimulus that came on for the trial.

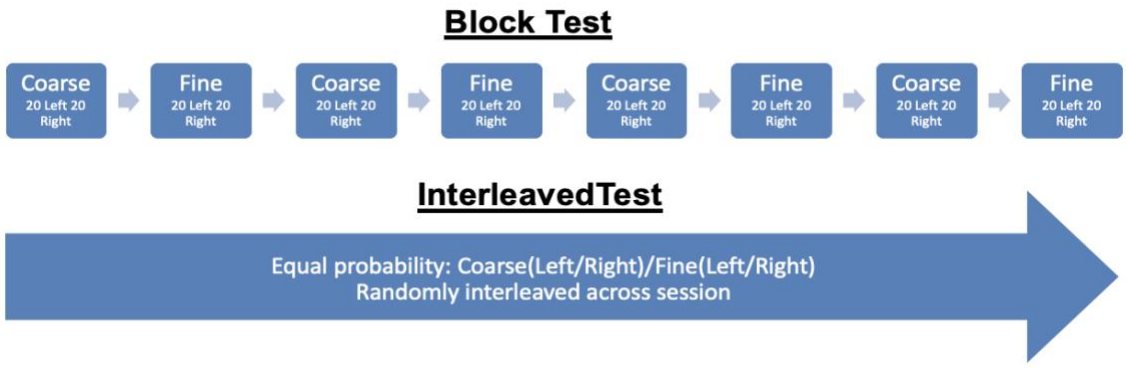

Figure 2.1 Test days schematic

On the first two days, rats performed the *block* test. In the block test, trials were composed of alternating blocks of fine and coarse stimuli. In a fine block for instance, only CSLeft and CSRight from the learned fine pair would come on, randomly within the block. Each session was composed of 320 trials or 8 blocks of 40 trials. Within each block, CSLeft and CSRight had an equal probability of happening. Sessions were terminated either at 400 trials or 320 attempted trials, whichever happened first.

On the third and fourth days, rats performed the *interleaved* task. The interleaved task is a similar 4-stimulus task, but instead of fine and coarse pair blocks, trials were fully randomly interleaved among the 4 stimuli. On any given trial, there's an equal probability of any of the 4 stimuli to come on. The interleaved test is designed to provide less predictability of the odor compared to the block test, hence a presumed higher demand for cognitive effort. However, we weren't sure how rats would use the lights, so for each interleaved session, we also added 10% of

trials with neutral light and 10% of trials with the wrong light signal. During the neutral light trials, instead of one of the lights rats under the informative condition has learned to associate with either an upcoming fine or coarse stimulus, the middle light was illuminated. During the trials with the wrong light for the informative group, the opposite light that was associated with the coming stimulus was illuminated.

Surgery and Electrophysiology

Once rats performed above 70% two days consecutively on the training odors, they were put back on ad lib to prepare for surgery. Surgeries were performed once rats came back to their previous ad lib weight. Bipolar electrodes (100 mm stainless steel, Formvar insulated;1–1.5 mm vertical tip separation, 100–200 kV impedance at 1 kHz) following our previously reported methods (Frederick et al., 2016) were implanted in the left main OB (8.5 mm anterior to bregma, 1.5 mm lateral, and 4.2 mm deep), left anterior PC (0.5 mm anterior to bregma, 3 mm lateral, and 7.5 mm deep at a 15° angle from vertical), left DG of dorsal hippocampus (3 mm posterior to bregma, 2.4 mm lateral, 3 mm deep), left dorsal CA1 of hippocampus (4 mm posterior to bregma, 3 mm lateral, 2 mm deep); a thermocouple electrode (0.005 inch, Teflon coated; catalog #5TC-TTK-36-36, Omega) was implanted ipsilaterally in the nasal cavity to measure respiration. Ground and reference screws were secured to head screws in the right parietal and frontal bones, respectively. Electrodes were visualized to pierce the pial surface, and signals were recorded as the electrode was lowered. A final location was selected if the signals on each electrode reversed themselves at or near the planned depth. If there was no reversal, the location within the desired stereotaxic depth with the largest amplitude was selected. Depths for reversals were previously estimated in published experiments. Each electrode was attached to an eighteen-pin connector

(Ginder Scientific). Rats recovered from surgery for at least 18 days, after which they were returned to the training regimen.

Recording sessions were conducted during the last stage of Phase 3 training on the training odor set and for the remainder of the training and test sessions for the experiment.

Raw data were digitized and amplified by an Intan RHD2132 headstage (http://intantech.com/RHD2132_RHD2216_amp_board.html), collected with an Open Ephys acquisition board (http://www.open-ephys.org/acq-board/), and preprocessed with Open Ephys GUI (http://www.open-ephys.org/gui/) on a computer running Windows 10. The raw data signals were band-pass filtered from 1 – 250Hz. Behavioral events were recorded by MedPC and at the same time, conveyed to Open Ephys with a TTL pulse. The TTL pulse was recorded in a separate channel of the session data file from the rest of the LFP data, but was of the same length. Post processing extracts the TTL timepoints to mark behavior events.

Analysis

Preprocessing and spectral analysis were done in MATLAB 2024a. All statistical analyses were performed in R Studio (2024.12.1) using R 4.4.3. The alpha value is set as 0.05.

Preprocessing

LFP raw signals were manually reviewed to exclude trials with unreasonable levels of 60Hz noise, static, or movement artifact. Each trial was inspected manually and marked good or bad. The inspected period of each trial spans from 3s before nose poke and 7s after. Any duration of unreasonable level of noise during this 10s window disqualifies the current trial from “good”. Further analyses were conducted on good trials only.

Using the Chronux(Mitra & Bokil, 2008) package in MATLAB, we detrended LFP raw signals (*locdetrend)*, then filtered out 60hz noise (*rmlinesc)*, and then normalized them by the

standard deviation of the session baseline. The session baseline was manually selected for each session. Before the behavioral program was started on MEDPC, OpenEphys was started to record a pre-session baseline for each rat on each session. A 10s period during which the rats were not moving around or grooming or actively exploring or sniffing from the ports was marked for later baseline extraction. The final length of the baseline was determined as a 7s period, as not all rats were able to maintain a relatively restful period for an entire 10s.

Spectral Analysis

Normalized LFPs were fed into spectral analysis functions to produce power density (*mtspectrumc)* or spectrogram weights (*mtspecgramc)*. Parameters were adjusted based on the length of the input data. We set the OpenEphys system to sample at 2000 Hz. We zero-pad the signal to extend the length to the next power of two. For analysis on data length smaller than 500ms, we set the time-bandwidth product as 2 and the taper number as 3. For analysis on data longer than 500ms, we set the time-bandwidth product as 3 and the taper number as 5. Both are the maximum numbers of tapers allowed given the time-bandwidth product. For spectrograms, the moving window is set as 0.3s, and the step size is 0.01s. We do not average signals or initial analyses over trials. This average is later performed manually based on analysis needs.

For each trial, we get the power density across 3-110Hz of each interval of analysis. The intervals of analysis included were centered around the trial events, including light on, nose poke, and nose withdraw. This resulted in 6 possible intervals of analysis: before and after light on, before and after nose poke, and before and after nose withdrawal. We also added a baseline interval, which is a 500ms interval beginning 1s before light on, to use as a trial baseline reference. Initial power analysis was performed at each event interval, spanning from 300ms to 500ms based on previous knowledge of LFP dynamics during a trial(Frederick et al., 2016).

Further statistical analysis excluded data window overlap between after nose poke and before nose withdraw or after light on and before nose poke. The final length of power analysis for each event interval were: baseline 500ms, before light on 500ms, after light on 500ms, before nose poke 400ms, after nose poke 400ms, before nose withdraw 400ms, after nose withdraw 400ms.

General Least Square Analysis

To account for the correlation in our data structure due to subject effects, we perform the general least square models (GLS). Compared to linear mixed-effects models, generalized least squares (GLS) models include random effects by modeling the correlation structure of the residuals directly. As a result, GLS models estimate the marginal (population-level) effects of the fixed terms. We expected the cue effect to be a general marginal effect preserved across subjects.

Variables

Possible independent variables for a given trial are: coarse/fine(type of olfactory stimulus); cue (informative or noninformative light cue; for interleaved tests, this variable also includes the values neutral or discordant light cue); test day(four days, the first two being the block tests and the last two being the interleaved test); event(including the six intervals mentioned earlier); sex; learning phase(is the odor set the 1^{st} or the 2^{nd} odor set that rats learned); block number(the first 40 trials of the session is block 1, 41-80 is block 2 etc.). It is reasonable to expect block effects given our design of the block test, and that a session may be long enough (1hr 15min to 1hr 45min) to show a session-wise learning effect. Hence, we conducted statistical analysis on block-averaged data points.

Dependent variables include mean power, mean coherence, mean accuracy, median sampling duration, and median response delay. Sampling duration is the period of time that rats sniff the odors, calculated as the time difference between when rats start sampling and when they

withdraw from the odor port. Response delay is the time rats take to make a left or right response after odor sampling. From previous work, we know the distribution of sampling duration and response delay both have a long tail on the right side; therefore, the median is a better statistical representation for their analysis.

All variables included either directly address our hypothesis or are known to be a factor in OB LFP and behavioral performance. Interaction terms that address our hypothesis (the three-way interaction between odor stimulus type, cue condition, and test day) are included in all models. When other interaction terms are needed, a likelihood ratio is performed to determine whether including the interaction term significantly improves model prediction. The interaction term in question was included if $p<0.05$.

Behavior

In general, the model for a behavioral variable was (with adapted interaction terms if needed):

behavior variable ~ odor stimulus type (coarse/fine) + cue (informative/non-informative) + day of test (1-4, 1,2=block, 3,4=interleaved) + sex (male/female) + learning phase (1/2=first OS learned) + block no. (1-8) + odor stimulus type *cue *day

We set the condition of the model as "correlation = corCompSymm(form = ~1 | rat)", this innate parameter to the *gls* function in the R *lmne* package allows the model to take into account random effects of "rat" by setting the correlation structures of the errors by each rat.

Power

The output of *mtspectrumc* by trial and other behavioral variables were stored in a .mat file to be processed in R for further statistical analysis. Saved .mat files are read by R with function *h5read* from the R package rhdf5 and then saved as an R signature data frame structure

for further analysis. Only good trials and trials with a sampling duration larger than 0.1s and smaller than 2s were used for spectral analysis. Trial-wise mean theta (3-12 Hz), beta (15-35 Hz), gamma (65-110 Hz), gamma2 (40-55 Hz) band power for each event interval was calculated. We further calculated the average mean power for each band across each 40 trials, or one block, during all event intervals, for each session. In the block test, our design allows a total of 8 forty-trial blocks.

The final block averaged mean band power and behavioral variable values were fed into the *gls* function of the lmne R package. The model for average power in each band range follows the formula (with adaptation for each model on the interaction, and event if needed):

log(mean band power) ~ odor stimulus type (coarse/fine) + cue (informative/non-informative) + day of test (1-4, 1,2=block, 3,4=interleaved) + event (pre/post lighton, nose poke, response) + sex (male/female) + learning phase (1/2=first OS learned) + block no. (1-8) + cue*event + coarse*fine*day

We adopted the same correlation structure "correlation = corCompSymm(form = ~1 | rat)", to account for random effects of rats. Further GLS may be performed if one particular event is of interest.

Coherence

We adapted the Chronux function *coherencyc* into *coherencyc_Zcoh*, to Z-transform the coherence output using the function *atanh*. Output of *coherencyc_Zcoh* by trial, and other behavioral variables were stored in a .mat file to be processed in R for further statistical analysis. Only good trials and trials with a sampling duration longer than 0.1s and smaller than 2s were used for coherence analysis. Furthermore, input to *coherencyc_Zcoh* requires the two signal matrices to be of the same size. So, for each combination of areas, the subset of trials that are

good for both areas was used. Trial-wise mean theta (3-12 Hz), beta (15-35 Hz), gamma (65-110 Hz), gamma2 (40-55 Hz) coherence over each event interval was calculated. We further calculated the average mean coherence for each band across each 40 trials, or one block, during all event intervals for each session.

The final block-averaged coherence and behavioral variable values were fed into the *gls* function of the lmne R package. The model for average coherence in each band range was:

mean band coherence ~ odor stimulus type (coarse/fine) + cue (informative/non-informative) + day of test (1-4, 1,2=block, 3,4=interleaved) + event (pre/post lighton, nose poke, response) + sex (male/female) + learning phase (1/2=first OS learned) + block no. (1-8) + cue*event + coarse*fine*day

We adopted the same correlation structure "correlation = corCompSymm(form = ~1 | rat)", to account for random effects of rats.

Multiple Comparison Tests

Model results from the *gls* function were used for multiple comparison tests to further estimate level values. For statistically significant prediction terms, multiple comparison tests were done with R package *emmeans*, using the Bonferroni correction method for significance and confidence interval estimations.

Coherence phase estimation

Coherence phase estimation was used to interpret the direction of connections between different areas. We did this in MATLAB using the phase result of function *coherencyc_Zcoh*. The phase output of the above function was fit to a linear model. The slope of the linear model indicates the directionality of directions. When the slope is positive, the second input matrix leads the first input matrix. The exact delay in s is derived by slope/2pi.

Chapter 3: Behavioral and OB oscillations in a 4-odor identification task based on TAC

In order to test the influence of cognitive demand on gamma oscillations in the OB, we designed a variation of the two-alternative choice (TAC). The variation of the TAC task manipulates task demand in three dimensions: (1) after rats learn one dissimilar odor stimuli pair (composed of one CSLeft and one CSRight), they continue to learn another pair of odor stimuli, but composed of combinations of enantiomers. Once rats learn both pairs, they were tested on two learned pairs together, making it a four-odor discrimination task (two CSLeft and two CSRight) (2) the testing phase included first two days of the four-odor discrimination task in a block manner, then immediately after two days of the four-odor discrimination task in an interleaved manner (3) half of the rats (4 total, 2M2F) learned the odor sets (not the training set which they never get tested on) with an informative cue. We replaced the normal house light of a TAC task with a light panel consisting of three lights in a horizontal traffic light fashion. When the light on the left came on, it signified that the trial that was about to start (500ms after light on) would be one of the conditioned stimuli from the dissimilar (coarse) pair. When the light on the right came on, it signified the coming trial with a stimulus from the enantiomers (fine) pair. We hypothesized that these three levels interact in influencing gamma oscillations in the OB. Half of the rats were in the informative group, half were in the non-informative group as a control for level 3. Total number of rats was 8, including 4 male and 4 female rats. We report the result for one OS2 in this dissertation and will further examine the differences in the two-odor set. The results we report here are largely similar across the two odor sets.

In this chapter, we report details of the OB LFP power across the theta, beta, gamma, and gamma2 bands with a focus on answering our hypothesis concerning the dynamics of the gamma

oscillations. Power densities were calculated by trial and events of a trial in Chronux and averaged over blocks (40 trials) by group within the event. The event intervals we include during a trial center around significant task timepoints: light on, start of odor sampling, and response. We take 400ms-500ms intervals around (before and after) the three timepoints, plus a 500ms interval before the pre-light period as a baseline. This results in 7 trial event intervals labeled: pre light baseline, pre light, post light, pre sampling, sampling, pre odor off, post odor off (see figure 3.1 for trial schematics). In reality, the time between when sampling can begin and when it actually does is extremely short (as short as 10ms, which is our recording unit limit) as rats often wait in the odor port prepared to sample the trial. Thus, the pre sampling period and after light period often overlap considerably (there is a 0.5s delay between when the cue light turns on and when the nosepoke can trigger the odor to start). After sampling the odor, the rats make their responses very quickly. The time between withdrawal of nose from the odor port and the nose poke in the response port is 54ms +/-15ms. Pre odor off may overlap with sampling. We report results of GLS and follow up multiple comparison tests. All GLS models used a specified correlation structure to account for random effect of rats. Based on the factor investigated and prior knowledge, either an overall GLS include all event data, or an event specific subset GLS is used. We report this when reporting results. Since there are overlapping event intervals, when using an overall GLS model, possibly overlapping events were filtered in the data set used for the GLS. Most often pre sampling and pre odor off were dropped. They were included in some models because the possibility of overlapping did not produce identical results for pre sampling and post light, or pre odor off and sampling.

.

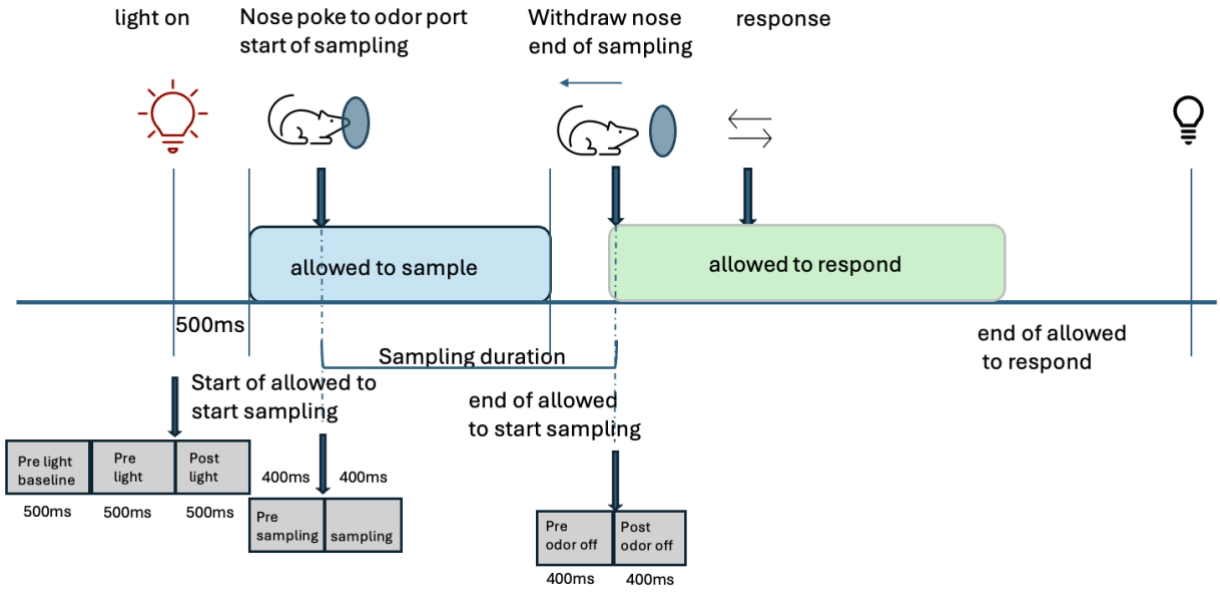

Figure 3.1 Trial schematic of the TAC task.
The variation of the task we use preserves this trial structure. Instead of normal house light we use a traffic light composed of 3 light bulbs at fixed locations on the light board. The light panel is fixed on the same side of the aluminum wall rats poke their nose for sampling and response. See methods for light variation details. We included a 500ms mandatory wait after light on to encourage rats to pay attention to the light. The major event timepoints of a trial include light on, start of sampling, nose withdraw and response. The grey boxes signify trial event intervals we perform our spectral analysis on.

Results

Two groups of rats were tested each in a variant of the two-alternative choice task (TAC). We tested the hypothesis that the cognitive load or amount of information available to solve the discrimination problem would modulate gamma power differently on the same odor sets. In the 4-odor block and interleaved task, one group (informative) was provided a cue which limited the upcoming odor to one of two odors. The other group (non-informative) had a neutral cue. We hypothesized that the non-informative group would face a more challenging task than the informative group and amplify OB gamma oscillations more than the informative group.

Informative and non-informative groups show different strategies and network states while performing the 4-odor discrimination task

We found significant differences between the informative and non-informative rats in a wide array of behavioral and electrophysiological variables. These differences indicate that the overall brain states for the two groups are different when performing the same tasks.

The behavioral variables we examined include response accuracy and sampling duration. The electrophysiological variables we examined include averaged power of oscillations in the theta (3-12Hz), beta (15-35Hz), gamma1 (65-110Hz) (referred to as gamma from now on), and gamma2 (40-55Hz) bands, during a trial (spans 0.5s before nose poke for odor sampling or 0.5s before light cue illuminates to 1s after), or during the seven event intervals of a trial (baseline before pre light, pre light, post light, pre sampling, sampling, pre odor off, post odor off). For each dependent variable, we fit a generalized least square (GLS) model, accounting for the random effect from rats. Data from both informative and non-informative groups (4 + 4 rats, 2F in each group), two block test days, and two interleaved test days are evaluated in this chapter. The independent variables we included vary by the dependent variable being examined. The model formulas mostly vary in interactions. The independent variables include cue condition (informative/non-informative, 1/0 in tables), stimuli type (coarse/fine, 1/2 in tables), day of test (days 1,2 are block tests, days 3,4 are interleaved tests), sex (male/female, 1/2 in tables), learning phase (1=first odor set learned, 2=second odor set learned), block number (each session has 8 blocks composed of 40 trials), and interaction terms that we expect to have an effect on the dependent variable examined. The block number was calculated as the absolute index of attempts during a session. If a trial was later excluded for noise or other reasons, it does not influence the block number of surrounding trials. For all models, all interaction terms related to our main

hypothesis, cue effect, were included. For other interactions, if an interaction term is questionable to be included or not, we perform a likelihood ratio test to see if excluding or including the term significantly improves the model. The significantly better model (difference between models for the likelihood ratio test has a $p<0.05$) is always chosen; if including the interaction term in question does not significantly improve the model, we choose the simpler model.

Accuracy

In the GLS performed on accuracy, we found odor stimulus type (odor from the fine or coarse pair) to be a significant predictor of accuracy (p= 0.0366, t= -2.0989, beta= -0.1100, SE= 0.0524), with no significant interactions. Rats performed better on odors from the coarse pair (Fig. 3.2a). There was also main effect of trial block number (2-5) on performance compared to the first block; the later blocks have significantly higher performance (block 2: p= 0.0119, t= 2.5294, beta= 0.0732, SE= 0.0289, block 3: p= 0.0471, t=1.9932, beta= 0.0540, SE= 0.0271, block 4: p= 0.0031, t= 2.9815, beta= 0.0869, SE= 0.0291, block 5: p= 0.0403, t= 2.059268, beta= 0.0562, SE= 0.02727497; Fig. 3.2b). First block performance is lower than the rest of the blocks (till block 5). The reason why blocks 6-8 didn't show significant improvement over block 1 could be that female rats tend to finish fewer trials than male rats (~200 trials compared to 320 trials), resulting in a difference in power in later blocks. There were no other significant terms, including no difference across the two cue conditions (informative vs. non-informative).

a b

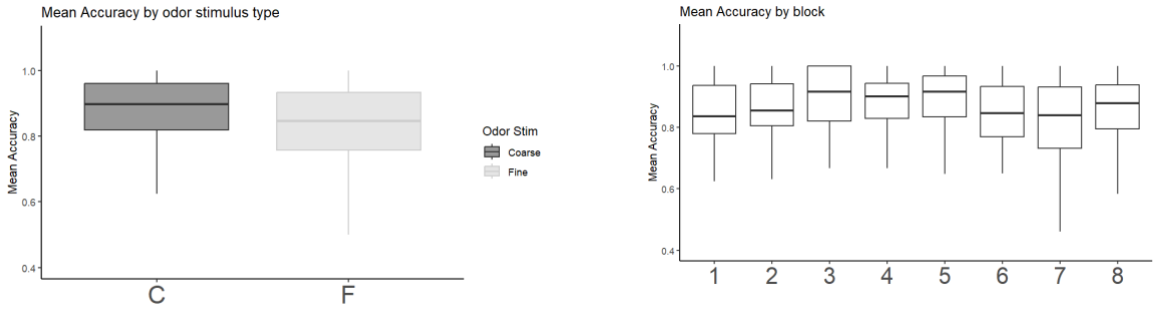

Figure 3.2 Accuracy effect of odor stimulus type and block number
Rats do better on coarse trials than fine trials by 11% (p= 0.0366, t= -2.0989, beta=, -0.1100 SE= 0.0524). b. block number. GLS result shows block 1 is significantly lower than block 2-5 by 7 (p= 0.0119), 5 (p= 0.0471), 9 (p= 0.0031), 6 (p= 0.0403) percent.

Sampling duration

Sampling duration, together with accuracy, has been used as an indicator of how difficult a rat may find a task. Several studies have talked about the idea of speed-accuracy trade-off in olfactory tasks(Abraham et al., 2004, 2012; Khan & Sobel, 2004), where rats and mice need more time to discriminate more closely related or complex odor stimuli compared to simple stimuli.

We found a main effect of odor stimulus type (coarse or fine pair) on sampling duration (p= 0.0316, t= 2.1595, beta= 0.0510, SE= 0.0236). Similar to previous studies, it takes rats longer to identify a stimulus from a fine odor pair, compared to a stimulus from a coarse odor pair. The difference in our experiment is about 51ms longer when sampling a fine pair odor. We also found a main effect of cue condition on sampling duration (p= 0.0491, t= 1.9756, beta= 0.1, SE= 0.0506). The informative group samples about 100ms longer compared to the non-informative group (Fig. 3b).

a

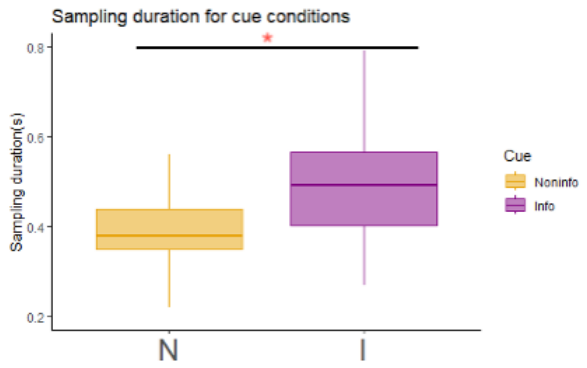

b

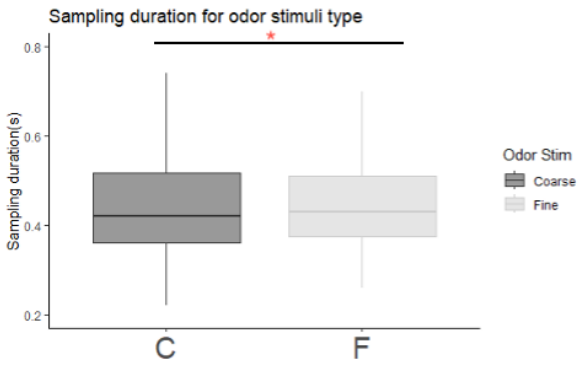

Figure 3.3 Sampling duration effects of cue and odor stimuli type
a. cue conditions. Informative group samples 100 ms longer than non-informative group (p= 0.0316). b. odor stimulus type. Rats sample for 51ms longer on fine versus coarse trials (p=0.0491).

We also found the block numbers to have a significant main effect on sampling duration. Starting with block 3, the sampling duration decreases by 33-104ms (Fig. 3.4). This means that throughout the session, rats learn and adapt their behavior. Later blocks (3-8) require lower sampling durations than the first 2 blocks.

a

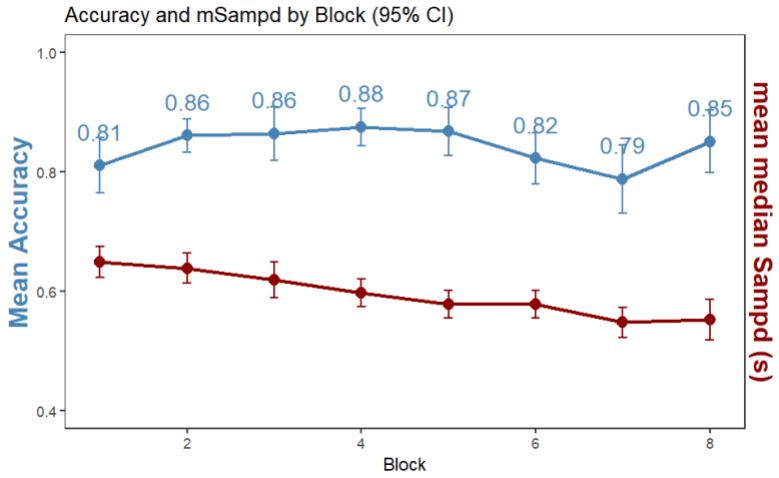

b

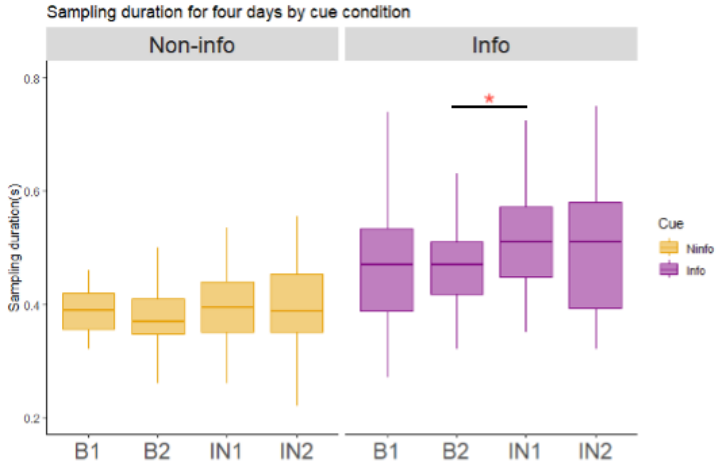

Figure 3.4 Sampling duration
a. Block effects on sampling duration and accuracy are plotted on the same x-axis with block number. Each point is a block average data point, with 95% confidence intervals calculated for each point. The GLS model on sampling duration show blocks (3-8) to be significantly lower than block 1(p= 0.0058 for block 3, p=0 for the rest). b. sampling duration for all test days by cue condition

Test day, sex, and learning phase (first odor set vs. second odor set learned) were not significant in the GLS model, nor was the three-way interaction term between odor stimulus, cue

and day significant. Since we expected rats to behave differently on different test days (block vs interleaved), to examine what the effect of odor stimulus type (coarse/fine) and cue (informative/non-informative) might look like on different days, we performed follow-up multiple comparison tests for sampling duration of each odor stimulus type by day and sampling duration for each cue type by day. After Bonferroni correction for p values, we found that for informative rats, sampling duration on day 3 was significantly longer than that on day 2 ($p = 0.0198$; Fig. 3.4a). No other multiple comparison tests survived the Bonferroni correction. (The reason why the main effects of GLS didn't survive multiple comparisons could be that the multiple comparison method we used with *emmeans* prioritizes interaction structures when included in the model, even though the three-way interaction was not significant. It was included because this interaction informs our hypothesis, and improved model fit (AIC and BIC).)

This difference in behavior between the informative rats and the non-informative rats shows that the variation of the TAC test we used successfully manipulated rats' behaviors. Rats can use an associated cue conveying information about the next trial to perform odor discriminations differently than if the cue is not informative. Adding the informative cue results in a longer sampling time. Even though there is no main effect of test day, when looking at the cue and odor stimulus effects throughout the 4 test days, we found that the non-informative group has similar behavior throughout the four days, while the informative group samples longer on day 3 compared to day 2. Similar to other studies, rats sample longer for fine odors compared to coarse odors, both the informative and the non-informative groups. We also found that throughout a session, both informative and non-informative rats adapt their sampling strategies; sampling duration for blocks 3-8 was shorter than blocks 1 and 2.

OB Gamma power

In the mammalian OB, we know that gamma oscillations are generated by the local circuitry. Gamma oscillations are modulated by sensory input and are theorized to be a signature of sensory pattern disambiguation. The functional role of elevated gamma power during odor sampling in fine discrimination supports this hypothesis(Martin et al., 2007; Nusser et al., 2001). Our previous studies showed different amounts of gamma power elevation in fine odor discrimination that varied by the difficulty of the tasks we used in different tasks (Beshel et al., 2007; Martin et al., 2007; Frederick et al., 2016). We therefore hypothesized that the cognitive structure of the task contributes to the role that gamma oscillations play in odor discrimination. Our hypothesis was that this sensory process would also be modulated by cognitive load, and we manipulated the tasks to create various levels of cognitive load. We predicted that OB gamma power changes as cognitive load changes.

To test this hypothesis, we first performed a GLS analysis accounting for random effects of rats on OB gamma power and odor stimulus type, cue condition, test day, marked event intervals (excluding overlapping event intervals), sex, learning phase, block id, interaction between cue condition and event and a 3-way interaction between cue condition, odor stimuli type and test day. The GLS informs us what further multiple comparison tests to perform, and if they should be grouped by other factors. We found significant effects on day 3 (beta=-0.5944, SE=0.0828, t=-7.1788, p=0) and day 4 (beta=0.416, SE=0.0844, t= 4.9320, p=0) in comparison to reference level (day 1), and these effects were modulated by cue. See table 3.1 for detailed OB gamma GLS results. These inform us that day 3 OB gamma power is lower than day 1, but this modulation differs by cue group. On day 4 OB gamma power is higher than day 1, and this modulation differs by cue group. We also found a significant interaction on day2:cue, meaning

cue modulates day 2 OB gamma power differently compared to day 1. Different cue conditions have different changes in OB gamma power on day 2. There were also significant effects of events: pre sampling, sampling, post odor off. The interaction between the event interval of post odor off and cue is also significant. We also found a significant effect on learning phase.

Table 3.1 GLS result on OB gamma power including all non-overlapping event intervals

Variable	**beta**	**SE**	**t**	**p**	
odor stimulus type	-0.0149	0.1003	-0.1489	0.8816	
cue1	0.1937	0.3194	0.6063	0.5444	
day2	0.1709	0.0929	1.8407	0.0658	
day3	-0.5813	0.0820	-7.0915	0.0000	***
day4	0.4127	0.0835	4.9401	0.0000	***
sampling	0.1931	0.0615	3.1403	0.0017	**
post odor off	0.1361	0.0615	2.2128	0.0270	*
pre light	-0.0053	0.0615	-0.0855	0.9319	
pre sampling	-0.2088	0.0615	-3.3949	0.0007	***
sex2	-0.4993	0.3024	-1.6511	0.0989	
learningph2	-0.7467	0.3024	-2.4691	0.0136	*
blockid2	0.0007	0.0554	0.0121	0.9904	
blockid3	-0.0038	0.0519	-0.0737	0.9412	
blockid4	0.0014	0.0558	0.0249	0.9802	
blockid5	-0.0670	0.0522	-1.2825	0.1998	
blockid6	-0.0301	0.0558	-0.5399	0.5894	
blockid7	-0.0610	0.0560	-1.0891	0.2763	
blockid8	0.0029	0.0672	0.0432	0.9655	
odor stimulus type:cue1	0.0191	0.1316	0.1449	0.8848	
cue1:day2	-0.3939	0.1303	-3.0218	0.0026	**
cue1:day3	0.5539	0.1130	4.9027	0.0000	***
Table 3.1 continued					
cue1:day4	-1.4598	0.1131	-12.9014	0.0000	***
odor stimulus type:day2	0.0007	0.1350	0.0054	0.9957	
odor stimulus type:day3	0.0604	0.1199	0.5037	0.6145	
odor stimulus type:day4	0.0297	0.1219	0.2433	0.8078	
cue1:sampling	-0.0353	0.0865	-0.4082	0.6832	
cue1:post odor off	-0.2122	0.0865	-2.4537	0.0142	*
cue1:pre light	0.0158	0.0865	0.1829	0.8549	
cue1:pre sampling	0.1175	0.0865	1.3589	0.1744	
odor stimulus type:cue1:day2	-0.1122	0.1894	-0.5920	0.5539	
odor stimulus type:cue1:day3	0.1424	0.1635	0.8712	0.3838	
odor stimulus type:cue1:day4	-0.0152	0.1617	-0.0938	0.9252	

Moreover, all interactions between cue and day are significant. These results show that there is a complex dynamic of gamma power change in the OB across a trial, by test day, and by event intervals. Cue condition adds another layer to these effects. To look at what these significant interactions mean for different event intervals, on different days in different cue groups, we performed multiple comparison tests on the level of interactions among these factors.

We know from previous studies that during sampling, OB gamma power is elevated in fine discrimination compared to coarse discrimination. Motivated by this phenomenon, we are testing the effect of cognitive load on OB gamma. Interestingly, we did not find any significant effect of odor stimulus type (coarse vs fine), including interaction terms in the GLS model. It's possible that group dynamics of different levels for coarse and fine subgroups are more complicated, resulting in a null main odor stimulus effect when we use a model like the GLS looking at marginal effect, which means effects are averaged by subgroups. The following analysis on OB gamma power combines both coarse and fine trials. This remains true for the GLS model on data during odor sampling alone.

During sampling

Because gamma is elevated during early odor sampling (Frederick et al., 2016), we dive into the OB gamma analysis on the sampling duration. We performed a GLS on OB gamma power during sampling, and odor stimulus type, cue condition, sex, learning phase, block number and the three-way interaction between odor stimulus type, cue and day (sublevels inclusive). See table 3.2 for detailed GLS result.

From the GLS analysis, we found a significant day effect for interleaved test days, day 3 has lower OB gamma during sampling than day 1 during sampling($p=0.0026$); day 4 has higher OB gamma during sampling than day 1 ($p=0.0071$). These are also modulated by cue

(day3*cue: p=0.0448, day4*cue: p=0). Further multiple comparison tests revealed (see table 3.3 for multiple comparison results) that on day 3, or first day of interleaved testing, cue difference in OB gamma power didn't survive, but the trend is that non-informative OB gamma power is lower than informative. On day 4, non-informative OB gamma power is significantly higher than informative (Fig. 3.5a).

Table 3.2 OB gamma power during sampling GLS result

Variable	**beta**	**SE**	**t**	**p**	
odor stimulus type	0.0715	0.2136	0.3349	0.7379	
cue1	0.2234	0.4336	0.5152	0.6068	
day2	0.1958	0.1977	0.9906	0.3226	
day3	-0.5291	0.1745	-3.0321	0.0026	**
day4	0.4815	0.1779	2.7074	0.0071	**
sex2	-0.6995	0.3918	-1.7854	0.0751	
learningph2	-0.8726	0.3918	-2.2274	0.0266	*
blockid2	0.0067	0.1179	0.0571	0.9545	
blockid3	-0.0287	0.1105	-0.2598	0.7952	
blockid4	-0.0432	0.1187	-0.3638	0.7163	
blockid5	-0.0186	0.1111	-0.1671	0.8674	
blockid6	-0.0270	0.1187	-0.2273	0.8203	
blockid7	0.0075	0.1192	0.0628	0.9499	
blockid8	0.0755	0.1430	0.5279	0.5979	
odor stimulus type:cue1	0.0430	0.2801	0.1537	0.8780	
cue1:day2	-0.4576	0.2775	-1.6493	0.1001	
cue1:day3	0.4844	0.2405	2.0142	0.0448	*
cue1:day4	-1.5506	0.2409	-6.4376	0.0000	***
odor stimulus type:day2	0.0307	0.2875	0.1068	0.9150	
odor stimulus type:day3	0.0482	0.2552	0.1888	0.8504	
odor stimulus type:day4	-0.0159	0.2595	-0.0614	0.9511	
odor stimulus type:cue1:day2	-0.1118	0.4033	-0.2773	0.7817	
odor stimulus type:cue1:day3	0.1301	0.3480	0.3738	0.7088	
odor stimulus type:cue1:day4	-0.0296	0.3442	-0.0860	0.9315	

We also found that the OB gamma power for the non-informative group differs by days in a different way from the informative group. For the non-informative group, on days 1 and 2, OB gamma power was not significantly different, but on the remaining days (except for days 2-4), comparisons on OB gamma power were all significantly different. For the informative group,

days 1-2 and day 1-3 were not significantly different, but the rest of the days OB gamma power comparisons were all significantly different (see Fig. 3.5b).

Table 3.3 Multiple comparison results on OB gamma power during sampling

Contrast	Estimate	SE	df	t.ratio	p.value	
Day 1: cue0 - cue1	-0.245	0.412	5.80	-0.594	0.5746	
Day 2: cue0 - cue1	0.269	0.414	5.90	0.650	0.5405	
Day 3: cue0 - cue1	-0.794	0.401	5.21	-1.981	0.1021	
Day 4: cue0 - cue1	1.321	0.400	5.18	3.299	0.0204	*
Cue 0: day1 - day2	-0.2112	0.144	318	-1.469	0.8566	
Cue 0: day1 - day3	0.5050	0.123	318	4.120	0.0003	***
Cue 0: day1 - day4	-0.4736	0.125	318	-3.794	0.0011	**
Cue 0: day2 - day3	0.7162	0.124	318	5.763	<0.0001	***
Cue 0: day2 - day4	-0.2624	0.126	318	-2.075	0.2326	
Cue 0: day3 - day4	-0.9786	0.102	318	-9.608	<0.0001	***
Cue 1: day1 - day2	0.3024	0.142	318	2.134	0.2016	
Cue 1: day1 - day3	-0.0444	0.124	318	-0.359	1.0000	
Cue 1: day1 - day4	1.0918	0.119	318	9.208	<0.0001	***
Cue 1: day2 - day3	-0.3468	0.128	318	-2.714	0.0421	*
Cue 1: day2 - day4	0.7895	0.123	318	6.394	<0.0001	***
Cue 1: day3 - day4	1.1363	0.102	318	11.121	<0.0001	***

a

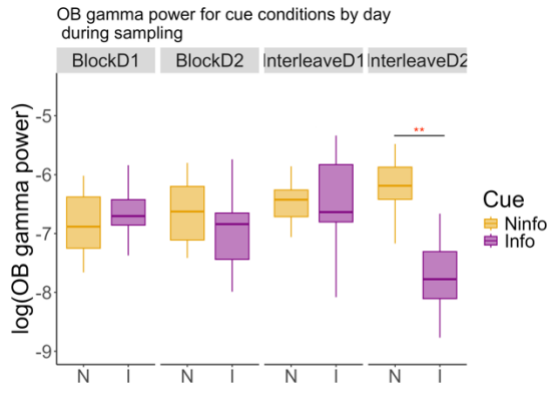

b

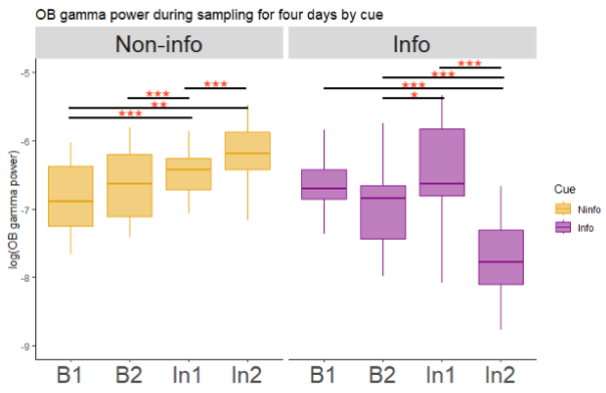

Figure 3.5 OB gamma power during sampling
OB gamma power during sampling plotted two ways. a. for cue by day, cue differences are significant on day 3&4 (p=0.0488&0.0086) not day 1&2. b. for day by cue, day differences are marked.
*=p<0.05,**=p<0.01,***=p<0.001

The non-informative group increases OB gamma power day by day over the 4 days. The informative group OB gamma power during sampling drops on day 2 compared to day 1, then goes up on day 3 and eventually drops to a level that's lower than even day 2. Looking at the

difference between day 1 and day 2 OB gamma power, unlike the non-informative group, the informative group shows decreased OB gamma power on day 2 compared to day 1. These results show that during sampling, OB gamma oscillations differ by cue group, and the difference is modulated by testing day. Moreover, on each day, the informative group and non-informative group adapt differently.

OB gamma power during all event intervals of a trial

To look at how gamma power in the OB changes by test days, and what may cause it, we expanded the time period to look at all events of a trial. Since day: cue and event: cue interactions are significant, we looked at day differences by cue and event (see Fig. 3.6). Multiple comparison tests of the OB gamma level between informative and non-informative groups by day and event (see table 3.4) show that for days 1 and 2 (block tests), OB gamma power during all events is not significantly different in the two cue groups. On day 3, OB gamma power is significantly different in the cue groups during the pre-sampling period (informative > non-informative). On day 4, OB gamma power is significantly different through all trial events, from 1s before the light comes on till 0.4s after they withdraw their nose and go to the response. However, the direction between these differences changes from day 3 to day 4. Driven by OB gamma power increase in the non-informative group, and OB gamma power drop in the informative group, on day 4, OB gamma power for the non-informative group is higher than for the informative group. Examining all events shows that OB gamma power is modulated by cue condition beyond odor sampling. Furthermore, the differences in gamma power in the two cue conditions on interleaved test days are not just about odor sampling.

Table 3.4 Multiple comparison result for OB gamma power for cue by day and event

Day	Event	Contrast	Estimate	SE	df	t.ratio	p.value	
1	bsl	cue0 - cue1	-0.2032	0.313	3.70	-0.649	0.5543	
2	bsl	cue0 - cue1	0.2467	0.314	3.73	0.787	0.4784	
3	bsl	cue0 - cue1	-0.8284	0.310	3.56	-2.673	0.0630	
4	bsl	cue0 - cue1	1.2641	0.310	3.55	4.081	0.0192	*
1	sampling	cue0 - cue1	-0.1679	0.313	3.70	-0.536	0.6223	
2	sampling	cue0 - cue1	0.2820	0.314	3.73	0.899	0.4227	
3	sampling	cue0 - cue1	-0.7931	0.310	3.56	-2.559	0.0703	
4	sampling	cue0 - cue1	1.2994	0.310	3.55	4.195	0.0176	*
1	post odor off	cue0 - cue1	0.0090	0.313	3.70	0.029	0.9786	
2	post odor off	cue0 - cue1	0.4589	0.314	3.73	1.463	0.2222	
3	post odor off	cue0 - cue1	-0.6162	0.310	3.56	-1.988	0.1265	
4	post odor off	cue0 - cue1	1.4763	0.310	3.55	4.767	0.0119	*
1	pre light	cue0 - cue1	-0.2190	0.313	3.70	-0.700	0.5256	
2	pre light	cue0 - cue1	0.2309	0.314	3.73	0.736	0.5051	
3	pre light	cue0 - cue1	-0.8442	0.310	3.56	-2.724	0.0600	
4	pre light	cue0 - cue1	1.2483	0.310	3.55	4.030	0.0199	*
1	pre sampling	cue0 - cue1	-0.3208	0.313	3.70	-1.025	0.3678	
2	pre sampling	cue0 - cue1	0.1292	0.314	3.73	0.412	0.7029	
3	pre sampling	cue0 - cue1	-0.9459	0.310	3.56	-3.052	0.0443	*
4	pre sampling	cue0 - cue1	1.1466	0.310	3.55	3.702	0.0257	*

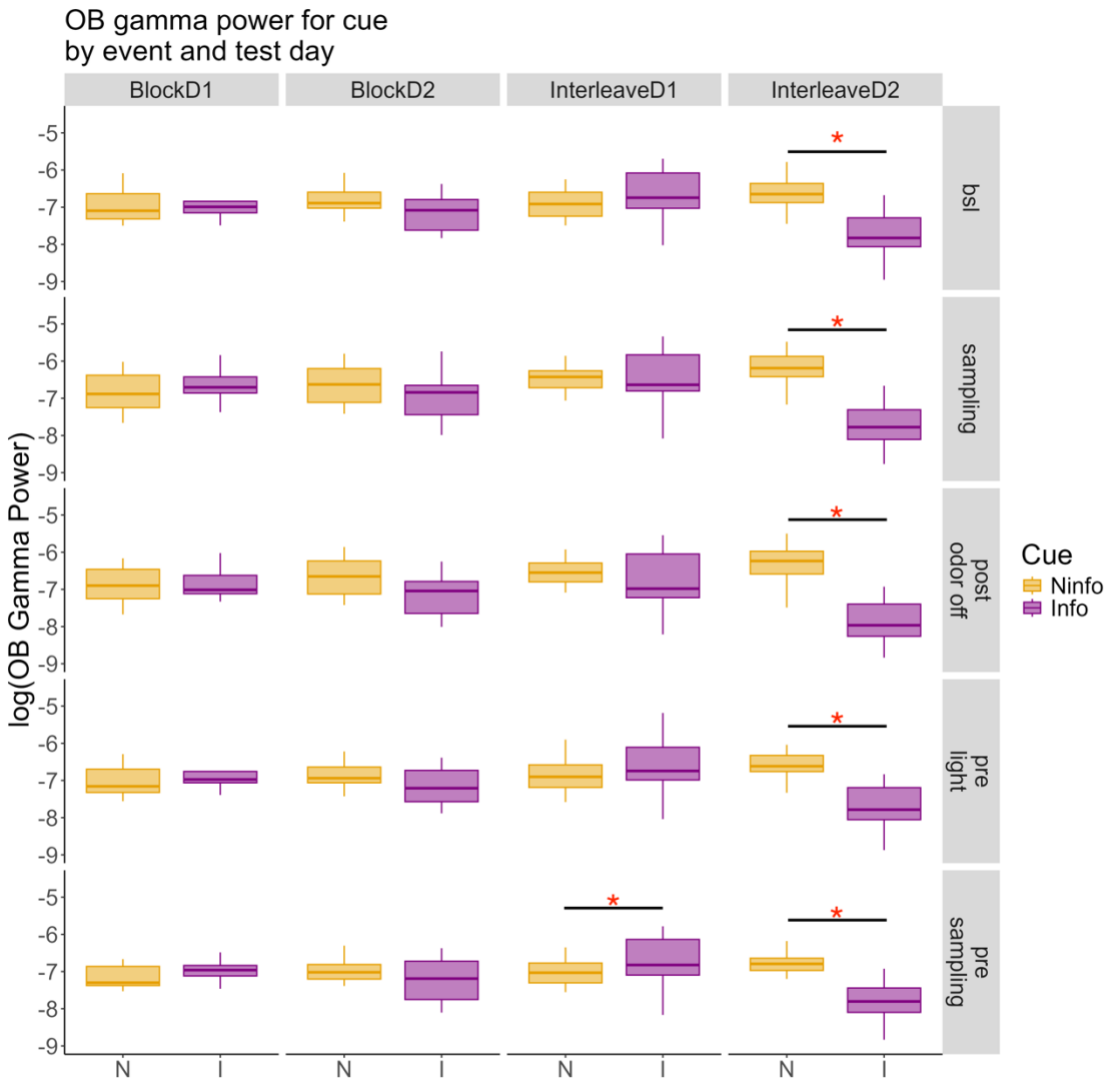

Figure 3.6 OB gamma power for cue by event and test day
Horizontal panels, test days. Vertical panels, events. Non-significant differences between cue conditions are not labeled. *=p<0.05,**=p<0.01,***=p<0.001 see table 3.5 for all p values

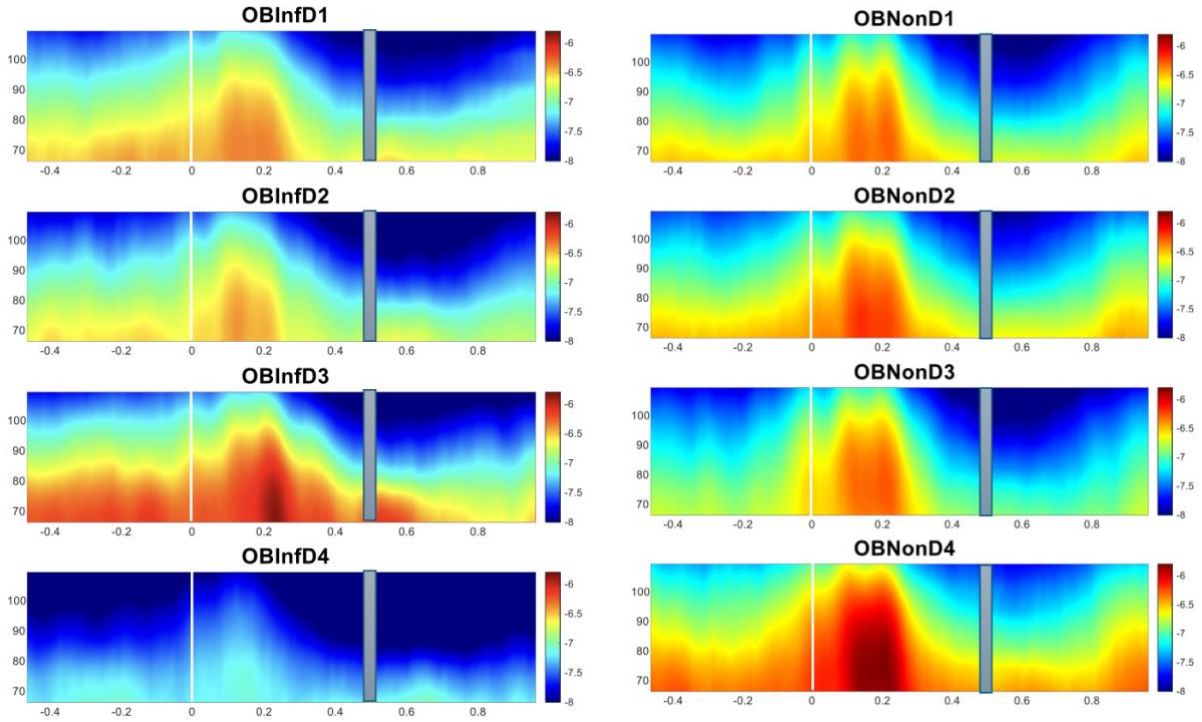

Figure 3.7 Spectrograms of OB gamma power by cue and test day
Spectrograms of OB power from 65-110 hz, -0.5s to 1s after start of sampling (t=0, white line). 90% CI of end of sampling marked by grey box.

OB Beta power

To further test our hypothesis, we examined beta band power in the OB to provide more information. Beta gives us a window into how top-down inputs and higher-order processes between structures might play out and influence the amount of gamma. Beta oscillations in the OB and surrounding areas have been associated with multiple-area communication. Moreover, we know that in the OB, the same circuit, the inhibitory feedback loop formed by mitral/tufted cells and granule cells, makes local gamma and beta oscillations(Osinski et al., 2018; Osinski & Kay, 2016). It has been previously observed that there is an interchange between dominating gamma and dominating beta(Frederick et al., 2016; Kay & Beshel, 2010), defined by task specifics. In the OB, beta power is higher during later periods of sampling and after rats

respond(Frederick et al., 2016; Martin et al., 2006; Martin & Ravel, 2014). Beta elevation is also associated with odorant volatility, motor effects, and associative learning(Aylwin et al., 2009; Hermer-Vazquez et al., 2007; Lowry & Kay, 2007; Martin et al., 2007; Ravel et al., 2003).

To examine OB beta power, we performed a similar GLS accounting for random effects of rats, including all events of interest throughout the trial. Independent variables we included were different than those of OB gamma power GLS model. Besides the interaction between cue condition and event, we included the interaction between odor stimulus type and event. Including the latter interaction term significantly improved model prediction ($p<0.001$) in a likelihood ratio test.

We found significant main effects in day 3 (p=0, t=-9.4234, beta=-0.7573, SE=0.0803), odor sampling event (p=,0.0001 t=3.8590, beta=0.3099, SE=0.0803), after odor off event (p=0, t=4.0686, beta=0.3267, SE=0.0803), sex (p=0.0001, t=-3.9862, beta=-0.6987, SE=0.1753), block 4 (p=0.0091, t=2.6123, beta=0.1428, SE=0.0547), and significant interactions of cue:day2 (p=0.0167, t=-2.3945, beta=-0.306, SE=0.1278), cue:day3 (p=0, t=6.6854, beta=0.7405, SE=0.1108), cue:day4 (p=0, t=-7.9459, beta=-0.8814, SE=0.1109), cue:event sampling (p=0.0447, t=2.0083, beta=0.1865, SE=0.0929), cue:event post odor off (p=0, t=4.3718, beta=0.4061, SE=0.0929). The interactions between odor stimulus type and two events are also significant: odor stimulus type and odor sampling (p=0.0010, t=-3.3072, beta=-0.3073, SE=0.0929), odor stimulus type and post odor off event (p=0.0007, t=-3.3845, beta=-0.3145, SE=0.0929). These differences we see in the OB beta power support the idea that cue condition modulates beta changes in the OB. OB beta power also differs by event, and this difference is modulated by odor stimulus type. We also found a robust sex difference in OB beta power. It's unclear what the effect of block 4 is driven by; we'll investigate this later in block-wise analysis.

To dive into how beta power in the OB changes by testing day in a cue modulated manner, we performed multiple comparison tests on beta power on each day by cue condition and event. We found that on day 3, OB beta power differs by cue during the pre-sampling period (p=0.0443). On day 4, OB beta power differs by cue during all events (see table 3.5 for multiple comparison results and figure 3.8 for the values over days and groups). Also, for the non-informative group, days 1 and 2 do not have significantly different beta power in the OB, but days 1-3 (p <.0001), days 2-3 (p<.0001), and days 3-4 (p<.0001) have significantly different beta power in the OB. For the informative group, day 1-2 (p <.0001), day 2-3 (p <.0001), day 3-4 (p<.0001), day 2-4 (p <.0001) and day 1-4 (p <.0001) are all significantly different.

Table 3.5 OB beta power multiple comparison result

Day	Event	Contrast	Estimate	SE	df	t.ratio	p.value	
1	bsl	cue0 - cue1	-0.2032	0.313	3.70	-0.649	0.5543	
2	bsl	cue0 - cue1	0.2467	0.314	3.73	0.787	0.4784	
3	bsl	cue0 - cue1	-0.8284	0.310	3.56	-2.673	0.0630	
4	bsl	cue0 - cue1	1.2641	0.310	3.55	4.081	0.0192	*
1	sampling	cue0 - cue1	-0.1679	0.313	3.70	-0.536	0.6223	
2	sampling	cue0 - cue1	0.2820	0.314	3.73	0.899	0.4227	
3	sampling	cue0 - cue1	-0.7931	0.310	3.56	-2.559	0.0703	
4	sampling	cue0 - cue1	1.2994	0.310	3.55	4.195	0.0176	*
1	post odor off	cue0 - cue1	0.0090	0.313	3.70	0.029	0.9786	
2	post odor off	cue0 - cue1	0.4589	0.314	3.73	1.463	0.2222	
3	post odor off	cue0 - cue1	-0.6162	0.310	3.56	-1.988	0.1265	
4	post odor off	cue0 - cue1	1.4763	0.310	3.55	4.767	0.0119	*
1	pre light	cue0 - cue1	-0.2190	0.313	3.70	-0.700	0.5256	
2	pre light	cue0 - cue1	0.2309	0.314	3.73	0.736	0.5051	
3	pre light	cue0 - cue1	-0.8442	0.310	3.56	-2.724	0.0600	
4	pre light	cue0 - cue1	1.2483	0.310	3.55	4.030	0.0199	*
1	pre sampling	cue0 - cue1	-0.3208	0.313	3.70	-1.025	0.3678	
2	pre sampling	cue0 - cue1	0.1292	0.314	3.73	0.412	0.7029	
3	pre sampling	cue0 - cue1	-0.9459	0.310	3.56	-3.052	0.0443	*
4	pre sampling	cue0 - cue1	1.1466	0.310	3.55	3.702	0.0257	*

For the non-informative group, OB beta power differences across days are driven by lower beta on day 3. For informative group, OB beta power differences follow a similar pattern to the of OB gamma power. This is contrary to our expectations since in previous studies we see high beta and high gamma powers in the OB alternate during a trial. Informative group have similar but not opposite OB power dynamics in the beta and gamma bands.

a

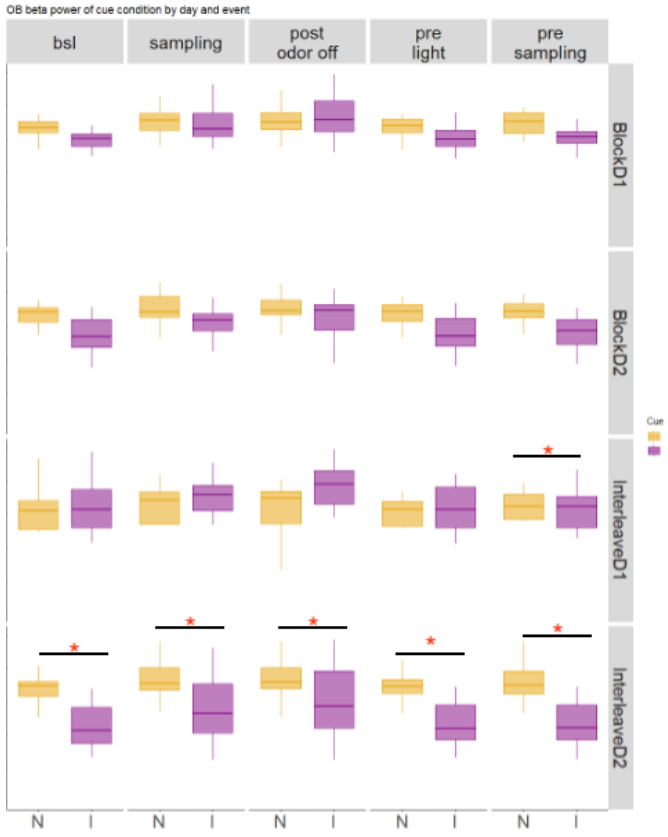

b

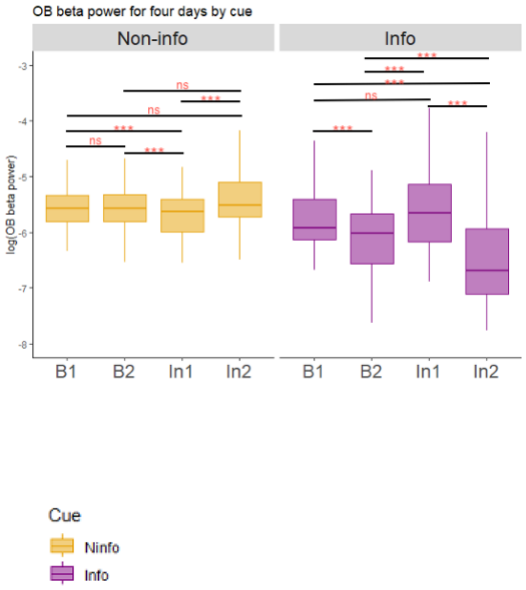

Figure 3.8 OB beta power multiple comparison panels
a. for cue by event and test day. b. for day by cue

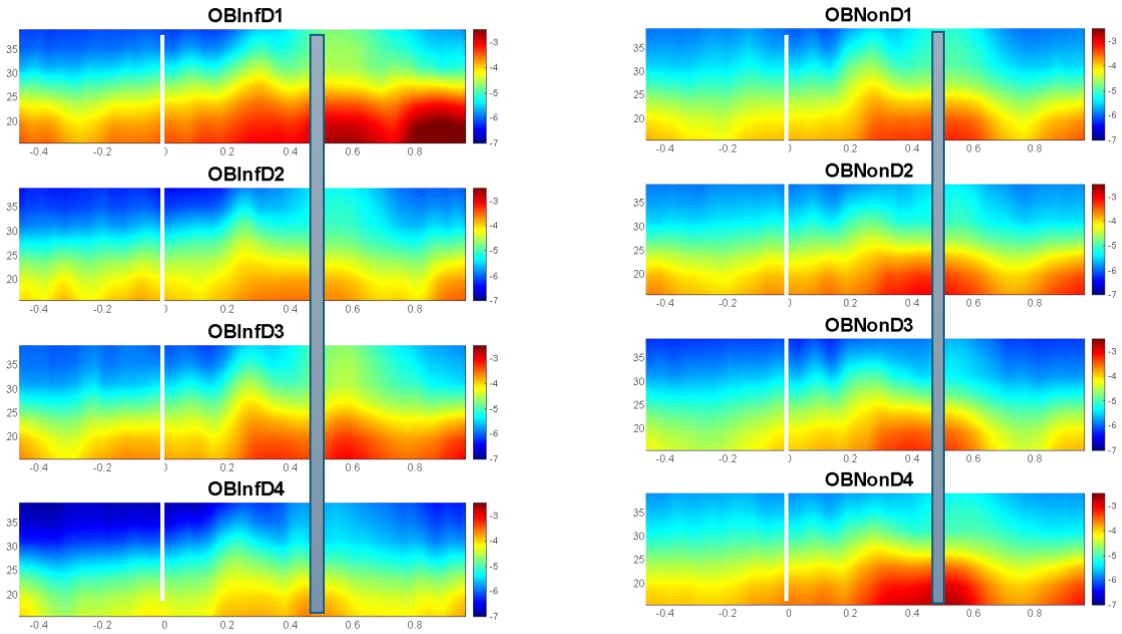

Figure 3.9 spectrograms of OB beta power for cue conditions by test day
Spectrograms of OB power from 15-40 hz, -0.5s to 1s after start of sampling (t=0, white line). 90% CI of end of sampling marked by grey box.

It has been observed that OB beta power increases during later sampling time (but varies by odor stimulus, Frederick et al., 2016) and as rats withdraw their noses and proceed to a response port. Here we see changes in OB beta power compared to a baseline period before the light was on during odor sampling, and even right after the light cue is illuminated. Moreover, odor stimulus type modulates OB beta power. Beta power in the OB is lower during fine discrimination trials compared to coarse discrimination trials, starting when the light cue comes on, and lasting until 400ms after the odor is off (Fig. 3.10).

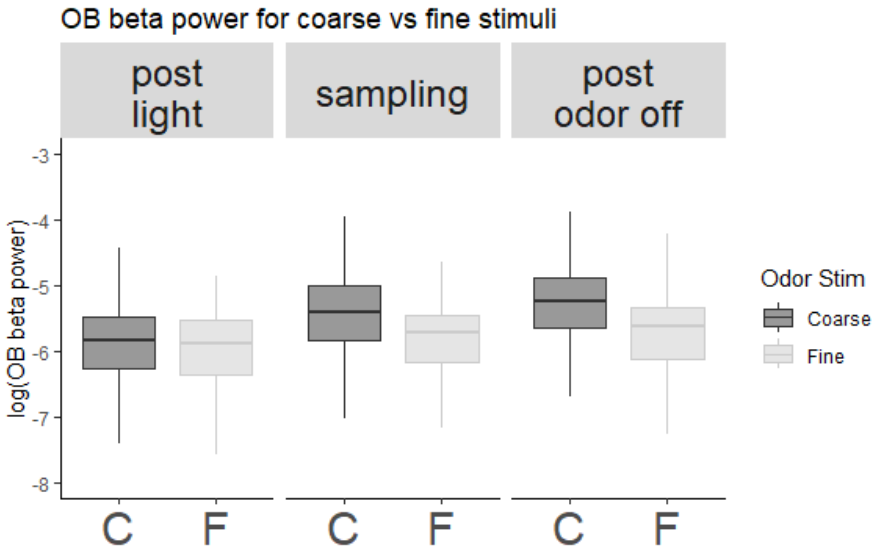

Figure 3.10 OB beta power for odor stimulus type by events
OB beta power is lower for fine trials compare to coarse trials, during post light ($p=0.0368$), sampling ($p<0.001$) and post odor off periods ($p<0.001$).

As we expected, cue condition has an overall effect on beta oscillations in the OB. On day 3 during sampling, the non-informative group had lower beta power in the OB compared to the informative group. On day 4, the non-informative group has higher gamma and higher beta power in the OB during pre-sampling compared to the informative group. The direction of OB beta power for the pre-sampling on day 3 for the non-informative group is the opposite of that of day 4 (Fig. 3.8a).

In summary, analysis of task behaviors enabled us to look at behavioral dynamics by the blocks within a session and across four testing days. Rats sample shorter and reach higher accuracy for both the informative and non-informative groups over the course of a session. Throughout a session, both informative and non-informative rats adapt their sampling strategies and perform at different accuracy levels across the 8 blocks. Accuracy for blocks 2-5 was higher than block 1, while sampling duration for blocks 3-8 was shorter than blocks 1 and 2.

The informative cue group samples longer than the non-informative group for the 4-odor task we designed based on TAC. There is also a main effect of odor stimulus type on accuracy. Rats are more accurate for coarse trials than for fine trials. Both these effects are marginal effects without significant interactions.

Analysis of OB gamma and beta power allowed us to investigate our hypothesis that task demand interacts with olfactory sensory stimulus type in modulating gamma oscillations in the OB. We found supporting evidence that shows OB gamma and beta power are both modulated by cue conditions. Contrary to what we expected, that OB gamma dynamics would be opposite to beta dynamics, we found that OB beta and gamma increase and decrease in a similar fashion on four test days but modulated by cue condition. The non-informative group increased beta and gamma power by day, while the informative group decreased beta and gamma power on day 2 compared to day 1 but increased beta and gamma power on day 3. For the gamma band, this increase in power is significant, while for the beta band, it is a trend. The informative group also drops gamma power significantly on day 4. The differences on block test days are less pronounced than the differences on interleaved days. We expected that the presumably harder interleaved test, compared to the block test, due to its low predictability, would cause more differences in OB power. We continue the same inquiry line by looking at coherence results within the olfactory and limbic systems we recorded on.

Chapter 4: Network coherence in a task with multiple levels of cognitive demands

The previous chapter described the change in behavioral variables and OB gamma power consistent with the hypothesis that cognitive load interacts with odor similarity to drive the increase in gamma oscillation power seen during fine odor discrimination. To further investigate how the dynamics of gamma oscillations in the OB are modulated, in this chapter, we report results on the network coherence between OB, PC, DG, and CA1 across theta, beta, gamma, and gamma 2 bands. Respiratory (theta) band coherence between the thermocouple probe and these areas is also reported. Results in each section generally contain two parts: coherence comparisons were modeled first by a GLS model for each band, and second is the presentation of multiple comparisons on significant or hypothesis-addressing levels.

OB-PC Coherence

We examined OB-PC coherence in theta/respiratory (3-12 Hz), beta (15-35 Hz), gamma (65-110 Hz), and gamma 2 (40-55 Hz) bands, and found cue-modulated effects in all bands.
GLS model results: For beta band coherence in OB and PC, we found a significant effect of odor stimulus type or coarse vs. fine odors (beta= -0.0593, SE=0.0162, t=-3.6536, p=0.0003), event of after odor off (p=1.9254e-07, t=5.2219, beta=0.1497, SE= 0.1497), and cue modulated beta change for after odor off (pre odor off:cue, beta=0.1217, SE=0.0166, t=7.3470, p=0; post odor off:cue, beta=0.1569, SE=0.0167, t=9.469793, p=0). Beta coherence in OB-PC is significantly higher for stimuli that belong to the coarse odor pair than for those that belong to the fine odor pair (Fig.4.1). Beta coherence in OB-PC during the 400ms after odor off is higher than a pretrial

baseline period (500ms starting 1s before light on) but differs by cue condition. We start to see this cue-modulated effect in OB-PC beta coherence starting 400ms before odor off or as the rat leaves the odor port, consistent with previous work (Frederick et al., 2016).

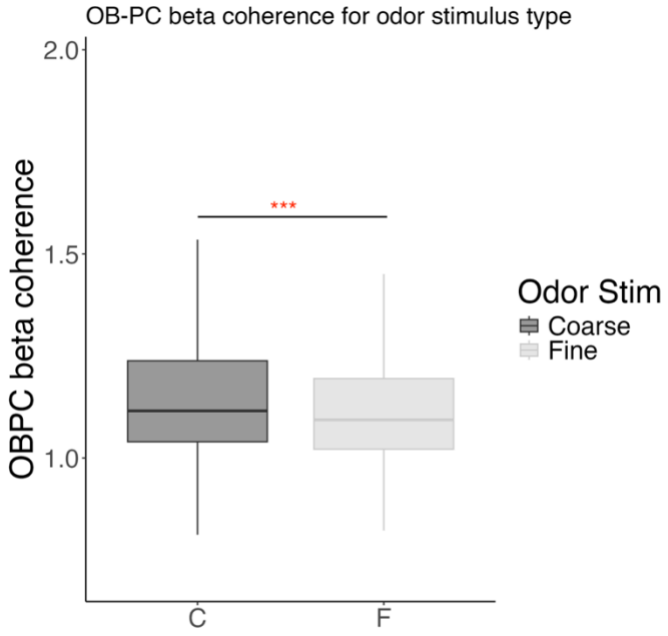

Figure 4.1 OB-PC beta coherence by odor stimulus type
Middle box line represents median, top of box is the 3rd quartile, bottom of the box is the 1st quartile. p<0.05=*, p<0.01=**, p<0.001=***

Multiple comparison tests with p values adjusted for Bonferroni correction found overall coherence difference in the beta band for all test days between the two cue conditions, although the onset and offset of when OB-PC beta coherence starts to differ during the behavioral trial vary by day. Starting with odor sampling until 400ms after response, OB-PC beta coherence differs between informative and non-informative groups (see Fig. 4.2, table 4.1 for p values). The informative group shows higher OB-PC beta coherence overall (see figure 4.5 for spectrogram).

Table 4.1 Multiple comparison results on OBPC beta coherence							
day	event	beta	SE	df	t.ratio	p.value	
1	Pre light bsl	-0.0671317	0.04871799	2362	-1.3779644	0.16834479	
2	Pre light bsl	-0.0923906	0.04928809	2362	-1.8745015	0.06098466	
3	Pre light bsl	-0.1044656	0.04479098	2362	-2.3322917	0.01976897	*
4	Pre light bsl	-0.0930492	0.0445554	2362	-2.0883933	0.03686922	*
1	Post light	-0.0713327	0.04871799	2362	-1.4641972	0.14327313	
2	Post light	-0.0477286	0.04928809	2362	-0.9683598	0.33296387	
3	Post light	-0.1170208	0.04479098	2362	-2.612598	0.00904266	**
4	Post light	-0.0887773	0.0445554	2362	-1.9925159	0.04642939	*
1	Post sampling	-0.1064847	0.04871799	2362	-2.1857362	0.02893279	*
2	Post sampling	-0.1507472	0.04928809	2362	-3.0584914	0.00224951	**
3	Post sampling	-0.1649758	0.04479098	2362	-3.6832366	0.00023546	***
4	Post sampling	-0.1446393	0.0445554	2362	-3.2462801	0.00118559	**
1	Post odor off	-0.2228214	0.04871799	2362	-4.5736986	5.04E-06	***
2	Post odor off	-0.2267085	0.04928809	2362	-4.5996604	4.46E-06	***
3	Post odor off	-0.3218801	0.04479098	2362	-7.1862692	8.89E-13	***
4	Post odor off	-0.2079972	0.0445554	2362	-4.6682818	3.21E-06	***
1	Pre light	-0.1099916	0.04871799	2362	-2.2577195	0.0240541	*
2	Pre light	-0.0882941	0.04928809	2362	-1.7913884	0.07335897	
3	Pre light	-0.1482959	0.04479098	2362	-3.310843	0.00094415	***
4	Pre light	-0.046916	0.0445554	2362	-1.0529816	0.29245714	
1	Pre sampling	-0.0865781	0.04871799	2362	-1.7771278	0.07567587	
2	Pre sampling	-0.095123	0.04928809	2362	-1.9299395	0.05373395	
3	Pre sampling	-0.1081969	0.04479098	2362	-2.4155955	0.01578495	*
4	Pre sampling	-0.0440818	0.0445554	2362	-0.9893704	0.32258331	
1	Pre response	-0.1890408	0.04871799	2362	-3.8803069	0.00010718	***
2	Pre response	-0.2058269	0.04928809	2362	-4.1759961	3.07E-05	***
3	Pre response	-0.2638857	0.04479098	2362	-5.8914909	4.37E-09	***
4	Pre response	-0.1849648	0.0445554	2362	-4.1513449	3.42E-05	***
P values are Bonferroni corrected. p<0.05=*, p<0.01=**, p<0.001=***							

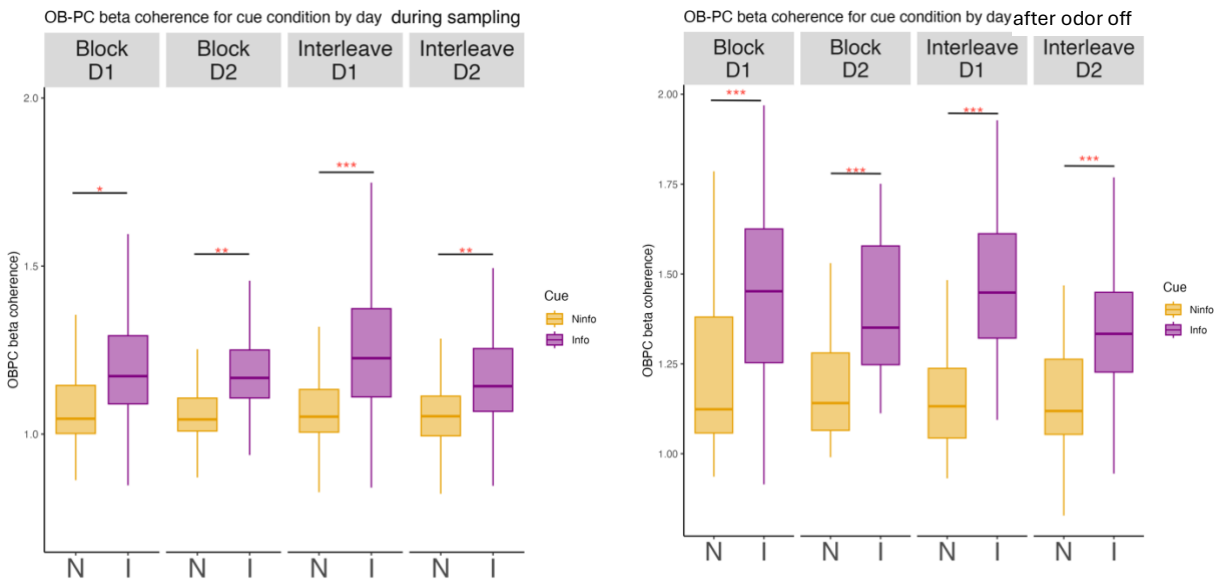

Figure 4.2 OB beta coherence for cue conditions during sampling and after odor off by days
a OB-PC beta coherence for cue condition by day during sampling event period. b OB-PC beta coherence for cue condition by day during the after odor off event period. Middle box line represents medial, top of box is the 3rd quartile, bottom of the box is the 1st quartile. p<0.05=*, p<0.01=**, p<0.001=***

We also found variation over days in OB-PC beta coherence after multiple comparison tests. On day 4, both informative and non-informative rats have a lower beta band OB-PC coherence during the after-response time window compared to day 1. For the rest of the events, only the informative rats vary OB-PC beta coherence by day. During odor sampling, informative rats have different OB-PC beta coherence on days 3 and 4 (day 3> day 4, p= 0.03434, t= 2.781, beta= 0.0555, SE= 0.0199). Non-informative rats do not vary by day during odor sampling. The informative rats show OB-PC beta coherence during other parts of the behavior that varies by day: pre-light period differences day1-4,2-3,3-4; pre-response period day 1-3,2-3,3-4; and pre-sampling period day 3-4, but there are no significant day differences for the informative group between day 1 and day 2. See figure 4.3.

a

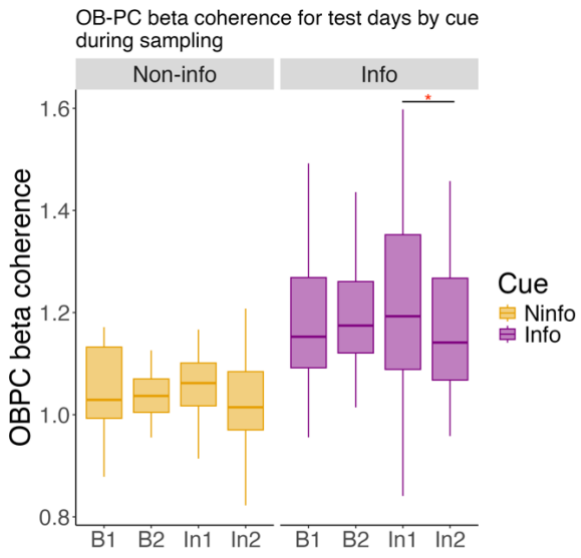

b

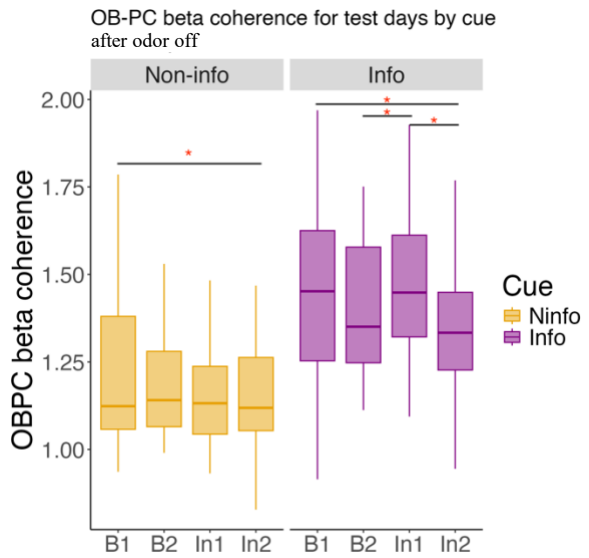

c

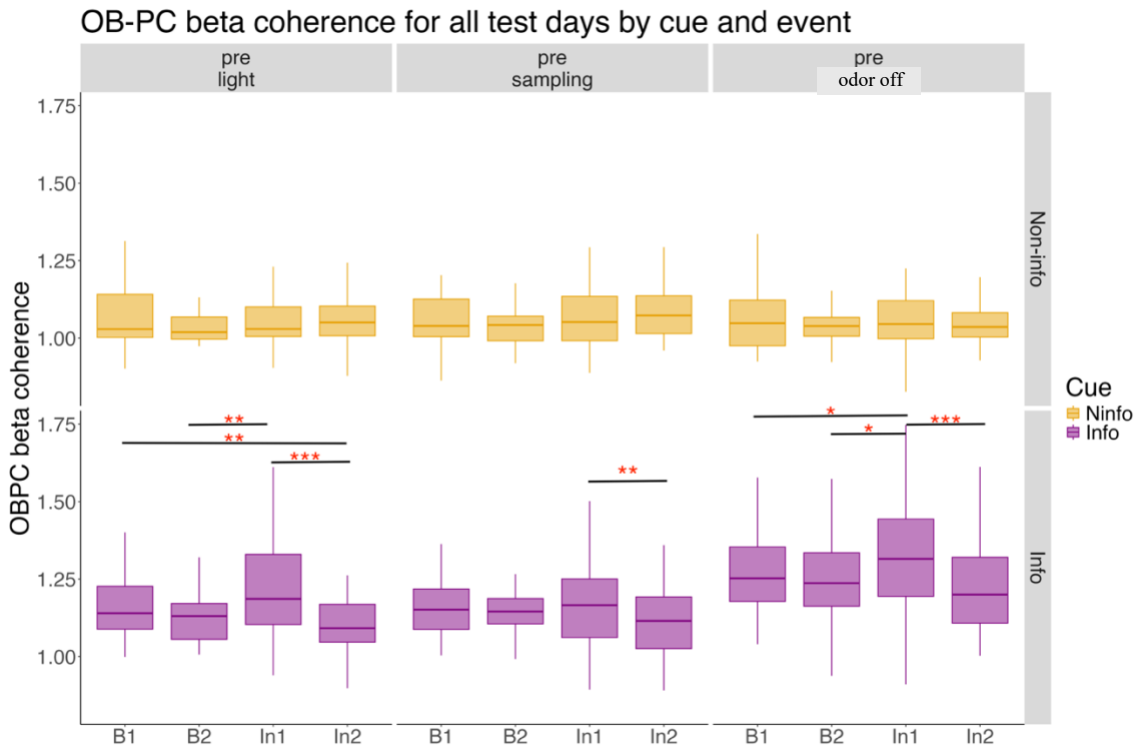

Figure 4.3 OB-PC beta coherence for days by cue for sampling and after odor off periods
a. during sampling b. after odor off c. pre light, pre sampling, pre odor off (late sampling) periods. Middle box line represents median, top of box is the 3rd quartile, bottom of the box is the 1st quartile. $p<0.05$=*, $p<0.01$=**, $p<0.001$=*** Unlabeled between day comparisons are non-significant.

For gamma band OB-PC coherence, the GLS model accounting for rat correlation structure found significant effects for sex (beta=-0.085, SE=0.0383, t=-2.2183, p=0.0266) and an interaction between cue (informative/non-informative) and the period after odor off (p=0.0375, t=2.081163, beta=0.0384, SE=0.0185). OB-PC gamma coherence for male rats is significantly higher than for female rats (see Fig. 4.4a). The cue type modulates OB-PC gamma coherence after odor off (see Fig. 4.4b).

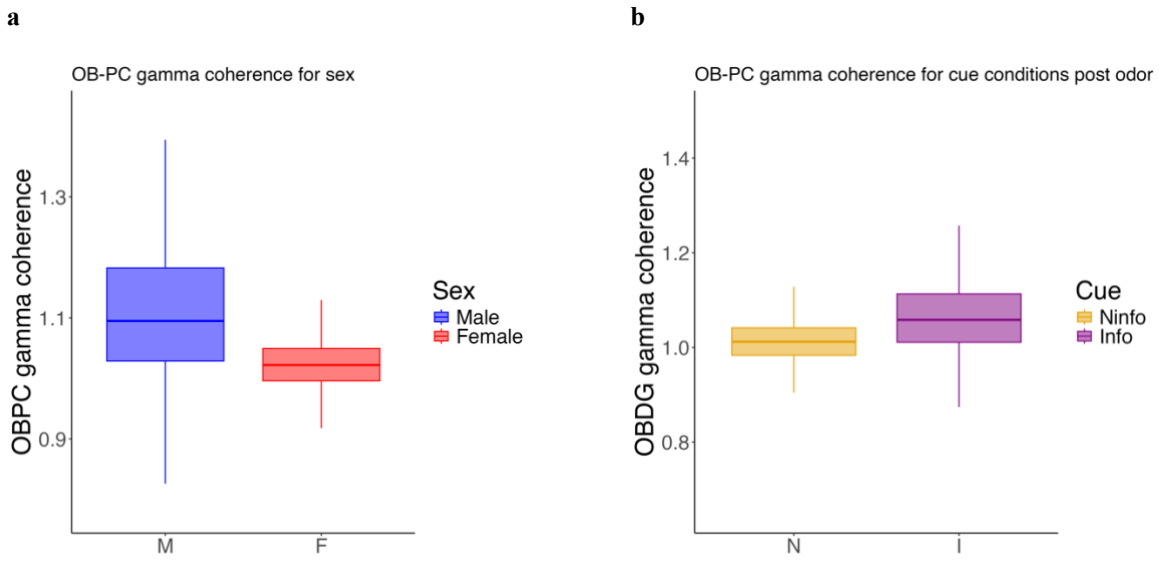

Figure 4.4 OB-PC gamma coherence for sex effect and cue modulation on post odor off
a. OB-PC gamma coherence for male is higher than female p=0.026 b. OB-PC gamma coherence is higher for informative group during post odor off period p=0.0375

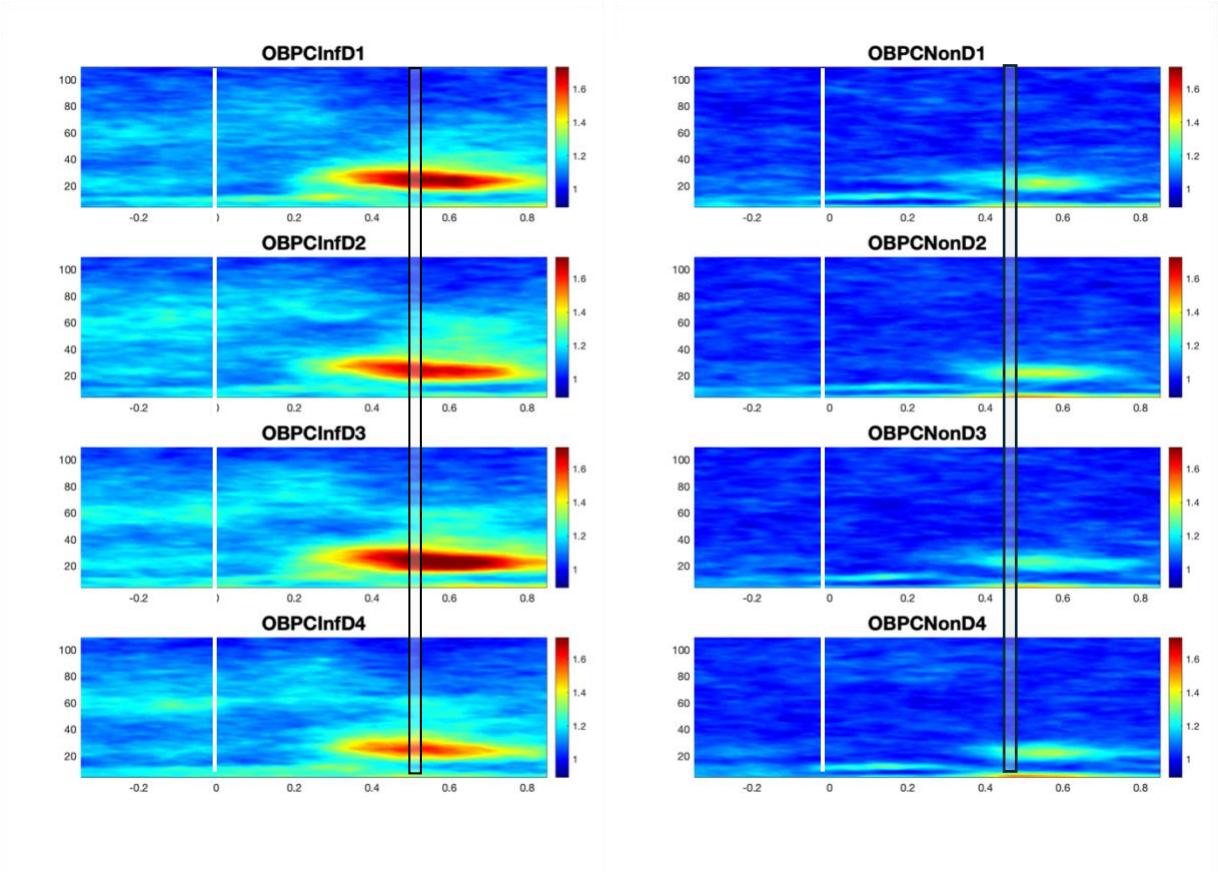

Figure 4.5 Coherence spectrograms for informative and non-informative groups on all test days
-0.5s to 1s after start of sampling (t=0, white line). 90% CI of end of sampling marked by grey box.

Interestingly for gamma2 band OB-PC coherence, we see persistent cue modulating effects. The interactions between cue, day and event are significant. Gamma2 OB-PC coherence changes by day and event, and this effect is modulated by cue. Follow-up multiple comparison tests show a large range of significant effects after strict Bonferroni correction. See table 4.2 for the multiple comparisons result on cue by day and event.

Table 4.2 OB-PC gamma 2 multiple comparison result, on cue by day and event

day	event	contrast	beta	SE	t.ratio	p.value	
1	Pre light bsl	cue0 - cue1	-0.0935	0.0498	-1.8776	0.0606	
2	Pre light bsl	cue0 - cue1	-0.1394	0.0501	-2.7807	0.0055	**
3	Pre light bsl	cue0 - cue1	-0.1435	0.0474	-3.0289	0.0025	**
4	Pre light bsl	cue0 - cue1	-0.1382	0.0472	-2.9253	0.0035	**
1	Post light	cue0 - cue1	-0.1354	0.0498	-2.7191	0.0066	**
2	Post light	cue0 - cue1	-0.1252	0.0501	-2.4961	0.0126	*
3	Post light	cue0 - cue1	-0.1385	0.0474	-2.9241	0.0035	**
4	Post light	cue0 - cue1	-0.1161	0.0472	-2.4587	0.0140	*
1	Sampling	cue0 - cue1	-0.1210	0.0498	-2.4297	0.0152	*
2	Sampling	cue0 - cue1	-0.1006	0.0501	-2.0063	0.0449	*
3	Sampling	cue0 - cue1	-0.1127	0.0474	-2.3794	0.0174	*
4	Sampling	cue0 - cue1	-0.0958	0.0472	-2.0293	0.0425	*
1	Post odor off	cue0 - cue1	-0.1709	0.0498	-3.4327	0.0006	***
2	Post odor off	cue0 - cue1	-0.1973	0.0501	-3.9339	0.0001	***
3	Post odor off	cue0 - cue1	-0.2327	0.0474	-4.9126	0.0000	***
4	Post odor off	cue0 - cue1	-0.1642	0.0472	-3.4774	0.0005	***
1	Pre light	cue0 - cue1	-0.1534	0.0498	-3.0808	0.0021	**
2	Pre light	cue0 - cue1	-0.1453	0.0501	-2.8977	0.0038	**
3	Pre light	cue0 - cue1	-0.1573	0.0474	-3.3201	0.0009	***
4	Pre light	cue0 - cue1	-0.1097	0.0472	-2.3230	0.0203	**
1	Pre sampling	cue0 - cue1	-0.1372	0.0498	-2.7564	0.0059	**
2	Pre sampling	cue0 - cue1	-0.1482	0.0501	-2.9544	0.0032	**
3	Pre sampling	cue0 - cue1	-0.1379	0.0474	-2.9106	0.0036	**
4	Pre sampling	cue0 - cue1	-0.0918	0.0472	-1.9432	0.0521	
1	Pre response	cue0 - cue1	-0.1711	0.0498	-3.4360	0.0006	***
2	Pre response	cue0 - cue1	-0.0971	0.0501	-1.9366	0.0529	
3	Pre response	cue0 - cue1	-0.0834	0.0474	-1.7612	0.0783	
4	Pre response	cue0 - cue1	-0.0798	0.0472	-1.6890	0.0913	

For theta band OB-PC coherence, the overall GLS does not show any significant effects. Since previously it has been shown that theta coherence in the OB and PC in the faster theta band is elevated during sniffing, we narrowed in more on OB-PC theta coherence during odor sampling and performed a GLS analysis on OB-PC theta coherence including all factors included

in the overall GLS models but took out factors related to events. We found a significant effect of odor stimulus type 400ms before rats leave the odor port (p= 0.0239, t= 2.2688, beta= 0.0278, SE= 0.0122). Theta coherence between OB and PC is significantly higher during fine discrimination than coarse for the late sampling time period (see Fig. 4.6).

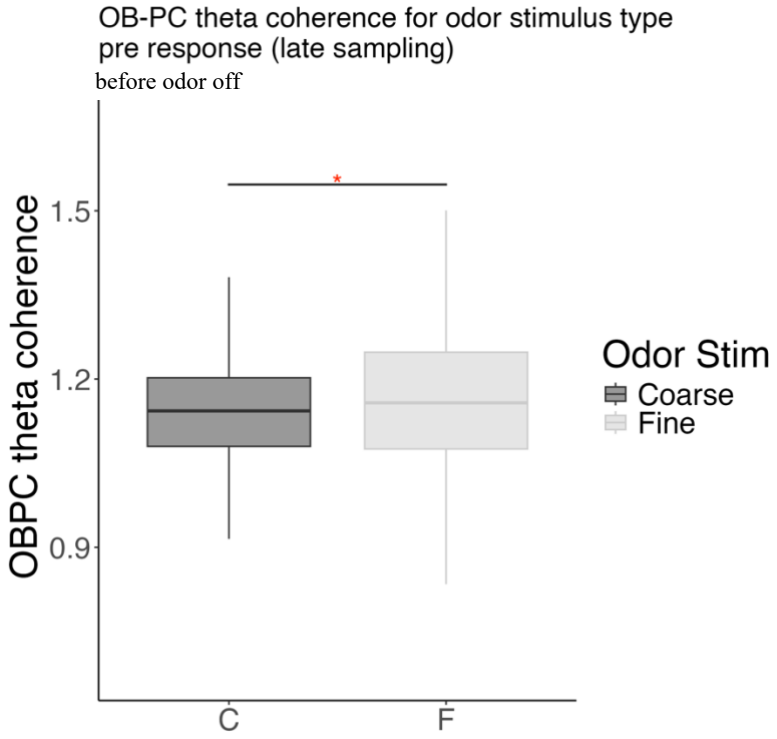

Figure 4.6 OB-PC theta coherence for odor stimulus type during late sampling
Middle box line represents median, top of box is the 3rd quartile, bottom of the box is the 1st quartile. p<0.05=*, p<0.01=**, p<0.001=***

OB-DG Coherence

We performed a GLS analysis on OB-DG coherence across theta, beta, gamma and gamma2 bands for each event separately. We report the OB-DG coherence GLS results by event and then follow up by multiple comparison tests to examine detailed differences.

In the pre-light period, 500ms before the cue light is illuminated, OB-DG coherence varies by cue conditions, and this difference is modulated by day (theta: cue*day2 p=0.0463, t=-2.0019, beta=-0.1194, SE=0.0596; beta: cue*day4 p=0.0236, t=-2.2753, beta=-0.1006, SE=0.0442). Multiple comparison tests showed OB-DG theta coherence to be different between informative and non-informative groups on days 3 and 4, with the informative group showing higher coherence. The informative group shows higher beta coherence on both days (see table 4.3 for details, figure 4.7). For the informative group, days 1-2 and days 2-4 have significantly different OB-DG theta coherence, driven by low theta coherence on day 2 for the informative group. The informative OB-DG beta coherence increases over days (figure 4.7c).

Table 4.3 OB-DG coherence during pre light period, significant multiple comparison terms

band	**cue**	**day**	**contrast**	**beta**	**SE**	**t.ratio**	**p.value**	
theta	-	3	cue0 - cue1	-0.0934	0.0364	-2.5680	0.0107	**
theta	-	4	cue0 - cue1	-0.1034	0.0346	-2.9883	0.0031	**
theta	1	-	day1 - day2	0.1163	0.0428	2.7193	0.0417	*
theta	1	-	day2 - day4	-0.1057	0.0338	-3.1296	0.0116	*
beta	1	-	day1 - day4	0.0970	0.0315	3.0838	0.0135	*
beta	1	-	day3 - day4	0.0712	0.0236	3.0167	0.0167	*

a

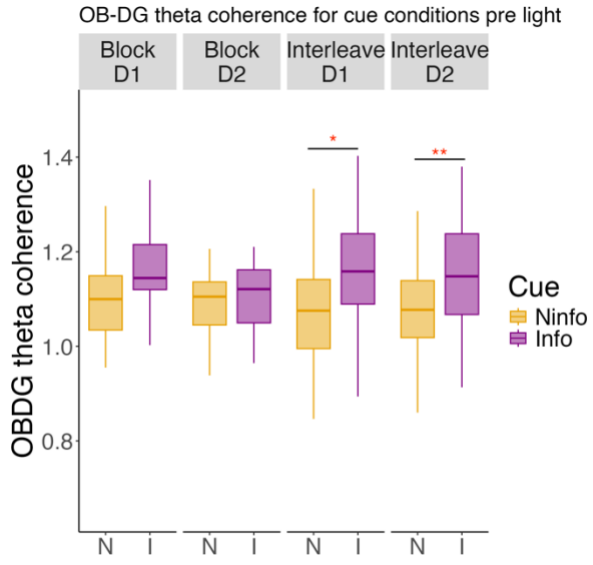

b

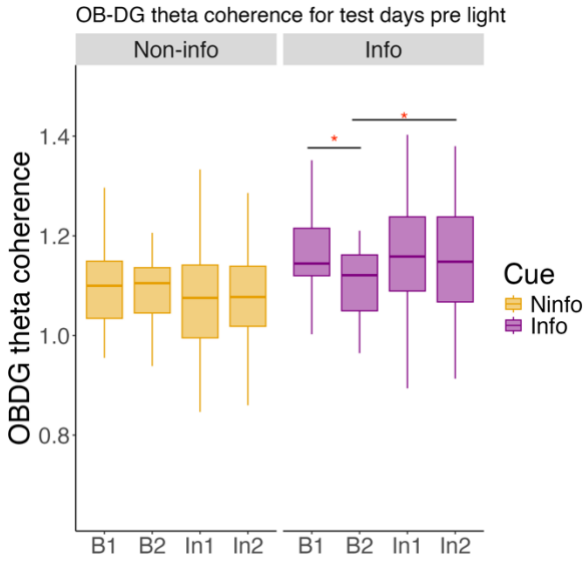

c

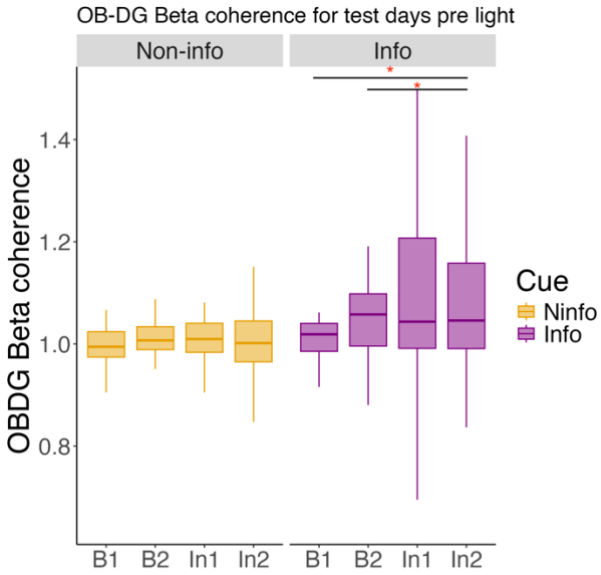

Figure 4.7 OB-DG theta and beta coherence during pre-light period
a. theta coherence for informative and non-informative groups by day b. theta coherence for test days by cue c. beta coherence for test days by cue. Middle box line represents median, top of box is the 3rd quartile, bottom of the box is the 1st quartile. p<0.05=*, p<0.01=**, p<0.001=***. Unmarked comparisons between days and cue condition are non-significant.

In the post-light period (0-500 ms after light on), the OB-DG coherence patterns look similar to the pre-light period, but there are two major differences: one is that OB-DG gamma coherence in the post-light period shows a difference by day for the informative group but not the non-informative group. The informative group has a higher gamma OB-DG coherence on

day 4 compared to day 2. Another difference compared to the pre-light period is that theta coherence is different between cue groups on day 1 as well, not just days 3 and 4. See table 4.4.

Table 4.4 OB-DG coherence multiple comparison result, post light period

band	cue	day	contrast	beta	SE	t	p
beta	1	-	day2 - day3	-0.0676	0.0230	-2.9422	0.0212
beta	1	-	day3 - day4	0.0722	0.0196	3.6772	0.0017
theta	-	1	cue0 - cue1	-0.1428	0.0600	-2.3795	0.0180
theta	-	3	cue0 - cue1	-0.1107	0.04731	-2.3398	0.0200
theta	-	4	cue0 - cue1	-0.0938	0.04571	-2.0524	0.0411
gamma	1	-	day2 - day4	-0.0413	0.01436	-2.8744	0.0261

a

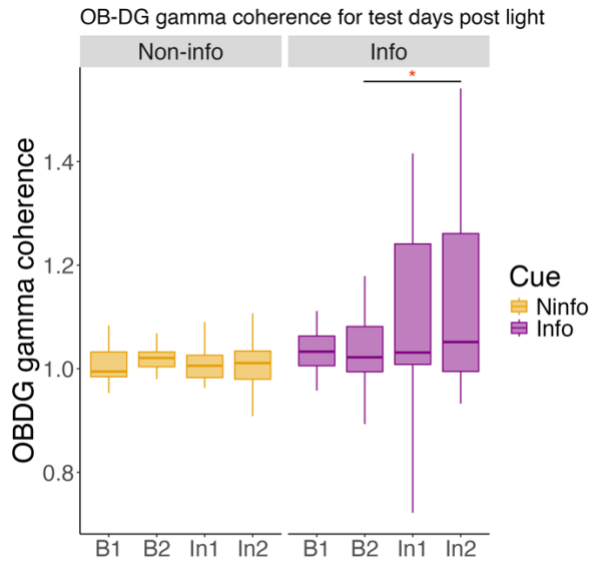

b

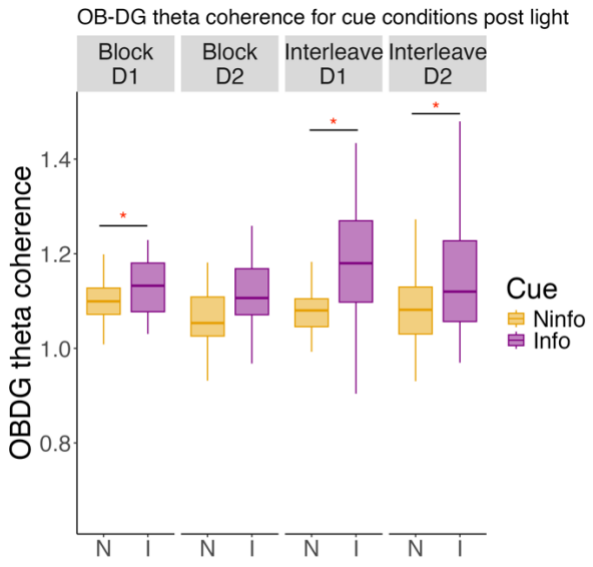

Figure 4.8 OB-DG gamma and theta coherence during post light
a. gamma coherence on test days by cue b. Theta coherence for cue by day. Middle box line represents median, top of box is the 3rd quartile, bottom of box is the 1st quartile. p<0.05=*, p<0.01=**, p<0.001=***. Unmarked comparisons between days and cue condition are non-significant.

During the odor sampling period (for the first 400ms after rats begin the nose poke into the odor port), the informative group OB-DG beta coherence is higher than that of the non-informative group. When looking at changes across days, the informative group only shows

different OB-DG beta coherence on day 3 compared to day 4 (p=0.0048, t=3.3878, beta=0.0669, SE=0.0197; Fig. 4.7). Day 3 OB-DG beta coherence is higher than that of day 4 for the informative group during sampling. Coherence between OB and DG on day 3 is high in general (see figure 4.9). The difference in OB-DG beta coherence between the informative and non-informative groups is also significant (p=0.0464, t=-2.0009, beta=-0.1382, SE= 0.0691).

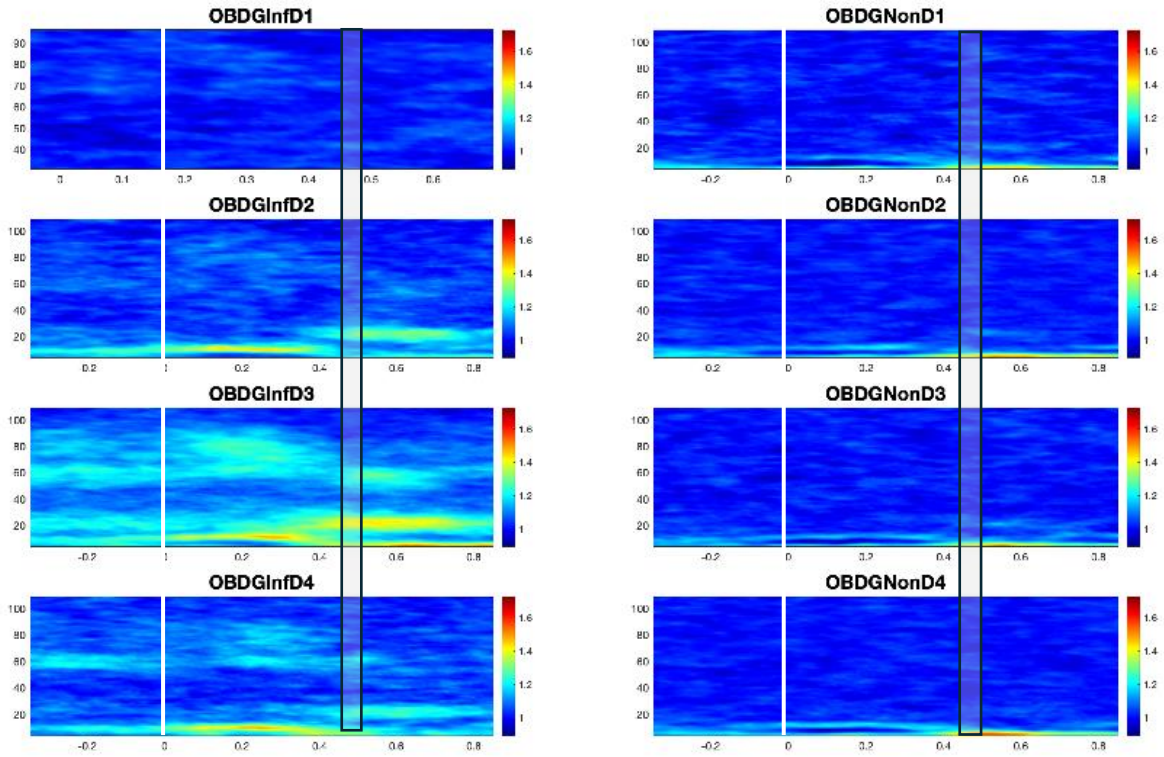

Figure 4.9 OB-DG coherence spectrogram
-0.5s to 1s after start of sampling (t=0, white line). 90% CI of end of sampling marked by grey box. a. OB-DG coherence for informative group by test day b. OB-DG coherence for non-informative group by test day. Beta band coherence is significantly higher for informative group than non-informative group. Informative group day 3 beta coherence is higher than day 4.

OB-CA1 Coherence

We expected to see activity coordination in CA1 and OB for the informative group, since the variation we introduced involved associative learning, and part of the CA1 has direct projections to OB. However, the OB-CA1 coherence does not differ by cue group, contrary to our expectations (Fig. 4.10). We did find a significant sex in OB-CA1 coherence effect for the theta, gamma, and gamma2 bands at specific events during the behavior (See table 4.5). There is an odor stimulus type effect for the theta and beta bands; coarse trials OB-CA1 beta and theta coherence is higher than fine trials during sampling (Fig. 4.11). Days 3 and 4 also separately show a significant difference compared to day 1 for gamma2 and beta coherence; this occurs during the pre-sampling and post-response periods separately. This means that interleaved tests may connect OB and CA1 differently than block tests. On the first day of interleaved testing, OB-CA1 gamma2 coherence in the 500ms before the start of odor sampling is significantly higher than during the period before the light is illuminated.

Table 4.5 OBCA1 coherence multiple comparison significant result

Area	**Frequency**	**Event**	**Term**	**Beta**	**SE**	**t**	**p**	
OBCA1	gamma2	Pre light bsl	sex	0.0139	0.0047	2.9294	0.0037	**
OBCA1	gamma2	Post light	sex	-0.0133	0.0055	-2.4245	0.0159	*
OBCA1	theta	Sampling	sex	0.1353	0.0651	2.0780	0.0386	*
OBCA1	gamma	Pre sampling	sex	0.0110	0.0020	5.5237	<0.0001	***
OBCA1	theta	Sampling	Odor stim	-0.0282	0.0136	-2.0684	0.0395	*
OBCA1	beta	Sampling	Odor stim	-0.0179	0.0084	-2.1473	0.0326	*
OBCA1	beta	Post odor off	Odor stim	-0.0317	0.0092	-3.4540	0.0006	***
OBCA1	gamma2	Pre sampling	day3	0.0413	0.0189	2.1911	0.0292	*
OBCA1	beta	Post odor off	day4	-0.0423	0.0182	-2.3232	0.0209	*
OBCA1	gamma2	Post light	Learning phase	0.0134	0.0054	2.4839	0.0136	*
OBCA1	gamma	Pre sampling	Learning phase	0.0062	0.0017	3.5549	0.0004	***

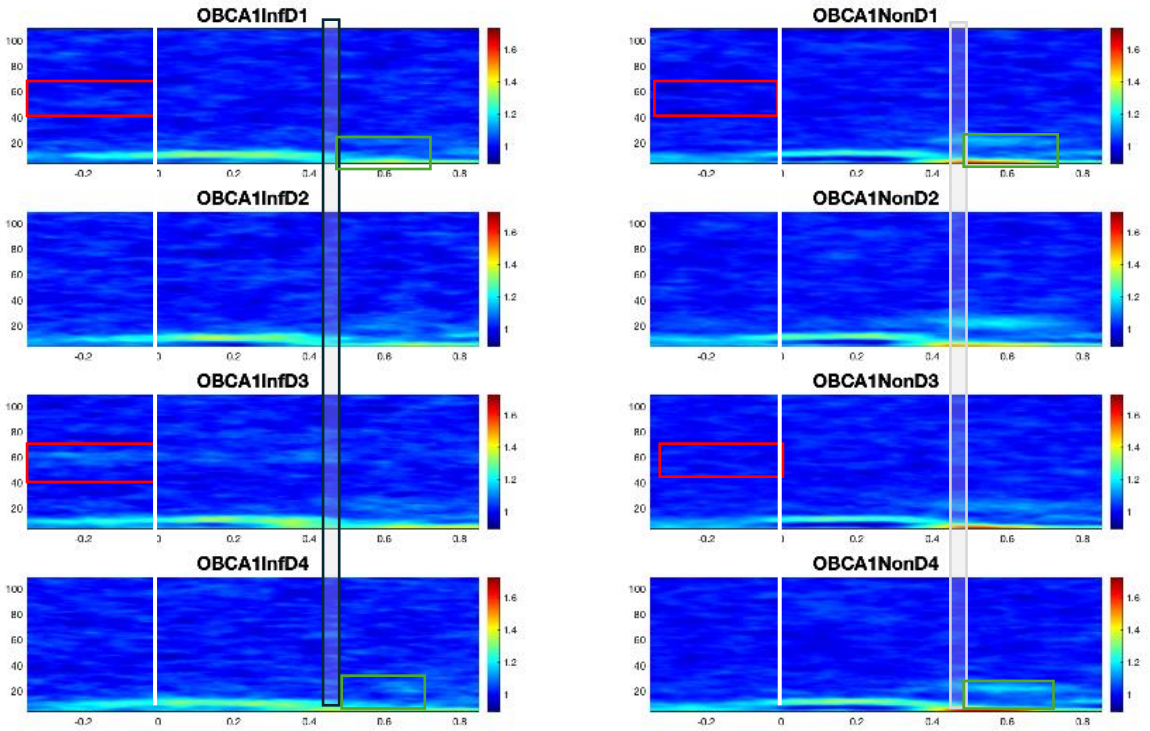

Figure 4.10 OB-CA1 Coherence spectrograms for cue by day
-0.5s to 1s after start of sampling (t=0, white line). 90% CI of end of sampling marked by grey box. a. OBCA1 coherence for informative group by test day b. OBCA1 coherence for non-informative group by test day. The OB-CA1 coherence does not differ by cue group. During pre sampling period, gamma 2 on day 3 is higher than day 1 (red boxes). During post odor off period, beta coherence on day 4 is higher than day 1.

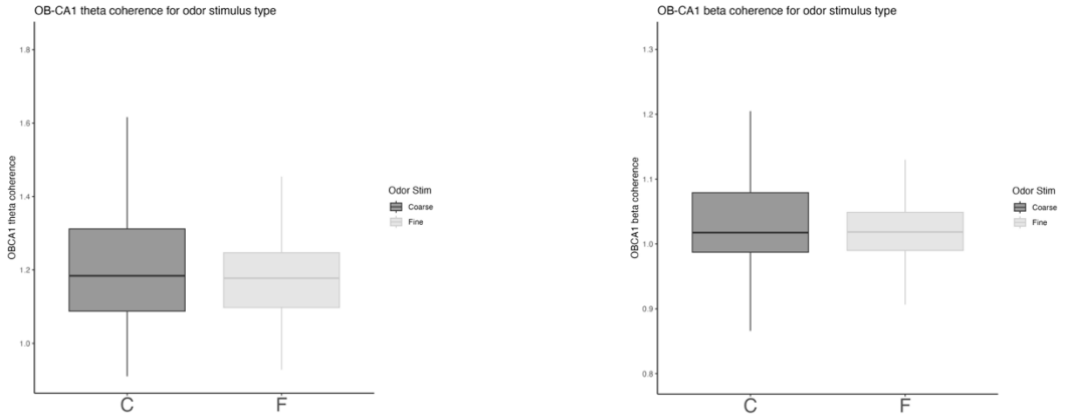

Figure 4.11 OB-CA1 beta and theta coherence during sampling for odor stimulus type
theta: coarse>fine, p=0.0395 b. beta: coarse>fine, p=0.0326

OB-Respiratory Coherence

The coherence strength between the thermocouple probe to measure respiration and the OB theta band (OB-TC) gives us information about whether or not sniffing may modulate neural dynamics differently for the informative and non-informative group at different times. The OB theta band activity generally tracks sniffing (but can also show hippocampal theta – see Heck et al., 2019; Kay, 2005), but for the two cue groups this relationship may differ across the events in a trial. We again performed a GLS account for the random rat effect in the correlation structure and performed multiple comparison tests to follow up on significant terms.

During odor sampling (400ms after start of odor, early sampling period), we found a significant odor stimulus type effect in the GLS model for OB-TC theta coherence (p=0.0385, t=2.07815115, beta=0.0360, SE=0.0173). For the late sampling period, (400ms before response), we also find an odor stimulus type effect (p=0.0306, t=2.1723, beta=0.0385, SE=0.0177) and a significant interaction between cue type and test day 3 (p=0.0144, t=2.4615, beta=0.1293, SE=0.0525). OB theta is more coherent with the TC during coarse compared to fine discrimination. The two cue condition groups have different theta coherence patterns throughout the four days. Based on follow-up multiple comparison tests, the non-informative group shows lower theta coherence than the informative group, both during early (p=0.0198, t=-2.3316, beta=-0.3787, SE=0.1624) and late sampling (p=0.0368, t=-2.0889, beta=-0.3393, SE=0.1624), or 400ms after odor starts and 400ms before odor off (these windows overlap but are aligned to different time points – sampling start vs. sampling end). For the informative group, theta coherence between OB and TC is different on day 3 than day 1 overall (p=0.0428, t=-2.7086, beta=-0.1041, SE=0.0384). Day 3 theta coherence between OB and TC is higher than that of day 1 by 0.1 unit.

a

b

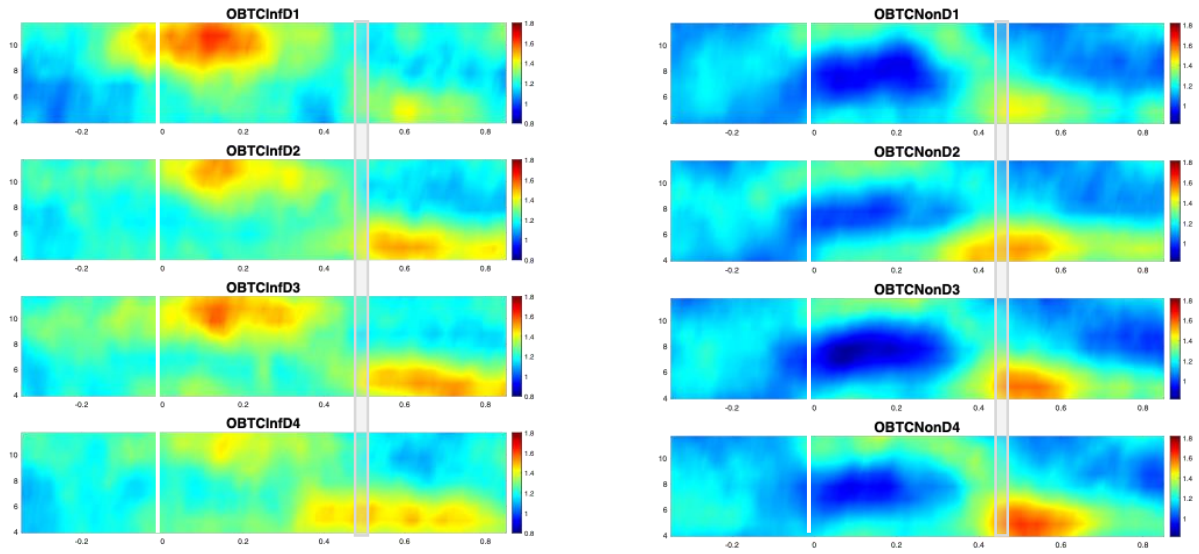

Figure 4.12 OBTC theta coherence spectrogram
a. informative group by day b. non-informative by day. -0.5s to 1s after start of sampling (t=0, white line). 90% CI of end of sampling marked by grey box.

PC-CA1 Coherence

We performed similar GLS accounting for rats' random effect by specifying coherence structures and following up with multiple comparison tests. Overall, to our surprise, PC is more coherent with CA1 for the non-informative group during sampling in the theta band, during post odor off period in the theta and beta bands (see figure 4.13.a-b). See table 4.6 for detailed GLS results; given the vast number of variables, only significant terms are listed.

Table 4.6 GLS result for PCCA1, significant terms							
Area	**Frequency**	**Term**	**beta**	**Std.Error**	**t.value**	**p.value**	
PCCA1	theta	Event sampling	0.1180	0.0308	3.8351	0.0001	***
PCCA1	theta	Event post odor off	0.1257	0.0308	4.0839	0.0000	***
PCCA1	theta	Event pre response	0.0776	0.0308	2.5216	0.0118	*
PCCA1	theta	cue:Event sampling	-0.1424	0.0463	-3.0777	0.0021	**
PCCA1	theta	cue1: Event sampling	-0.0913	0.0463	-1.9718	0.0488	*
PCCA1	theta	day3: Event sampling	-0.0815	0.0375	-2.1733	0.0299	*
PCCA1	theta	cue1:day2: Event sampling	0.1834	0.0666	2.7557	0.0059	**
PCCA1	theta	cue1:day3: Event sampling	0.1536	0.0580	2.6491	0.0081	**
PCCA1	theta	cue1:day4: Event sampling	0.1150	0.0568	2.0250	0.0430	*
PCCA1	beta	Event post odor off	0.1625	0.0269	6.0475	<0.0001	***
PCCA1	beta	Event pre response	0.0816	0.0269	3.0365	0.0024	**
PCCA1	beta	cue1: Event post odor off	-0.1481	0.0404	-3.6667	0.0003	***
PCCA1	gamma	Event post odor off	-0.0305	0.0133	-2.2825	0.0226	*
PCCA1	gamma	Event pre sampling	-0.0293	0.0133	-2.1954	0.0282	*
PCCA1	gamma2	Event sampling	-0.0438	0.0219	-2.0018	0.0454	*

Follow-up multiple comparison tests show that PC-CA1 theta coherence during odor sampling is significantly higher for the non-informative than the informative group on test day 1 (figure 4.13c). PC-CA1 beta band coherence after odor off is larger for the non-informative group on days 1,2 and 3 (figure 4.13e), on day 4 in the theta band (figure 4.13d). For the informative group, PC-CA1 coherence differ in the theta and gamma2 band. During pre sampling period for the informative group, theta coherence on day 4 is significantly higher than day 1 and 3 (figure 4.13f). See table 4.7 for multiple comparison results.

a

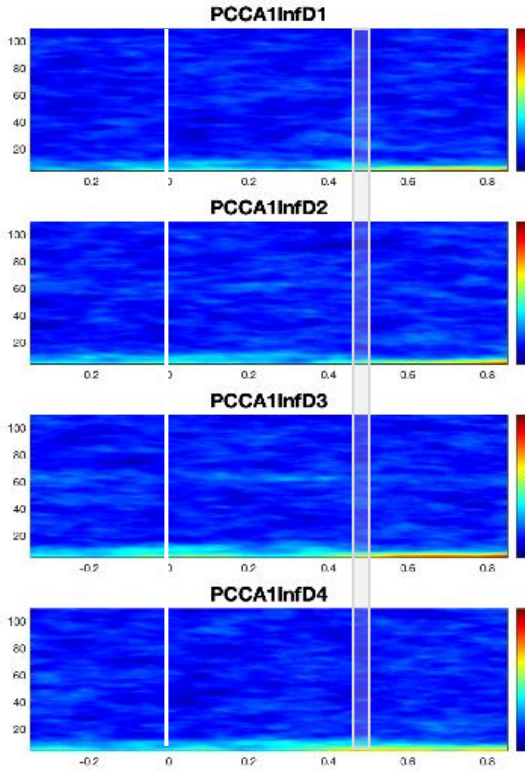
PCCA1InfD1
PCCA1InfD2
PCCA1InfD3
PCCA1InfD4

b

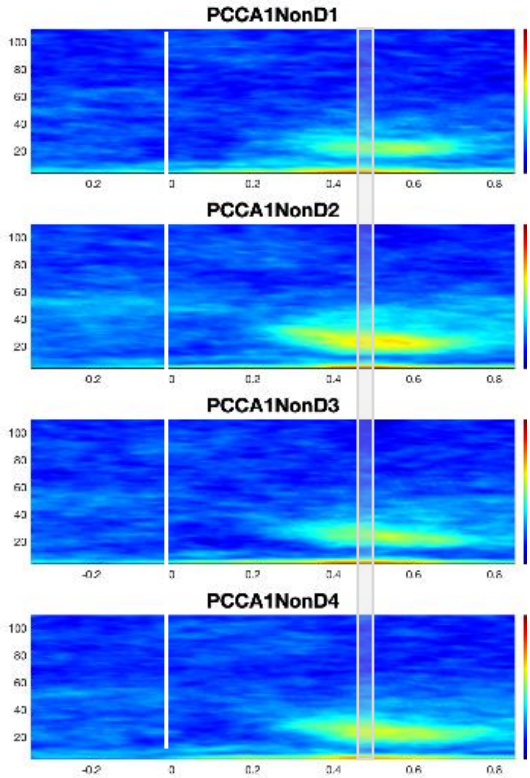
PCCA1NonD1
PCCA1NonD2
PCCA1NonD3
PCCA1NonD4

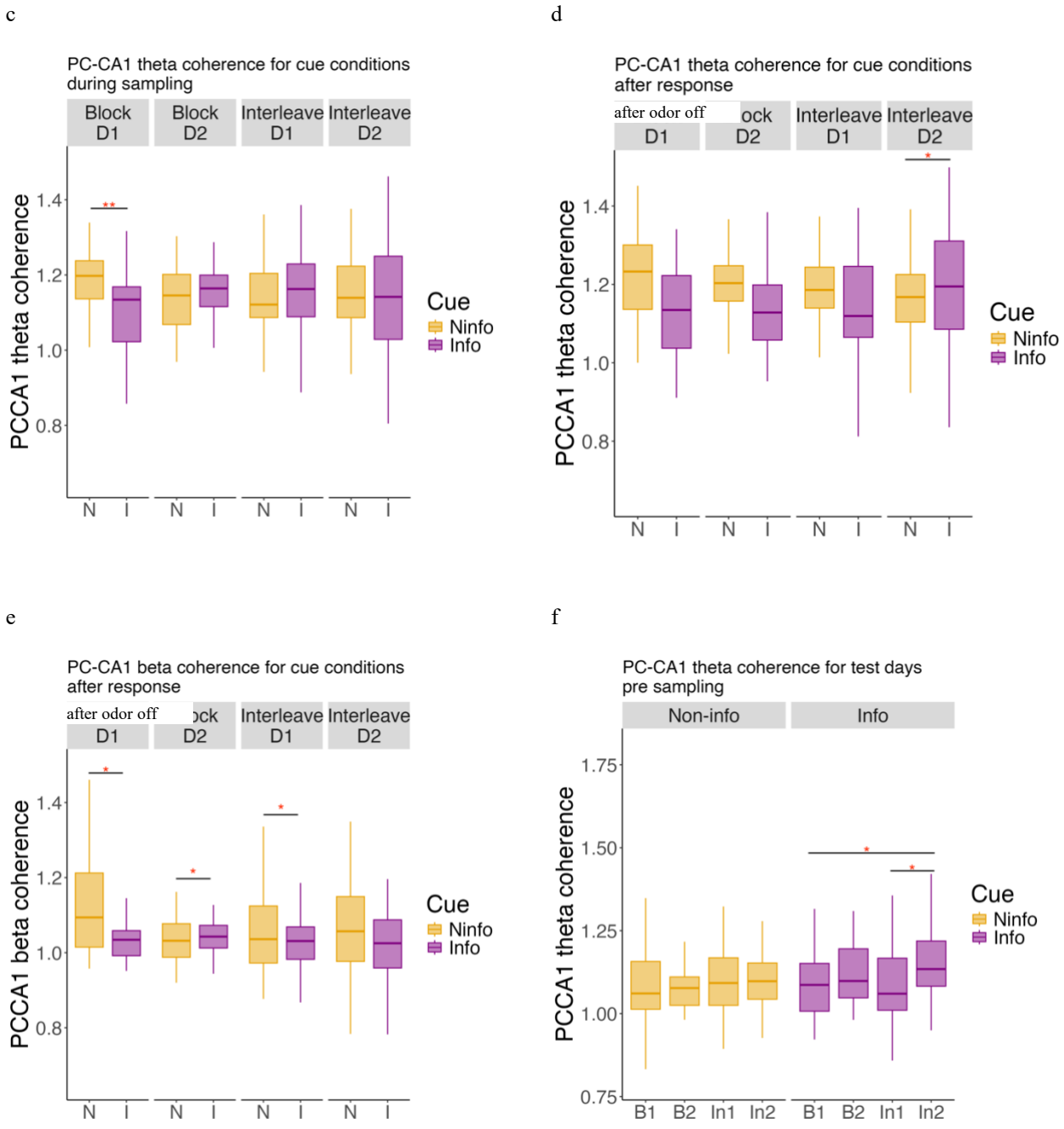

Figure 4.13 PC-CA1 Coherence
a-b. spectrograms -0.5s to 1s after start of sampling (t=0, white line). 90% CI of end of sampling marked by grey box. c.d. theta coherence during sampling and after odor off, cue and comparisons f. theta during pre sampling day comparison e. beta coherence during after odor off period, cue comparison. Unlabeled comparisons are not significant. $p<0.05$=*, $p<0.01$=**, $p<0.001$=***.

Table 4.7 PC-CA1 coherence multiple comparison result, significant terms									
Band	Cue	Day	Event	Contrast	Beta	SE	t	p	
beta	.	1	postnspkoff	cue0 - cue1	0.2292	0.1027	2.2324	0.0257	*
beta	.	2	postnspkoff	cue0 - cue1	0.2037	0.1023	1.9781	0.0481	*
beta	.	3	postnspkoff	cue0 - cue1	0.2067	0.1010	2.0474	0.0407	*
theta	.	1	postnspk	cue0 - cue1	0.0975	0.0366	2.6626	0.0078	**
theta	.	4	postnspkoff	cue0 - cue1	-0.0623	0.0285	-2.1879	0.0288	*
theta	.	4	postnspkoff	cue0 - cue1	-0.0907	0.0449	-2.0207	0.0442	*
theta	1	.	postnspkoff	day2 - day4	-0.0893	0.0331	-2.7002	0.0440	*
theta	1	.	prenspk	day1 - day4	-0.0839	0.0275	-3.0495	0.0150	*
theta	1	.	prenspk	day3 - day4	-0.0665	0.0239	-2.7777	0.0350	*
gamma2	1	.	prenspk	day2 - day4	-0.0555	0.0201	-2.7573	0.0372	*
gamma2	1	.	prenspk	day1 - day4	-0.0609	0.0226	-2.6952	0.0447	*

PC-DG Coherence

PC-DG coherence overall is higher in the informative group than the non-informative group, which is opposite to the cue difference for PC-CA1 coherence (see Fig 4.14.a-b, Fig 4.14.d-e). We performed GLS and followed up with multiple comparison tests. GLS shows that there are cue-modulated effects in the theta and gamma 2 bands. The effect for after response is particularly robust. Interestingly, theta coherence is modulated by cue before sampling starts (after light on). PC-DG theta coherence is also different by sex. Male rats have a higher PC-DG theta coherence by 0.05 unit. See Table 4.8 for GLS significant terms details.

Table 4.8 PC-DG coherence GLS result							
Area	Frequency	Term	Beta	Std.Error	t.value	p.value	
PCDG	theta	sex	-0.0482	0.0225	-2.1356	0.0328	*
PCDG	theta	Event post odor off	0.1146	0.0466	2.4590	0.0140	*
PCDG	theta	cue1:Event pre sampling	-0.1367	0.0676	-2.0218	0.0433	*
PCDG	gamma2	cue1:day3:Event post odor off	0.1067	0.0524	2.0386	0.0416	*

Despite a non-significant effect from the GLS model on beta and gamma bands, we still performed follow-up comparisons on these bands, because PC gamma and beta coherence concern our main hypothesis. Multiple comparison tests show that cue effects may even start 1s before light on. PC-DG gamma coherence during odor sampling on day 4 differed by cue condition with non-informative stronger than informative. The difference in gamma coherence between the cue groups starts 500ms before the light comes on for days 3 and 4 (see table 4.9 for details). The non-informative group in general has stronger PC-DG beta, gamma and theta coherence compared to the informative group during the interleaved tests, with the exception of theta 1s before light on day 4. The reason why these differences didn't show up in GLS could be that GLS estimates marginal effects and may mask level differences when they are in different directions or more complex in dynamics.

Table 4.9 PC-DG multiple comparison result, significant terms

band	**day**	**Event**	**contrast**	**beta**	**SE**	**t.ratio**	**p.value**	
beta	3	pre light on bsl	cue0 - cue1	-0.0926	0.0359	-2.5771	0.0100	**
beta	3	Post light	cue0 - cue1	-0.1020	0.0359	-2.8385	0.0046	**
beta	1	Post odor off	cue0 - cue1	-0.1190	0.0424	-2.8085	0.0050	**
beta	2	Post odor off	cue0 - cue1	-0.0977	0.0392	-2.4933	0.0127	*
beta	3	Post odor off	cue0 - cue1	-0.1435	0.0359	-3.9943	0.0001	***
beta	4	Post odor off	cue0 - cue1	-0.0740	0.0353	-2.0973	0.0361	*
beta	3	Pre light	cue0 - cue1	-0.0743	0.0359	-2.0669	0.0389	*
beta	3	Pre response	cue0 - cue1	-0.0933	0.0359	-2.5958	0.0095	**
gamma	4	Post light	cue0 - cue1	-0.0699	0.0325	-2.1535	0.0314	*
gamma	4	Sampling	cue0 - cue1	-0.0792	0.0325	-2.4393	0.0148	*
gamma	4	Pre light	cue0 - cue1	-0.0652	0.0325	-2.0094	0.0446	*
gamma	4	Pre sampling	cue0 - cue1	-0.0826	0.0325	-2.5444	0.0110	**
gamma2	3	Post odor off	cue0 - cue1	-0.0796	0.0379	-2.1029	0.0356	*
gamma2	4	Pre sampling	cue0 - cue1	-0.0749	0.0372	-2.0134	0.0442	*
theta	4	1s before light on	cue0 - cue1	-0.0773	0.0365	-2.1182	0.0343	*
theta	2	Post odor off	cue0 - cue1	0.1316	0.0457	2.8823	0.0040	**

a

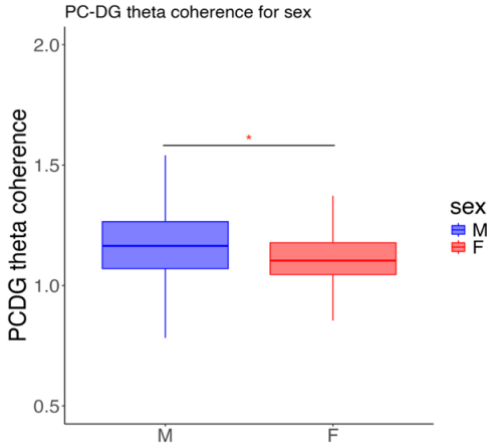
PC-DG theta coherence for sex
PCDG theta coherence
2.0
1.5
1.0
0.5
M
F
*
sex
M
F

b

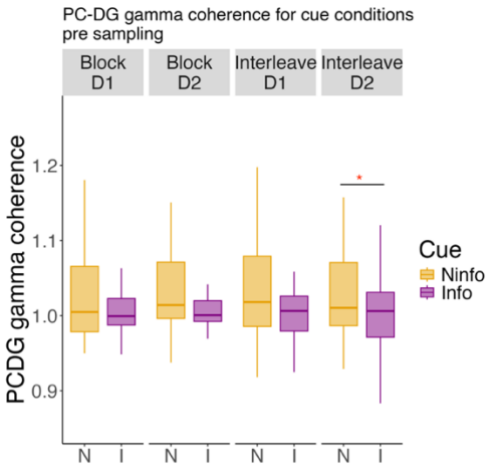
PC-DG gamma coherence for cue conditions
pre sampling
Block D1
Block D2
Interleave D1
Interleave D2
PCDG gamma coherence
1.2
1.1
1.0
0.9
N
I
*
Cue
Ninfo
Info

c

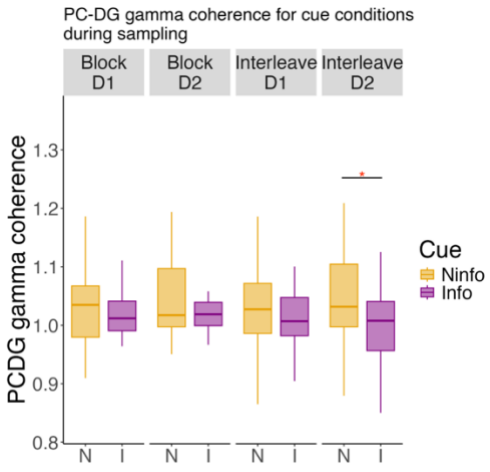
PC-DG gamma coherence for cue conditions
during sampling
Block D1
Block D2
Interleave D1
Interleave D2
PCDG gamma coherence
1.3
1.2
1.1
1.0
0.9
0.8
N
I
*
Cue
Ninfo
Info

d

e

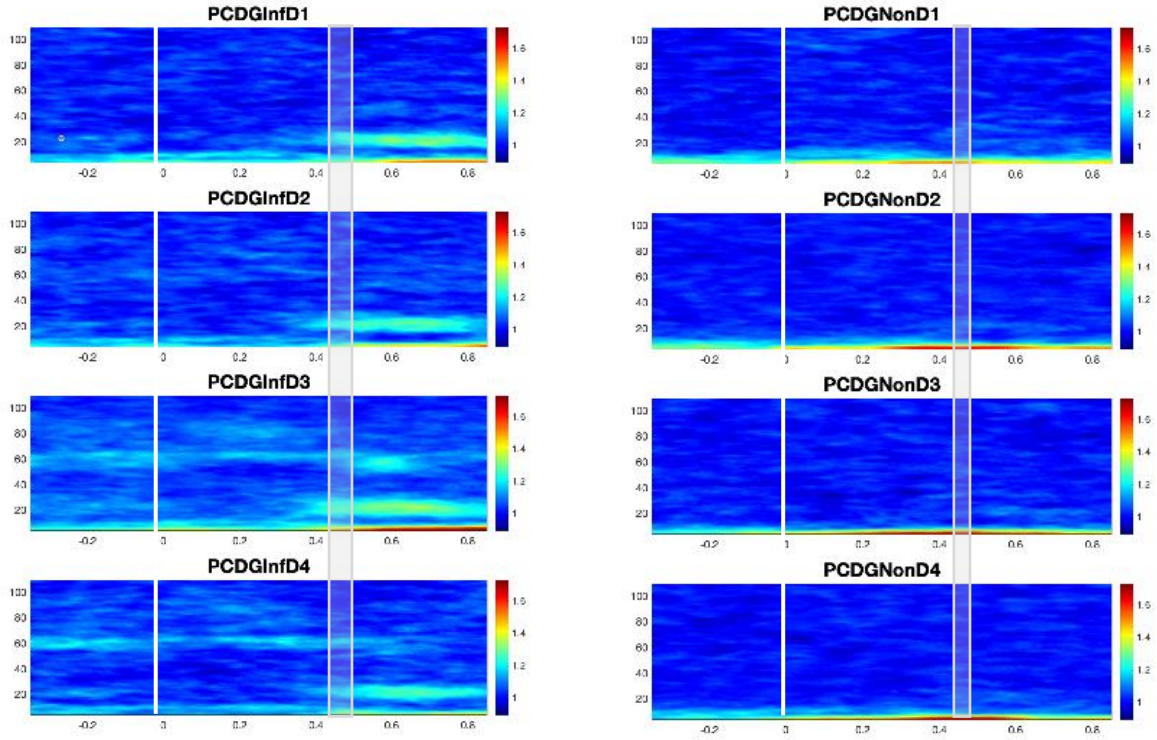

Figure 4.14 PC-DG Coherence
Non-informative gamma coherence higher than informative on day 4. a. theta coherence sex difference: male higher than female. b-c. gamma coherence pre sampling and during sampling, cue comparison by test day. d-e coherence spectrograms -0.5s to 1s after start of sampling (t=0, white line). 90% CI of end of sampling marked by grey box.

DG-CA1 Coherence

A GLS model incorporating rat random effects in the correlation structure shows that coherence within the hippocampus (DG-CA1) in beta and gamma bands is higher in the informative condition compared to the non-informative condition. In the beta band, this increase for the informative group is also modulated by events, meaning that the pattern is variable across the events within the behavioral trial. In the theta band, there are widespread effects of event, cue, test day and odor stimulus type. Interestingly, none of the above-mentioned effects survived the multiple comparison tests.

Table 4.10 DG-CA1 GLS result, significant terms						
Frequency	**Term**	**beta**	**Std.Error**	**t.value**	**p.value**	
theta	Post odor off	0.1011	0.0442	2.2854	0.0224	*
theta	cue1: day3	0.1300	0.0581	2.2378	0.0254	*
theta	cue1: sampling	0.1863	0.0672	2.7710	0.0056	**
theta	cue1: Post odor off	0.1387	0.0672	2.0622	0.0393	*
theta	cue1: Post odor off	0.1475	0.0672	2.1930	0.0284	*
theta	cue1:day3: post light	-0.1938	0.0821	-2.3605	0.0184	*
theta	cue1:day3: sampling	-0.2050	0.0821	-2.4974	0.0126	*
theta	cue1:day4: sampling	-0.1755	0.0803	-2.1842	0.0291	*
theta	cue1:day3: Post odor off	-0.2260	0.0821	-2.7534	0.0060	**
theta	cue1:day4: Post odor off	-0.1675	0.0803	-2.0847	0.0372	*
theta	cue1:day3: Pre odor off	-0.1774	0.0821	-2.1616	0.0308	*
beta	cue1	0.0979	0.0478	2.0497	0.0406	*
beta	cue1: Pre odor off	-0.0984	0.0432	-2.2764	0.0229	*
gamma	cue1	0.0536	0.0267	2.0041	0.0452	*

a **b**

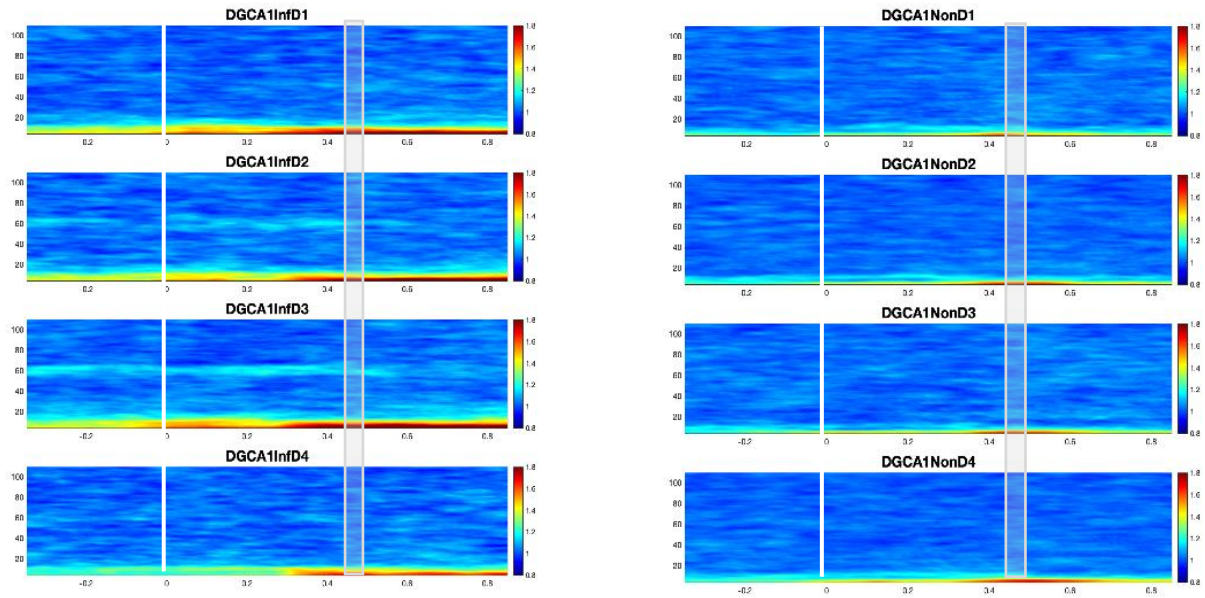

Figure 4.15 DG-CA1 coherence spectrograms
a. informative b. non-informative. -0.5s to 1s after start of sampling (t=0, white line). 90% CI of end of sampling marked by grey box.

TC-hippocampus Respiratory Coherence

The thermocouple allows us to track airflow in the nose and permits testing coherence between all recorded areas and the respiratory cycle. CA1 and TC theta/respiratory coherence is modulated by odor stimulus type (coarse>fine, beta=-0.0161, SE=0.0081, t=-1.9994, p=0.0457). Multiple comparison testing on cues by event and day showed that on day 4, non-informative rats have higher coherence between this area of the hippocampus and respiration 500ms before sampling starts.

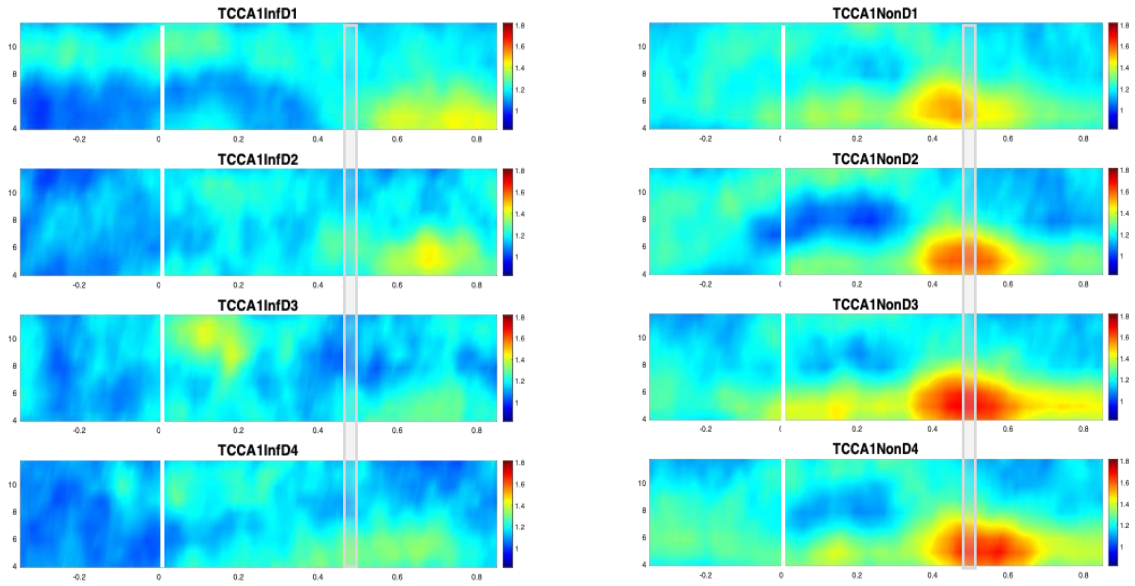

Figure 4.16 CA1-TC theta coherence
Spectrograms of CA1-TC theta coherence by cue group and test days, -0.5s to 1s after start of sampling (t=0, white line). 90% CI of end of sampling marked by grey box.

Respiratory coherence with DG showed main effects of day 4 (<day 1, p=0.045), sampling (>pre light baseline, p=0), post odor off (>pre light baseline, p=0), cue and post odor off interaction (p=0) (See table 4.11 for multiple comparison result). Cue effects on DG-TC theta coherence appear on days 1 and 2 during odor sampling, and on all days for post odor off period (non-informative respiratory DG coherence is higher than informative. See figure 4.17).

Table 4.11 DG-TC multiple comparison result

day	**event**	**contrast**	**beta**	**SE**	**df**	**t.ratio**	**p.value**	
1	pre light bsl	cue0 - cue1	0.0552	0.0340	25.4	1.6200	0.1175	
2	pre light bsl	cue0 - cue1	0.0264	0.0324	21.2	0.8160	0.4238	
3	pre light bsl	cue0 - cue1	0.0181	0.0308	17.2	0.5870	0.5648	
4	pre light bsl	cue0 - cue1	0.0194	0.0302	16.0	0.6420	0.5299	
1	post light	cue0 - cue1	0.0267	0.0340	25.4	0.7850	0.4395	
2	post light	cue0 - cue1	-0.0020	0.0324	21.2	-0.0620	0.9509	
3	post light	cue0 - cue1	-0.0103	0.0308	17.2	-0.3350	0.7419	
4	post light	cue0 - cue1	-0.0090	0.0302	16.0	-0.2980	0.7697	
1	sampling	cue0 - cue1	0.0985	0.0340	25.4	2.8920	0.0077	**
2	sampling	cue0 - cue1	0.0697	0.0324	21.2	2.1530	0.0430	*
3	sampling	cue0 - cue1	0.0614	0.0308	17.2	1.9910	0.0626	
4	sampling	cue0 - cue1	0.0627	0.0302	16.0	2.0740	0.0546	
1	post odor off	cue0 - cue1	0.1991	0.0340	25.4	5.8500	<0.0001	***
2	post odor off	cue0 - cue1	0.1704	0.0324	21.2	5.2620	<0.0001	***
3	post odor off	cue0 - cue1	0.1621	0.0308	17.2	5.2560	0.0001	***
4	post odor off	cue0 - cue1	0.1634	0.0302	16.0	5.4030	0.0001	***
1	pre light	cue0 - cue1	0.0159	0.0340	25.4	0.4670	0.6446	
2	pre light	cue0 - cue1	-0.0129	0.0324	21.2	-0.3970	0.6952	
3	pre light	cue0 - cue1	-0.0212	0.0308	17.2	-0.6860	0.5016	
4	pre light	cue0 - cue1	-0.0199	0.0302	16.0	-0.6560	0.5210	

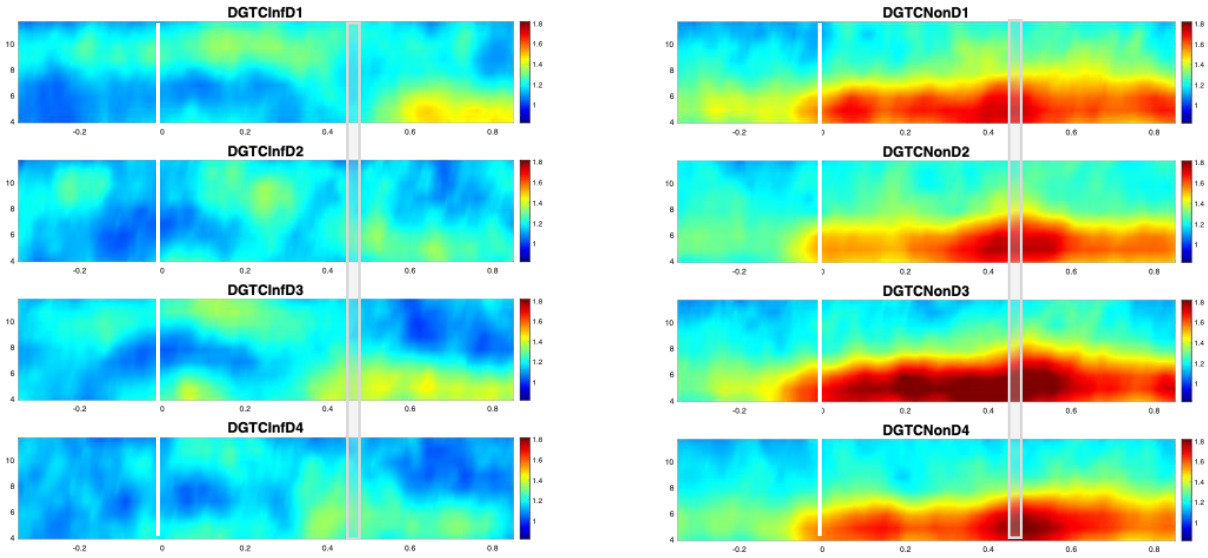

Figure 4.17 DG-TC theta coherence spectrogram
Spectrograms of CA1-TC theta coherence by cue group and test days, -0.5s to 1s after start of sampling (t=0, white line). 90% CI of end of sampling marked by grey box.

Coherence by events

While event effects are covered in the previous sections, looking at the results by event instead of by anatomical pairs can inform us more fully about what happens during the course of a behavioral trial. In this section we evaluate some of the more salient events regarding coherence patterns.

Beta coherence during the post odor off period is high in OB-PC for both informative and non-informative groups but stronger for the informative group. However, during this post odor off period, the informative group beta is also more coherent for PC-DG. At the same time, the non-informative group shows stronger OB-CA1 beta coherence. Moreover, during the pre-light baseline period, the informative group also shows elevated OB-PC beta coherence. The elevation in beta coherence during pre-light baseline and post odor off period between OB and PC is

highest on the first day of the interleaved test (day 3). On the same day, the OB-DG gamma coherence during sampling is also elevated for the informative cue group, which is not the case for the non-informative group.

Informative

a

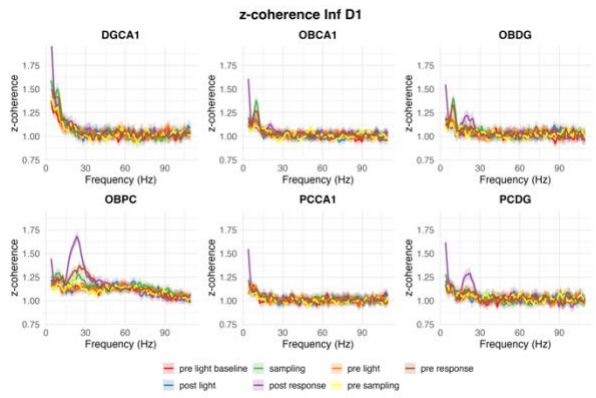

b

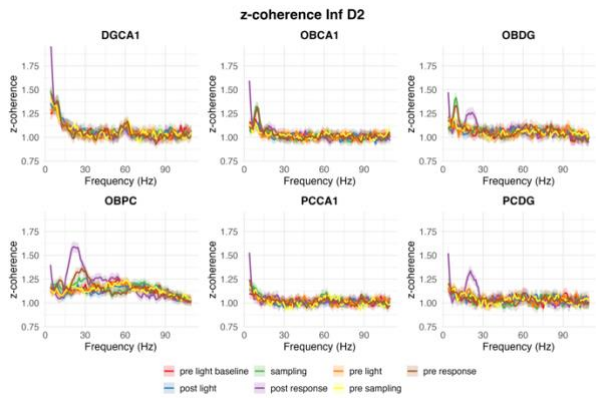

c

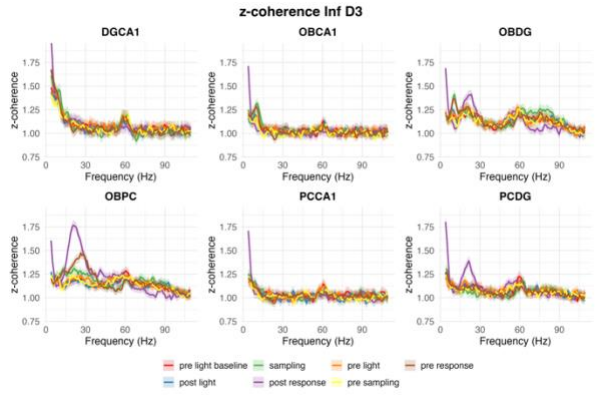

d

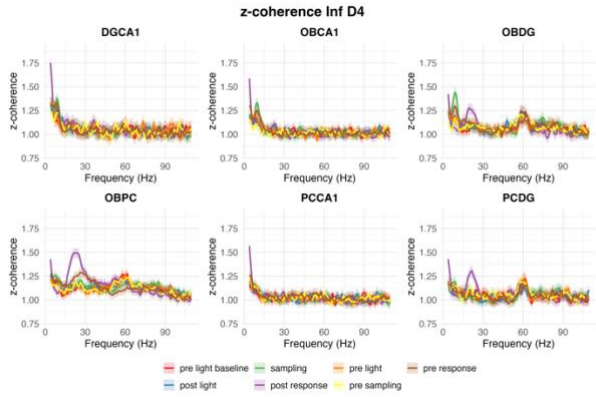

Non-informative

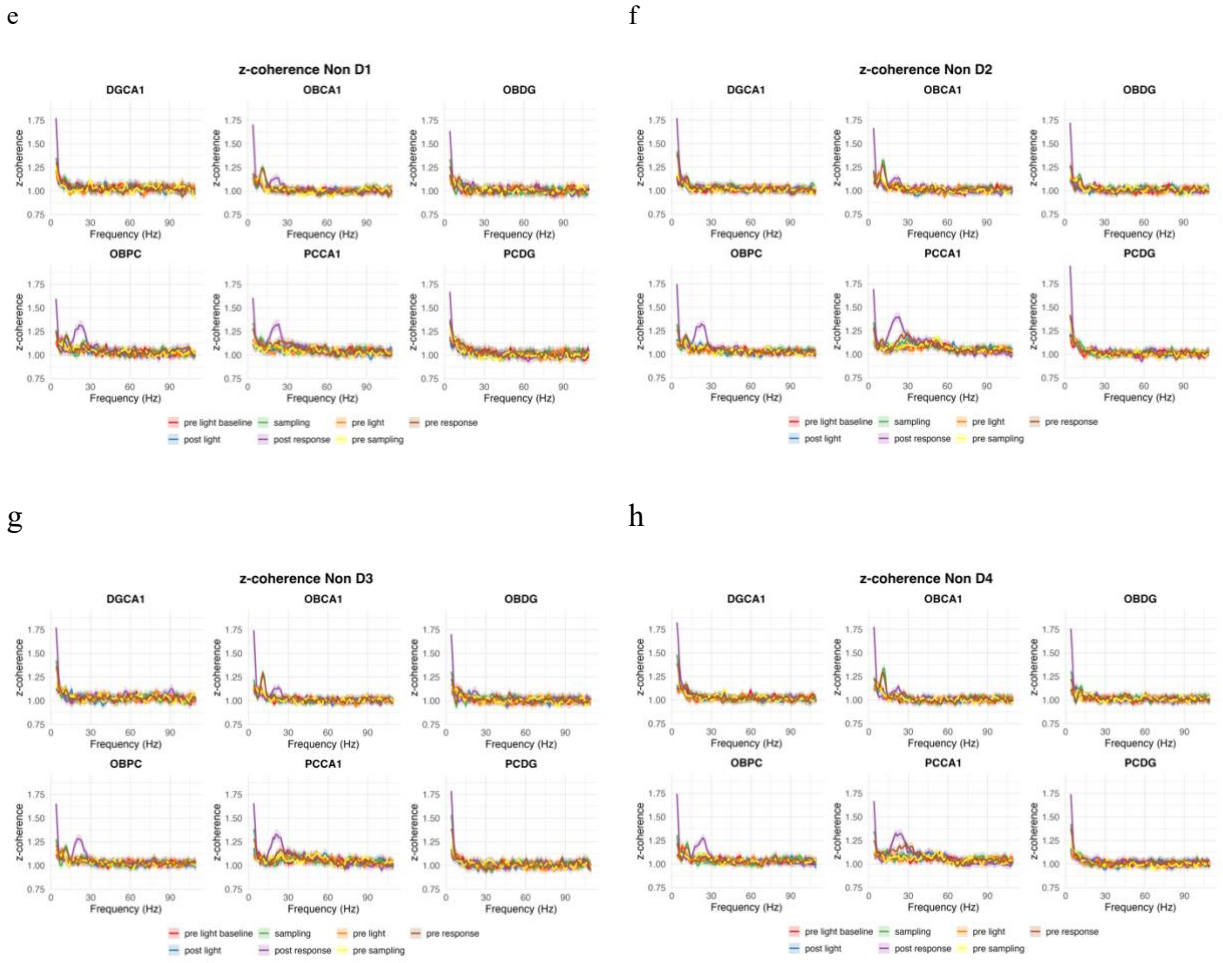

Figure 4.18 Coherence confidence intervals by frequency for all events
Coherence across area combinations for 3-110 Hz. a-d, informative group. e-h, non-informative group. Event indicted by color; shadowed band signifies 95% confidence intervals.

During odor sampling, rats using the informative cue show higher coherence in the fast-sniffing band (6-12 Hz) compared to the non-informative group, and this seems to be consistent to varying degrees across the coherence between TC and the four areas we recorded from (Fig.

4.18). While there is the expected high coherence with respiration and the OB during odor sampling, there is very low coherence with the PC, just one synapse away from the OB. Interestingly, there appears to be greater coupling between respiration and the hippocampal areas during odor sampling than there is with the PC.

Informative

a

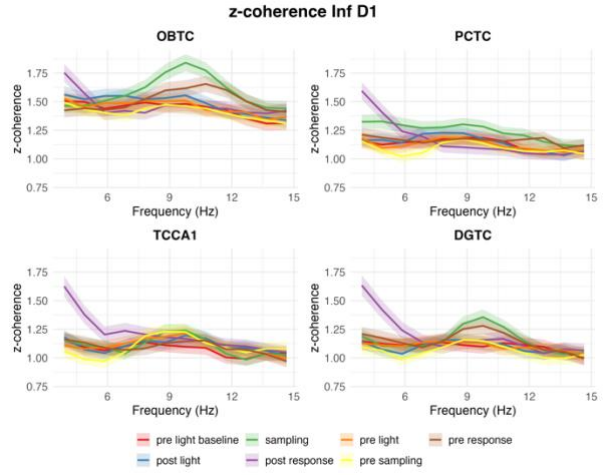

b

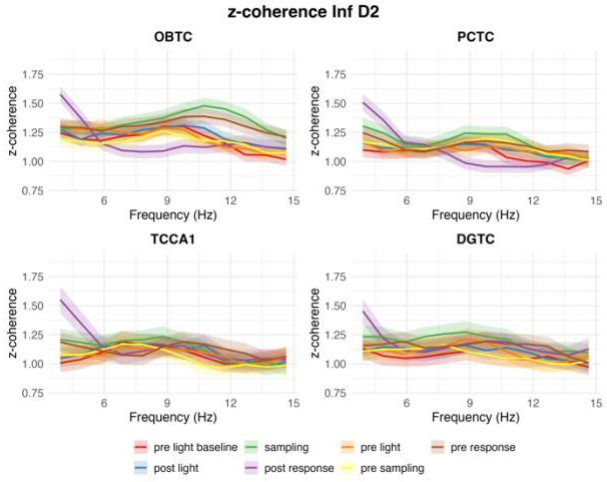

c

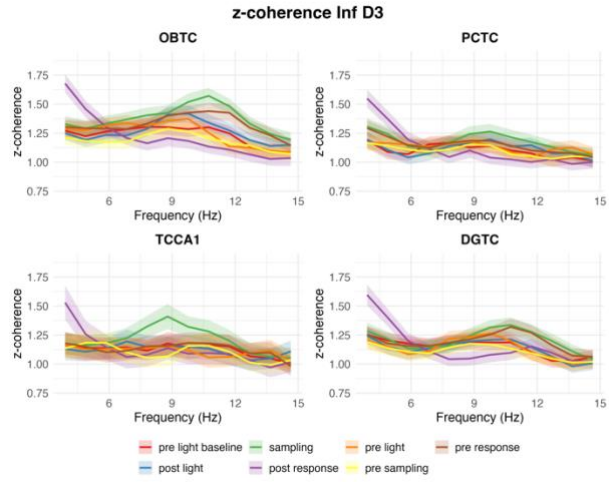

d

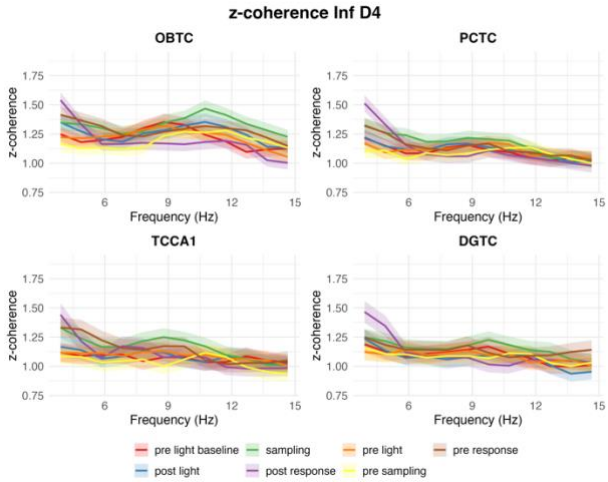

Noninformative

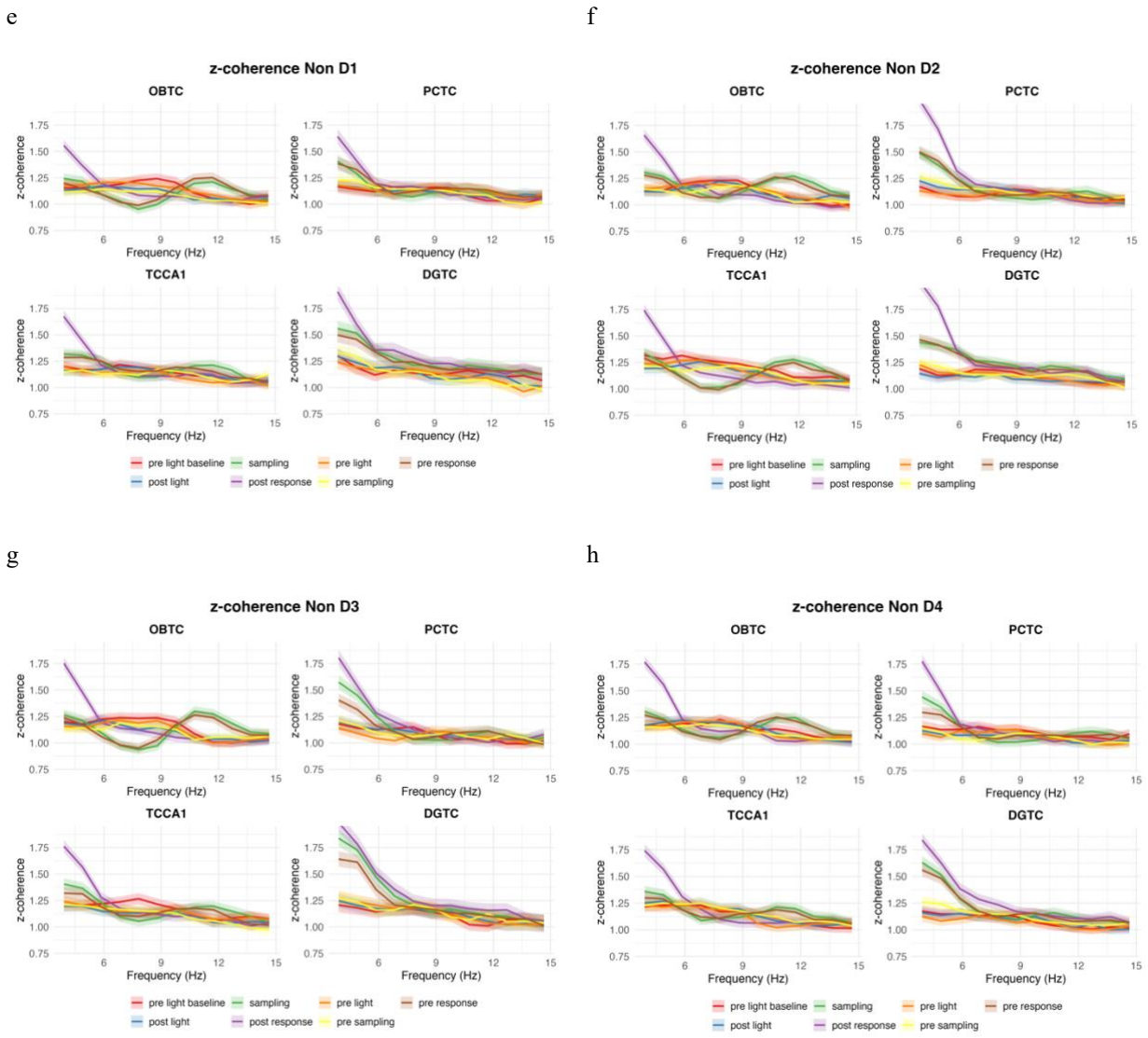

Figure 4.19 Respiratory coherence in all areas by cue group and events
Coherence across area combinations for theta band (3-15Hz). a-d, informative group. e-h, non-informative group. Event indicted by color; shadowed band signifies 95% confidence intervals.

In summary, analysis on the network coherence between OB, PC, DG, CA1 and their respective respiratory coherence allowed us to investigate further what the changes we see in OB

gamma and beta power modulated the task demand may be related to the olfactory-hippocampal network. We found that the informative and non-informative condition recruits the networks differently for the same task, one with a cue providing information of the immediate context, one without. The informative group has a higher OB-PC coherence than the non-informative group, and this change is persistent through all test days. Furthermore, the first day of the interleaved test brought out more differences in informative and non-informative groups. The non-informative generally have similar coherence patterns across days. For the informative group, we see many changes in the network start emerging on day 3. For the informative group, we start to see coherence differences during the late sampling period become more pronounced in OB-PC on day 3, the first day of the interleaved test where the cue light should become the most useful. Also, on day 3 in OB-DG coherence, we start to see non-informative and informative group differences in theta coherence. On day 3 in the informative group, we start seeing differences in OB-CA1 beta and gamma2 coherence compared to day 1. On day 3, OB respiratory theta coherence in the informative group is higher than day 1. PC-DG gamma coherence for the informative group emerges on day 3 compared to day 1 and 2. All of these day 3 effects show that the interleaved task can be differentiated from the block task on a neural level. Rats trained with and without an informative cue in the same olfactory learning task adapt their strategies for cognitive demand increase differently.

Chapter 5: Investigating cue effects during training and testing phase, learning interaction and sex effect

The large number of significant effects in the previous chapters beg the question when these differences arose in learning or testing and whether they are specific to the four-odor task. The counterbalancing of odor sets in our experimental design also allows us to ask if there is an effect of experience when rats finish one odor set and then learn the second set. The following analyses address these questions and also examine the sex differences that appeared in some of our previous results.

In the previous chapters, we saw that whether the odor set is the first odor set or the second set that the rats learned had a significant effect on OB gamma power, and OB-CA1 gamma and gamma 2 coherence. For a given odor set, composed of one fine pair and one coarse pair, when rats learned it as the first set of odors, OB gamma power was higher than if rats learned it as the second odor set. During the period between the cue light turning on and the beginning of odor sampling, OB-CA1 gamma coherence was higher for a given odor set if it was the second set of odors learned.

We also saw sex effects in the full task. OB beta power on day 3, is lower for females than for males. OB-PC gamma coherence for females is lower than males. Sex also modulates OB-CA1 theta, gamma, and gamma2 coherence at various events.

In this chapter, we look more into these factors and incorporate phase 3 data to ask two questions: 1. Are there sex effects modulated by task phase? 2. Does learning phase (first vs. second odor set) interact with the multiple changes we see on the first interleaved test day (day 3) in the two groups of rats? Our hypothesis is that learning phase and sex both modulate effects related to cue group (informative vs. non-informative).

First, we conducted the GLS analysis again including phase 3 data, using session averaged data points, to include the changes that occur from learning the associations for each odor set before the four-odor block and interleaved tests. Phase 3 data included here are from the last day rats trained on the coarse pair and the last day rats trained on the fine pair, before they moved on to phase 4. We expect to see a difference in behavior and LFP signals for the same odor set when encountered in these different phases. During the time rats were learning the first odor set, there were two possible transition points. The first was the first day that they performed the block test, as it was the first time they encountered four odors in the same session. The second transition point was the first day (test day 3) of the interleaved test, as it was the first time they encountered a four-odor test with higher unpredictability. In Chapters 3 and 4, we saw phase 4 day 3 effects in sampling duration, OB gamma power, OB beta power, OB-PC beta coherence, OB-DG theta coherence, OB-DG beta coherence, OB-CA1 beta and gamma2 coherence, OB-TC theta, PC-DG theta, all of which are modulated by cue condition (informative vs. non-informative).

We first focus on sampling duration and OB power, performing multiple comparison tests including the last days of phase 3 training for coarse and fine odor pairs combined (TD -1) and four days of phase 4, by addressing learning phase and cue. The multiple comparison test is based on the fitted values of a GLS analysis including phases 3 and 4 data, three-way interactions between learning phase, cue and day and sex, cue and day, at the same time accounting for the random effect of rats in the correlation structure and significant interactions relating to the levels compared. Then we examine coherence measures on TD -1 and day 3 by learning phase (first or second learned odor set) and cue to look at the effect of prior learning on

network coherences. For each section, we focus on learning phase and sex effects since we have reported effects of other variables previously.

The analyses in Chapters 3 and 4 did not include the two three-way interactions mentioned above but did include main effects of learning phase and sex. Moreover, the previous analyses included block id as a term to account for changes over a session. The significant effects from the two analyses are similar, despite including phase 3 data here. Differences in significant effects between current and previous analyses are noted below.

We found a sex difference in OB beta power and coherence during phase 4 analysis. A recent study from the lab by Maheshwar et al. 2025 found robust differences in sampling times and OB gamma and beta power between male and female Long Evans rats for an odor habituation task. The analyses including phase 3 and phase 4 data in the current experiment examine the details of sex effects. We first conducted a GLS and then followed up on sex and significant interactions with sex and other factors.

Sampling duration

Analysis of sampling duration shows significant effects of the odor stimulus type (coarse vs. fine; beta=0.065, SE=0.0240, t=2.7132, p=0.0099) and cue type (informative vs. non-informative; beta=0.1825, SE=0.0365, t=4.9955, p=0). The difference we see in sampling duration combining phase 3 and phase 4 data and adding interaction terms for learning phase and sex, is that the cue effect on sampling duration is modulated by odor stimulus type (cue:odor type, beta=-0.0844, SE=0.0360, t=-2.3465, p=0.0241), meaning that the informative / non-informative difference changes depending on whether the rats are sampling fine or coarse pair odors (longer for fine overall, as in Chapter 3, Fig. 3.3a).

Learning phase differences in sampling duration

We found significant three-way interactions between learning phase (first or second odor set learned), cue and day in the current analysis (cue1:day1:learningph2, beta=-0.1257, SE=0.0494, t=-2.5431, p=0.0151, cue1:day4:learningph2, beta=-0.2094, SE=0.0494, t=-4.2374, p=0.0001), confirming multiple comparison tests are needed to evaluate group levels. Multiple comparison tests with Bonferroni correction on the three-way interactions showed that differences in sampling duration between the informative and non-informative groups are present on the last training day in phase 3. During the last day of training in phase 3, informative rats sample longer, indicating that the group difference is present even before the tasks are more explicitly different. For the first odor set learned, the difference is about 118ms (p=0.0006); for second odor set learned, the difference is about 84ms (p=0.0095). On days 1,2 and 4, cue effects on sampling duration were not significant for the second odor set learned but were significant for 1st odor set learned. On day 3, differences in sampling duration between cue conditions were significant on both 1st and 2nd odor sets learned. Informative cue rats sample longer on the first day of an interleaved test than non-informative cue rats, for the first odor set learned 175ms (p<0.001), for second odor set learned 96ms (p=0.0029). See figure 5.1.

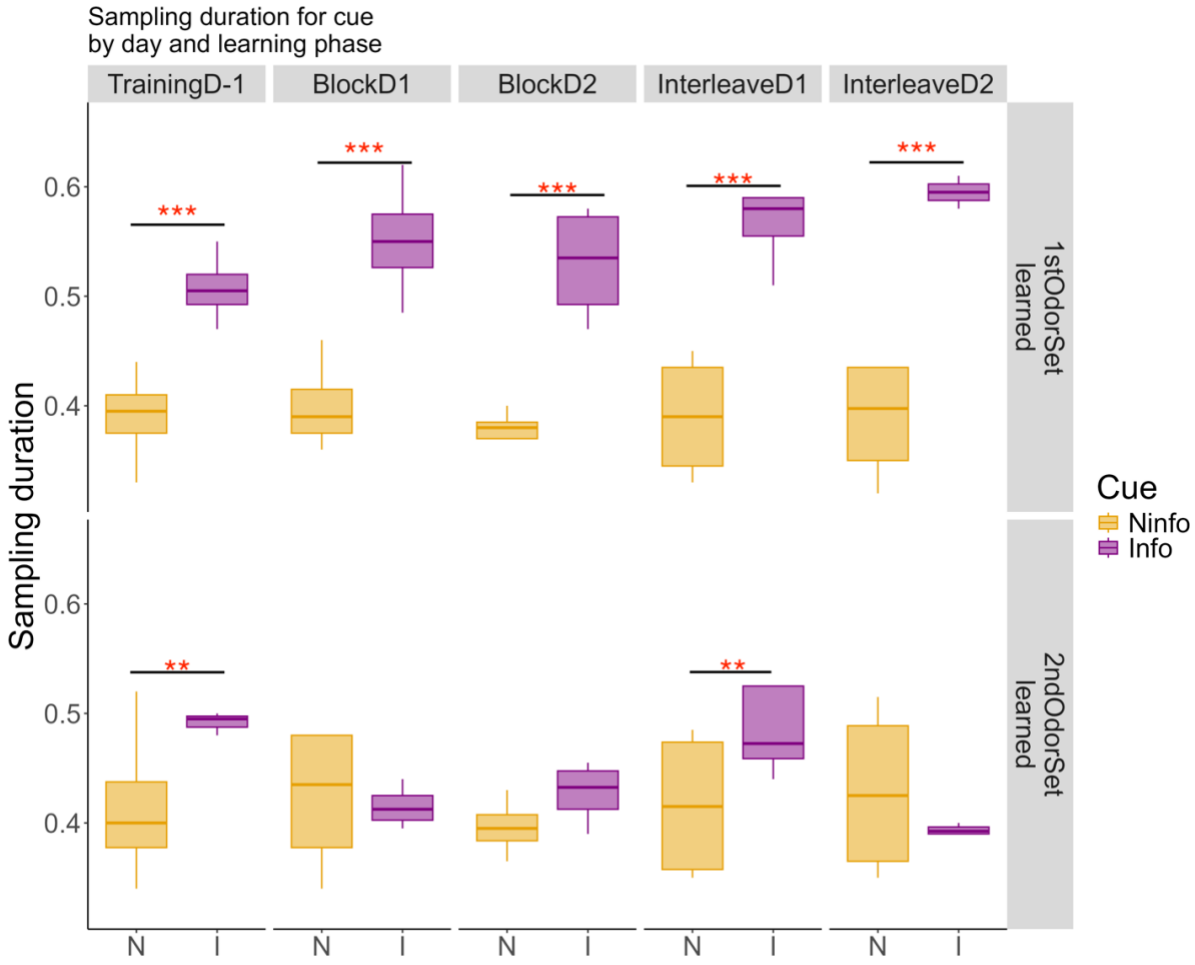

Figure 5.1 Sampling duration for cue conditions by day and learning phase
Top panel, 1st odor set learned. Bottom panel, 2nd odor set learned.

Sex differences in sampling duration

A pronounced sex effect in sampling time was evident for the last day of learning in phase 3 (beta=0.0800, SE=0.0264, t=3.0271, p=0.0044). Females sampled 80ms longer than males. No other interaction terms were significant. This difference was shorter than for the phase 4 behavior, which showed a sex difference of 51ms.

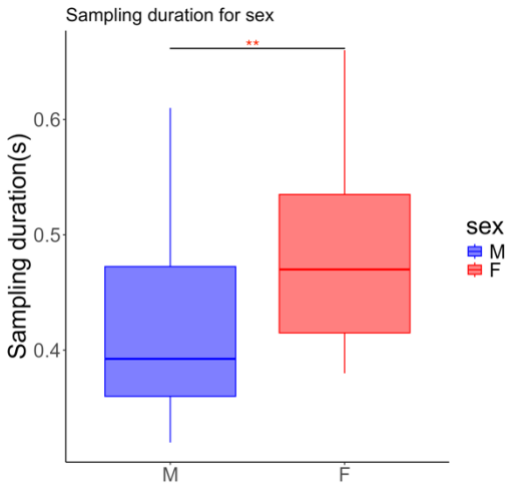

Figure 5.2 Sampling duration for sex including phase 3
Sampling duration for sex calculated by pooled phase 3 and 4 data (include last day of training for both coarse and fine pairs and four days of testing).

OB gamma power

When including the last training day (phase 3) data, OB gamma power analysis shows similar main effects of day and events compared to phase 4 analysis alone, but more interaction terms are significant in the GLS, including those that involve odor stimulus type (coarse vs. fine), which were not significant in phase 4 analysis alone. This is likely due to including

interactions for learning phase and sex, which lead to more levels in group analysis, hence capturing more interaction group variance. See table 5.1 for GLS significant variables result.

Table 5.1 GLS on OB gamma power significant terms				
Term	**beta**	**SE**	**t**	**p**
day3	0.8762	0.1386	6.3205	0.0000
day4	0.7965	0.1386	5.7456	0.0000
eventpostnspk	0.1847	0.0759	2.4319	0.0154
eventprenspk	-0.2137	0.0759	-2.8140	0.0051
day2:sex2	0.3399	0.1386	2.4521	0.0146
day3:sex2	-1.1328	0.1386	-8.1717	0.0000
cue1:day1	-0.4921	0.1960	-2.5099	0.0124
cue1:day3	-1.0052	0.1960	-5.1272	0.0000
cue1:day4	-1.8451	0.1960	-9.4113	0.0000
coarsefine2:cue1	-0.4224	0.1475	-2.8646	0.0044
day3:learningph2	-1.5030	0.1386	-10.8419	0.0000
cue1:day3:sex2	1.2514	0.2024	6.1831	0.0000
cue1:day4:sex2	1.1369	0.2024	5.6176	0.0000
coarsefine2:cue1:day3	0.5154	0.2024	2.5466	0.0112
cue1:day1:learningph2	0.7069	0.2024	3.4927	0.0005
cue1:day2:learningph2	-0.6341	0.2024	-3.1332	0.0018
cue1:day3:learningph2	1.7335	0.2024	8.5655	0.0000
cue1:day4:learningph2	-0.4924	0.2024	-2.4330	0.0154

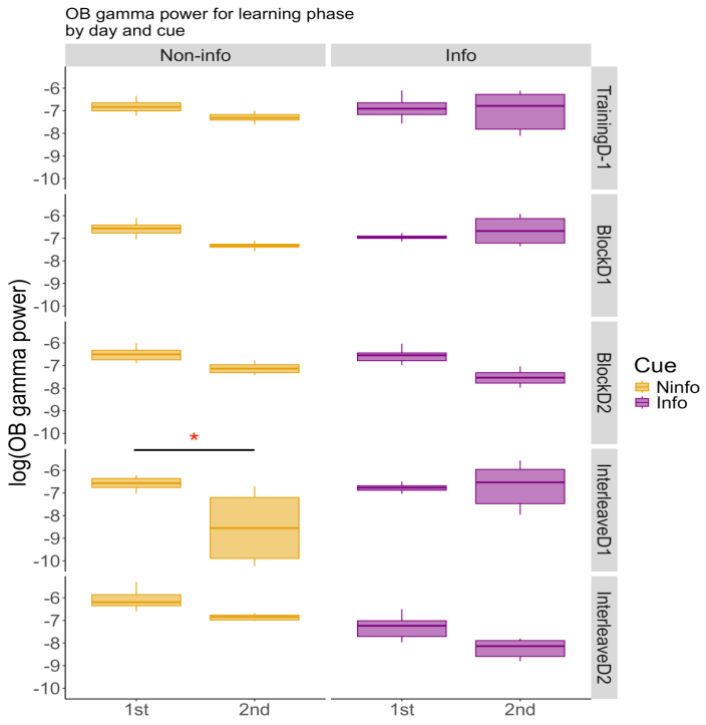

Figure 5.3 OB gamma power including phase 3 by three interactions of cue, day, learning phase
Horizontal: cue conditions; vertical: test days. Non labeled comparisons for learning phase 1 and 2 aren't significant. *p<0.05

A multiple comparison test with Bonferroni correction shows that OB gamma power on the first interleaved day for non-informative rats is higher for the first odor set learned than the second (p=0.0491, see figure 5.3). There was no sex difference in OB gamma power.

OB beta power

We examined beta power in a GLS including phase 3 and 4 data, including analysis of interactions of sex and learning phase. We found a main effect odor stimulus type. Fine odor trials produce less beta power in the OB compared to coarse trials. One difference emerged when including the Phase 3 data as compared to the Phase 4 data alone. The odor stimulus and event interactions that were significant for phase 4 data now are not significant when phase 3 is included. Instead, we observe a uniform odor stimulus fixed effects across events. This indicates that beta oscillation patterns in the OB become more complicated in their dynamics during phase 4. We also found a main effect of the first day of interleaved testing (day 3) and significant interactions between cue and day as we saw in phase 4 analysis. OB beta power is lower on day 3 compared to the last day of training. Learning phase was not significant in predicting beta power in the OB, including interactions, meaning that beta power did not vary dependent on whether the odor set was the first or second set learned. Sex was a significant predictor of OB beta power, as it was when including only the phase 4 data. Beta power in the OB is lower for females than for males.

Table 5.2 GLS on OB beta power significant terms

Variable	**beta**	**SE**	**t**	**p**
Odor stimulus type	-0.3926	0.1550	-2.5321	0.0117
day3	-0.8928	0.1550	-5.7584	0.0000
sex2	-0.9126	0.2702	-3.3782	0.0008
cue1:day3	0.9580	0.2292	4.1803	0.0000
cue1:day4	-0.6381	0.2292	-2.7844	0.0056
cue1:eventpostnspkoff	0.3829	0.1709	2.2402	0.0256

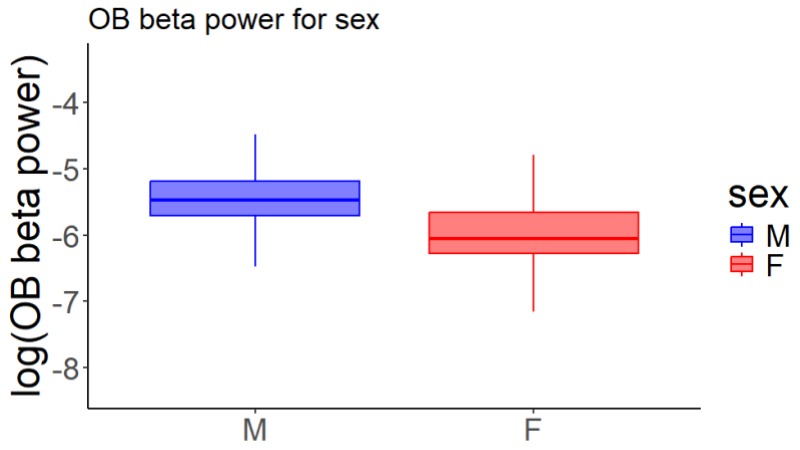

Figure 5.4 OB beta power by sex including phase 3 data

Coherence

To address the question whether there is a difference in the network depending on whether the odor set is learned as the first or second set of odors tested , we examined coherence across the network we recorded (OB, PC, DG, CA1, and TC) on last day of training (TD or day -1), and day 3 of testing, or first day of interleaved test. We calculated the 95% confidence intervals of coherence during each event period for each area pair. We choose day 3 to compare to the TD because day 3 was when most coherence effects appeared in phase 4 analysis (Chapter 4). Coherence during the first odor set last day of training shows visible differences from that during the second odor set last day of training, as well as on day 3.

For the informative group, on TD and day 3, OB-DG coherence across theta, beta and gamma bands and across events is higher in learning phase 2 (when the odor set was learned second) compared to learning phase 1 (the odor set was learned first). OB-PC beta coherence during pre- and post-response is higher for the second odor set than the first. PC-DG beta coherence is higher for learning phase 2 than learning phase 1. See figure 5.5.

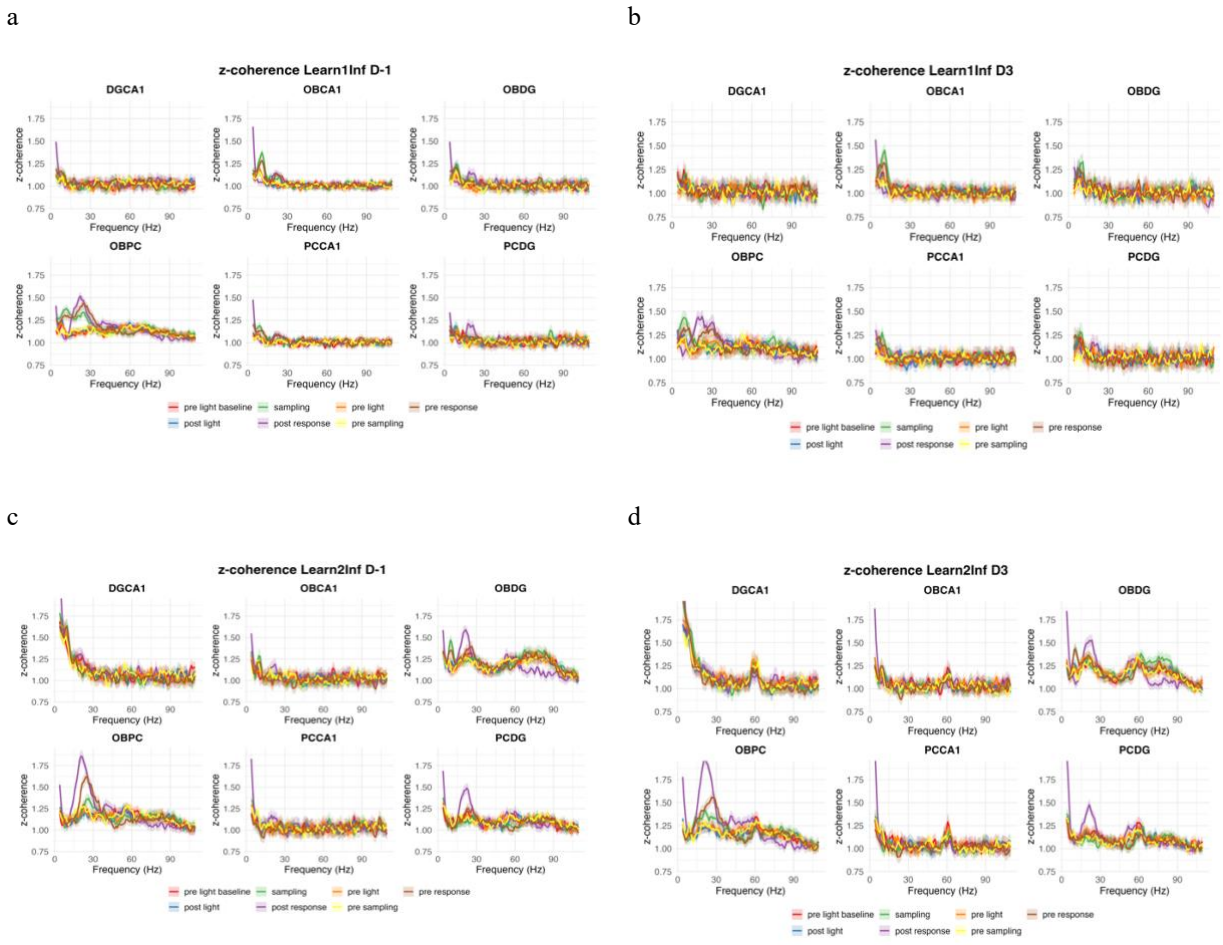

Figure 5.5 Network coherence between OB, PC, DG, CA1 for informative group
a-b. learning phase 1 c-d. learning phase 2 a.c. Last day of training b.d. first day of interleaved test
Event intervals indicated by colors

For the non-informative group, we found a pattern of higher coherence in beta and gamma bands for the second relative to the first learned odor set. On both TD and day 3, OB-PC beta coherence around the response time (during the pre- and post-response period) was higher for the second learned odor set than the first. On TD, PC-CA1 beta coherence during odor sampling and around the response time and gamma2 coherence during the periods from just before odor sampling until after the response was higher for second learned odor set than the first. On day 3, PC-CA1 beta coherence around the response and gamma2 and gamma coherence before and during odor sampling was higher for second than the first learned odor set. From TD to day 3 for second odor set, during odor sampling, PC-CA1 coherence also shifts up in frequency, from ~20 to ~40 Hz.

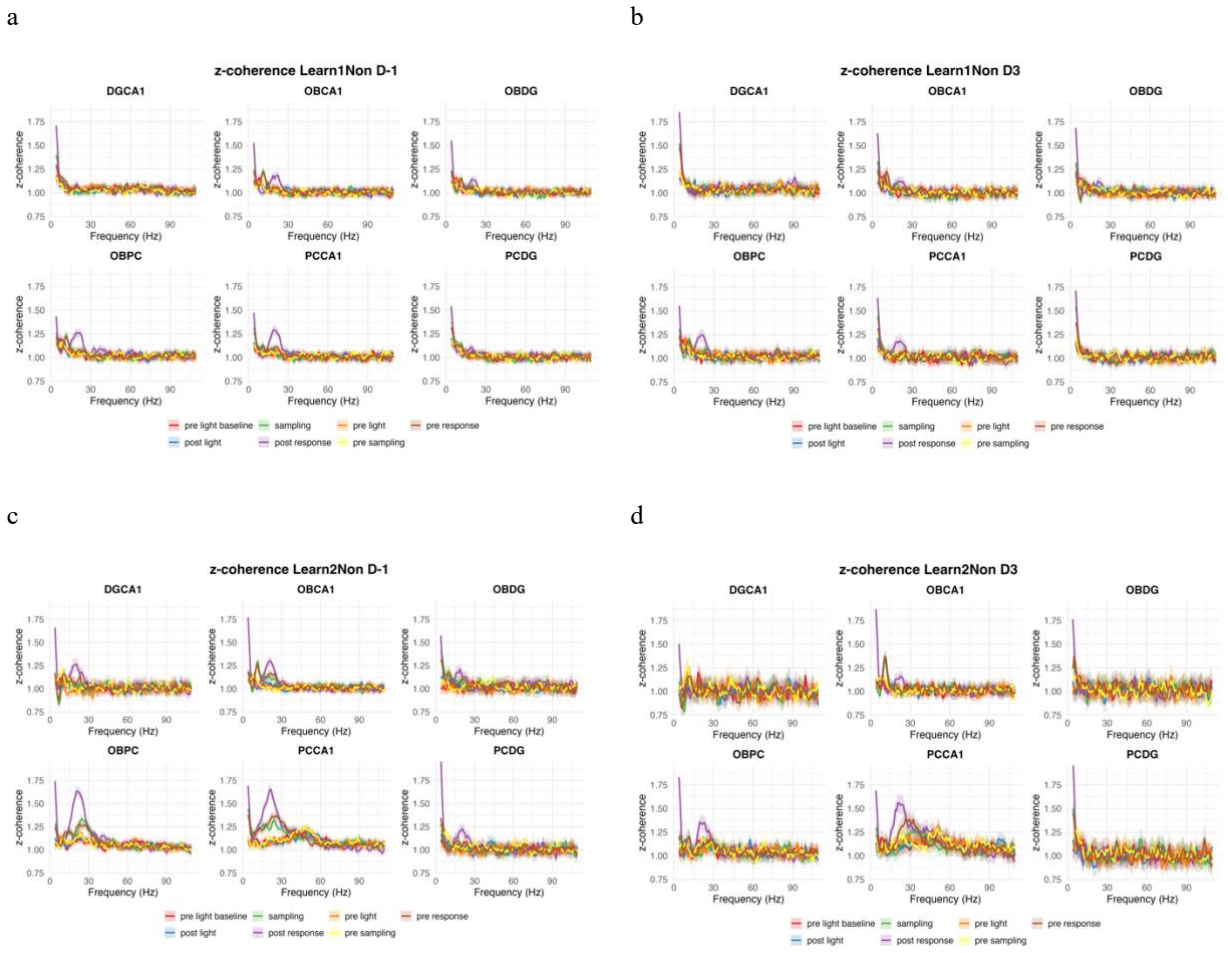

Figure 5.6 Network coherence between OB, PC, DG, CA1 for non-informative group
a-b. learning phase 1 c-d. learning phase 2 a.c. Last day of training b.d. first day of interleaved test
Event intervals indicated by colors

For the informative group, respiratory coherence showed effects of learning phase. Coherence in the theta band between CA1 activity and respiration was elevated for the odor set learned second compared to that learned first, on both the TD and day 3, across events. While for the first odor set learned, from the TD to day 3, respiration coherence in all areas increased during odor sampling, this was not the case for the second odor set.

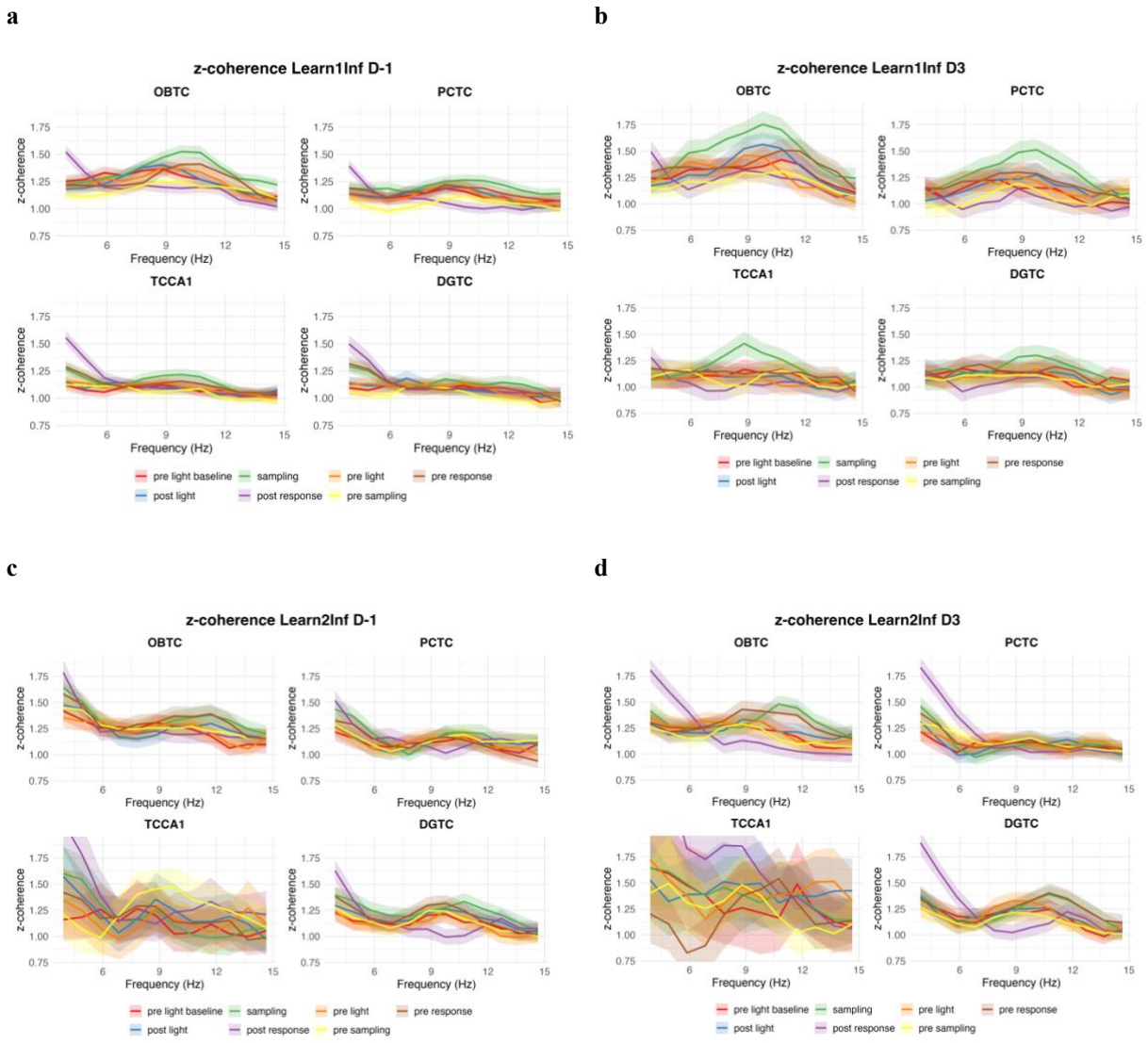

Figure 5.7 Respiration coherence with OB, PC, DG, CA1 for informative group
a-b. learning phase 1 c-d. learning phase 2 a.c. Last day of training b.d. first day of interleaved test
Event intervals indicated by colors

For the non-informative group, respiration coherence with OB on day 3 is elevated during pre-light baseline and before odor sampling for the first odor set learned but not the second. DG respiration coherence on TD during odor sampling and before the response is higher for second learned odor set than for the first.

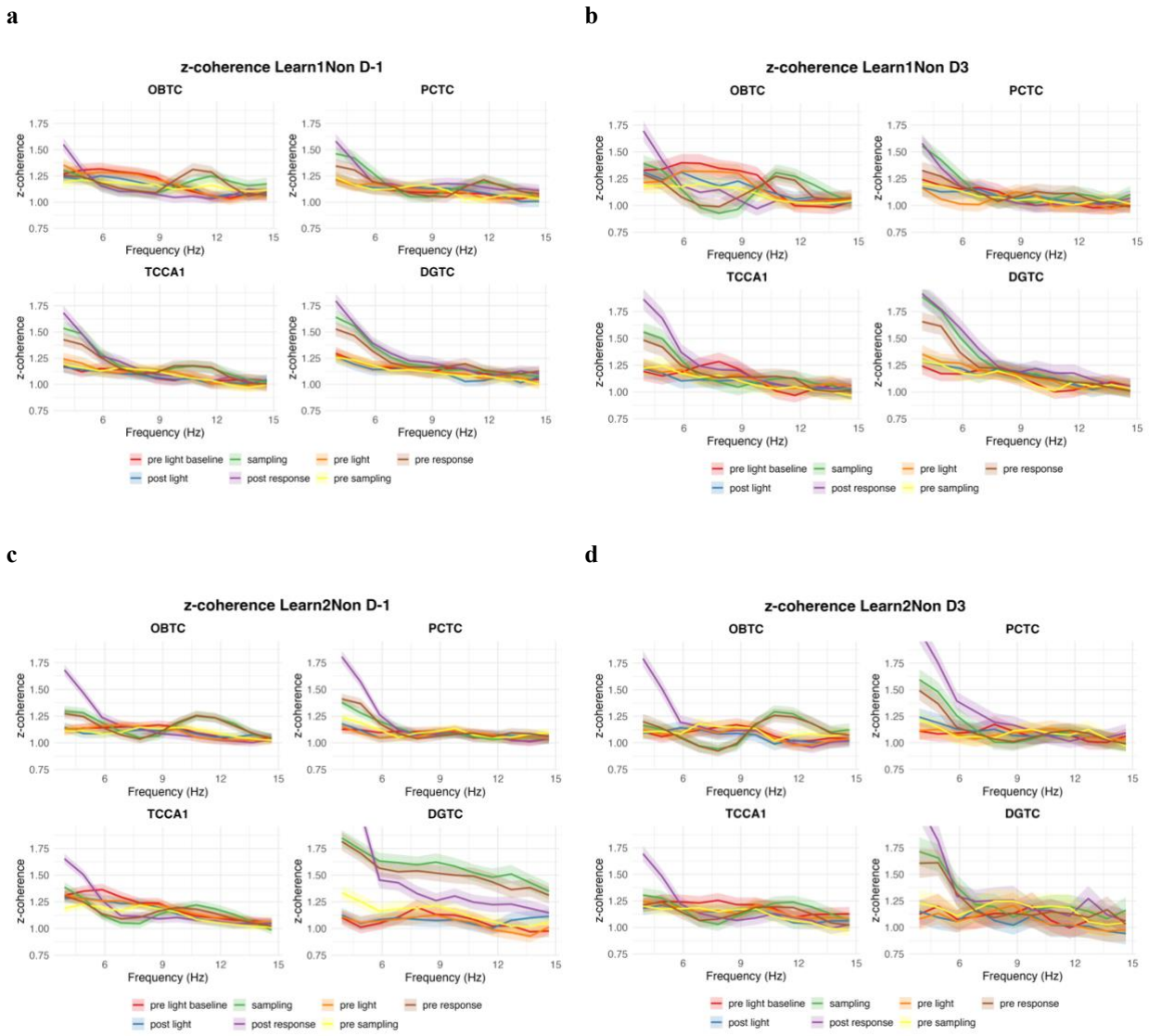

Figure 5.8 Respiration coherence with OB, PC, DG, CA1 for non-formative group
a-b. learning phase 1 c-d. learning phase 2 a.c. Last day of training b.d. first day of interleaved test
Event intervals indicated by colors

In summary, by including analysis of the temporal learning order including the learning of individual fine and coarse odor pairs, we uncover changes that occur in behavior, OB dynamics, and system connectivity when the rats move from the less difficult task (2-odor discrimination) to the more difficult 4-odor identification task and as they do this a second time as compared to the first time that they encounter the 4-odor interleaved task. The findings are

consistent with the idea that the first-time rats encounter a change in task is different than the second time they encounter the same change in the same task. The olfactory-hippocampal network adapts to the changes in the task and reflects the adaptations through changes in behaviors and neural dynamics. Behavior differences become smaller in the second odor set learning between the informative group and non-informative groups, but neural dynamic differences start appearing the first time they encounter the 4-odor task and become larger during the second time they perform the task. The two groups of rats in different cue conditions adapt differently.

One puzzling question is the large difference in sampling times between the two groups on the last day of fine and coarse training for the first odor set. The only difference in training or testing to this point is the cue light. The informative group rats trained with the left light as a cue to start the trial for several days with the coarse odor set, followed by several days with the right light while they learned the first fine odor set. At no point did these lights confer extra information for the upcoming odor until the rats were presented with the first four-odor test. Is it possible that this small change in the environment is enough to drive a large difference in behavior?

This analysis also allows us to explicate sex differences that appeared in the previous chapter. We replicate other findings in the lab in which we've identified sex differences in sampling time, with females sampling for more time than males in operant tasks(Kay, 2025) and less time than males in non-appetitive odor habituation(Maheshwar et al., 2025). We also found here that females show lower power beta oscillations than males, similar to our findings in that same study, but we did not find that females had lower amplitude gamma oscillations as that

study showed. We expect that this difference is driven by the difference between the operant appetitive task and the habituation condition.

Chapter 6: Trigeminal and olfactory interactions

This chapter is based on a published manuscript. We investigated the effect of trigeminal system input on the olfactory system. While the previous chapters address the cognitive processes related to olfaction, chapter 6 supports further investigations on factors that impact olfactory perception on the sensory side.

Introduction

The ability to discriminate and identify odors plays an important role for many animal species, because they rely on the sense of smell to eat, mate and detect danger. Most natural odors are compounds of large numbers of molecules. For instance, a natural floral scent could contain hundreds of components(Levin et al., 2003). Despite the complexity of natural odors, most olfactory research in rodents has relied on monomolecular odorants or has used mixtures assuming that equal concentrations result in equal perceptibility. Understanding the quality of mixtures appears a simple problem at first – examine the receptor or glomerular input patterns and add them together in the way that one might for different colors of light that combine to form a visual percept. However, predicting what a mixture of even just two odorants will smell like remains a difficult task(Frederick et al., 2011; Kay, 2005). While similarity in quality between complex mixtures can be predicted to some degree in humans(Ravia et al., 2020), we still do not understand the physiological mechanism for this process in rats or humans.

The factors that lead to the complexity of odor mixtures often stem from peripheral effects. Odorant sorptiveness can affect the detectability of components in a binary mixture(Rojas-Líbano & Kay, 2012). Glomerular activation patterns from mixtures can be quite

different from their components(Grossman et al., 2008). Early work hinted at nonlinear effects due to inhibition in mixtures at receptors(Araneda et al., 2000), and knowing about these interactions can help predict some aspects of odor quality(Kay, 2003). Recent work from the Firestein lab shows massive inhibitory interactions occur among components of odor blends at the level of the odor receptors on the olfactory sensory neurons(Xu et al., 2020). This inhibition may be the force behind the subtlety of perfumery and odor accord profiles.

The trigeminal profile of component odorants may also affect mixture quality. Trigeminality or chemesthesis is responsible for the sensations of hot, cold and irritation from substances like chiles, mint and CO_2, and these sensations are supported by many types of Transient Receptor Potential (TRP) cation channels on the trigeminal nerve. Research on TRP channels and their role in trigeminal sensations has provided evidence for the integral role the trigeminal system plays in olfactory experience(Baxter et al., 2021; Hansen & Finger, 2008; Silver et al., 2006).

Most odorants have trigeminal properties, and stimulation of the trigeminal nerve in the nasal epithelium can influence odor detection and recognition(Hummel & Livermore, 2002; Jacquot et al., 2004, 2010), sensitivity(Buron et al., 2009; Frasnelli et al., 2011; Galliot et al., 2012), perceptual memorability(Han et al., 2018) and intensity(Kobal & Hummel, 1988; Livermore et al., 1992; Murphy & Cain, 1980).

There is a direct neuromodulatory route from the trigeminal ganglion to the olfactory bulb (OB)(Schaefer et al., 2002). Trigeminal nerve endings release CGRP and substance P in the nasal epithelium when stimulated, and some collaterals of the trigeminal nerve enter the olfactory bulb with the olfactory nerve, where the same neuromodulators can affect OB neuron firing in response to odors(Finger & Böttger, 1993; Genovese et al., 2017; Messlinger et al.,

2020; Schaefer et al., 2002; Stanić et al., 2010). Trigeminal stimulation has been shown to influence the intensity of odorants both positively and negatively in humans(Kobal & Hummel, 1988; Livermore et al., 1992; Murphy & Cain, 1980).

All of these factors suggest a role for trigeminal stimulation in the perceptual quality of mixtures. The perceptual quality of binary mixtures can be categorized as elemental (component odors are recognized), configural (synthetic percepts in which the components are not recognized), and overshadowing (the mixture smells like one of the odorants)(Coureaud et al., 2009, 2020; Kay, 2003; Kay et al., 2003, 2005; Linster & Smith, 1999; Wiltrout et al., 2003). We hypothesize here that because trigeminal stimulation can affect detection of odorants, it could play a significant role in binary odor mixture perception. Specifically, we expect that trigeminal activation can contribute to overshadowing in binary mixtures. Our paradigm is designed to examine detectability of individual odorants in mixtures. Trigeminal activation can make odors more or less detectable. Thus, we expected that strong trigeminal stimulation would boost or suppress detection or learning of individual odors, contributing to differences in detectability of the components of a binary mixture. This would show up perceptually as overshadowing.

Based on limited knowledge of the trigeminal profiles of a few odorants, we test our hypothesis by controlling the trigeminal difference in the two component odorants in binary mixtures. We expect an odor mixture with component odorants of greater trigeminal difference to show greater overshadowing of one component by the other, or greater differences in detectability of the two odorants.

We tested the overshadowing effects of binary odor mixtures at varying combination ratios to determine the degree of overshadowing. We trained rats to respond to the two pure mixture components and then show us in a partial reinforcement two-alternative choice (TAC)

paradigm whether various mixture ratios smell more like one or the other component. We expected binary odor mixture psychophysical curves to have inflection points which depend on the difference in trigeminality instead of symmetric curves with inflection points at equal vapor phase concentration of the two odorants.

We further expected that the more different the trigeminal intensities of the components, the further away the point at which the two components are equally recognizable (inflection point) would be from equal concentrations of the two odorants. The direction of shift was predicted to be either toward the more or less trigeminal odorant.

Materials and Methods

Subjects

Adult Sprague Dawley rats were purchased from Envigo, Indianapolis, IN and began training at 8-10 weeks of age. We began with 6 males and 6 females, but 1 male and 1 female were excluded for failure to learn the task. We did not track estrus stage of the female rats, because female rats and mice do not produce more variable results than males across many measures(Becker et al., 2016; Prendergast et al., 2014), and we assumed that testing over the many weeks would randomize any rhythmicity in female rats' variability. Furthermore, testing of the ten rats was not synchronous, smaller subgroups were trained and tested in sequence, which would further smooth out any possible rhythmicity. Therefore, all rats were trained and tested in the same way regardless of sex.

Rats were dieted to 85% of their *ad libitum* weight before beginning training and were maintained on a restricted food schedule for the duration of the experiment. All rats were housed singly in standard housing cages with filter tops and maintained on a 14/10 hour light/dark cycle

(lights on at 8:00 A.M. CST). All experiments were performed during the light phase between 9 am and 6 pm CST to avoid exposing rats to light during the dark phase(Bedrosian et al., 2013; Travlos et al., 2001). To avoid variance within subjects across days due to circadian effects and to enable behavioral entrainment to the rewards given at the time of testing, each rat was tested in a set time window on each testing day(Carneiro & Araujo, 2012). All experimental procedures were done under veterinary supervision with approval and oversight by the University of Chicago Institutional Animal Care and Use Committee, according to the Association for Assessment and Accreditation of Laboratory Animal Care guidelines.

Apparatus

All experiments were conducted in two identical operant chambers with identical odor delivery systems. Operant chambers (ENV-008, Med Associates, Georgia, VT) and odor delivery systems were modified based on established protocols in our lab (Frederick et al. 2011), to be able to deliver 7 combinations of binary mixtures (Solenoid manifolds were NR Research 225T092, and flow meters were MasterFlex MFLX32003 series). Saturated vapor was maintained by bubbling clean air through columns of pure liquid odorants. To control for differences in volatility between the odorants in an odor set, flow rates of each component odorant in each odor set were adjusted in inverse ratio to the ratio of the theoretical vapor pressures of the two odorants. For mixtures, separate lines for each odorant were combined and then combined with plain air. See Table 6.1 and Section 2.4 (Testing) for details on ratios. All odorized air was combined with a diluting clean air stream of 1 LPM. The odor lines were charged for one second before the rats could trigger odor delivery, with odorant removed by the

vacuum line just before the odor port until the nosepoke occurred. Timing of event inputs and outputs were controlled and logged by a computer running MedAssociates MedPC IV software.

Two-Alternative Choice paradigm - training

All rats were trained to perform a Two Alternative Choice (TAC) behavior once they reached their respective 85% *ad libitum* weights. The TAC protocol trains rats to associate each of two different monomolecular odorants (saturated vapor from a single odorant mixed into the plain air stream) with one of two nose poke ports (left/right) in three phases. Rats were trained to associate odor A with the left port and odor B with the right port for all odor sets. Previous experiments have shown that in this TAC task, rats do not maintain a side bias after training, and therefore we did not balance the side of the two odors across subjects(Frederick et al., 2011, 2017).

Phase 1: Rats were trained to poke their nose into the odor port on the center of the front aluminum wall upon house light signal onset. Every time rats poked into the odor port, one 45 mg sugar pellet was dispensed as a reward (Bioserv 45 mg Dustless Precision Pellets). The odor port delivered odorants when rats had their nose inside the port, which was detected by an infrared (IR) detector situated at the edge of the odor port. For phases 1 and 2, the odor was amyl acetate. A vacuum line was always on, removing any odor from the supply line just before the odor port, unless the IR beam was disrupted. Thus, odor delivery, triggered by IR beam interruption during the nose poke, had a very short delay, on the order of a few tens of milliseconds. The odor stayed on as long as the beam was disrupted. Only one odor sampling period was allowed during each trial. Rats successfully learned phase 1 (50 correct trials) in 2.3+/-0.5 days.

Phase 2: Rats were trained to associate Odor A with the left response port. Every time rats sampled from the center odor port and then nose poked at the left response port within 5s, one sugar pellet was dispensed as a reward. Rats reach above 95% accuracy in 2.6+/-1.3 days.

Phase 3A: Rats were trained to associate Odor B with the right response port. During training, odor B was anisole. Odor A or B was randomly chosen on each trial. Rats received a reward for all correct responses (left port Odor A and right port Odor B) made within 5 seconds after nose withdrawal from the odor port. Rats trained on Phase 3A (8.7 +/-3.4 days) until they performed at 70% accuracy or better for two consecutive days.

Phase 3B: Rats were trained to perform the learned association with partial reward, Starting at 90% reinforcement and dropping to 60% in 10% decrements. Each rat was trained at 100% reinforcement for each odor pair and then reduced to 60% reward probability. By the end of phase 3B, all rats included completed 300 attempts in one session on each training day and performed at over 70% accuracy with 60% reward probability for two consecutive days.

Testing

Rats performed the above training with two sets of training odors before being tested on treatment odor sets. The first training set was for task learning; the second training set was to avoid transition (rule transfer) effects(Frederick et al., 2017). Training of the first training odor set (OS0) was composed of Phases 1, 2, and 3 described above. Training of all other odor sets began with phase 3. Only treatment odor sets were used in Phase 4, the testing phase.

Phase 4: Rats performed the same odor discrimination task they had learned, not only with odorants A and odorant B, but also with binary mixtures of odorants A and B. On each trial, either a pure odorant was chosen randomly between odorant A(100%A-0%B) and odorant

B(0%A-100%B), or a binary mixture at one of 5 ratios was selected. The 5 ratios were 75%A-25%B, 55%A-45%B, 50%A-50%B, 45%A-55%B, 25%A-75%B (the percent symbol for combination ratios are omitted in later passages for convenience). Percentages reflect partial flows of the respective pure odorants' saturated vapor.

Flow rates were adjusted to account for the relative theoretical vapor pressures (volatilities) of the two odorants, and all odorants were then mixed with plain air. Pure odorant A and pure odorant B flows were calculated so that the ratio of flows equals the inverse ratio of their respective theoretical vapor pressures at 25 deg C. In other words, theoretical intensities of 100% A and 100% B are controlled to be the same. A binary mixture composed of 50% flow of odorant A's pure odorant and 50% flow of odorant B's pure odorant thus has, theoretically, two equal components in terms of vapor phase concentration. In the binary mixture, when the percentage of odorant A is higher, it reflects that the binary mixture is composed of more A than B molecules. The odor flows (ranging from 0.01 LPM to 0.2 LPM) were then mixed with plain air at 1 LPM.

The number of trials was controlled so that there were 300 total trials, composed of 200 pure A or B trials (evenly divided between odorant A and odorant B) and 100 mixture trials (evenly divided between the five kinds of mixture types) with the order of all trial types randomized. The reward probability for monomolecular odorant (odorant A or B only) correct trials was 80%, and the reward probability for all mixture trials was 20%, regardless of which odor port was chosen. This enabled the overall reward probability to be kept at 60% without biasing rats' responses to mixture trials due to learning a reward influence. For each trial, the rat's response (left or right port) was recorded. If a response to a pure odorant (100% A or B)

trial was incorrect, the normal 7s penalty delay was imposed. There was no penalty for not responding and no penalties on mixture trials.

Phase 4 spanned 2 days for each odor set. During these two consecutive days, rats performed the session described above. A session ended when rats completed 300 trials. All rats were able to meet this criterion for at least 2 odor sets not including training and transition odor sets. Due to shutdown of the lab at the beginning of the pandemic, long delays between odor sets resulted in failure of some rats to reach criterion performance on some of the odor sets. The final number of rats that completed odor sets 1-4, respectively, is 6, 10, 7, 8.

Odors

Research with humans who are anosmic provides a psychological measure of trigeminal intensity for some odorants. Combining such information with the list of agonists and antagonists of the relatively well-studied TRP channel families, we selected 4 sets of odorants as the component odorants of binary mixtures. Odorants are matched based on their estimated trigeminal profiles (from human data) and volatilities. Table 6.1 displays all odor set pairing details.

Table 6.1 Odor sets specifics								
	Odorant A	VP @ 25C (Pa)	TRP	100% Flow (LPM)	Odorant B	VP @ 25C (Pa)	TRP	100% Flow (LPM)
OS0 (Training)	Amyl acetate	650	-	0.15	Anisole	472	-	0.15
OS00 (Transition)	Butyl acetate	1533	-	0.15	Hexanol	124	-	0.15
OS1	Eugenol	2.95	V1, V3, A1, M8	0.2	PEA	11.57	-	0.05
OS2	Eucalyptol	253.31	A1, M8	0.16	(+)-Limonene	205.5	A1	0.2
OS3	Eugenol	2.95	V1, V3, A1, M8	0.2	Cinnam-aldehyde	3.85	A1	0.16
OS4	Citral	12.17	V3	0.19	PEA	11.57	-	0.2

Of the four odor sets (OS), OS1 (eugenol/PEA) and OS4 (citral/PEA) have the best documented large trigeminal difference(Doty et al., 1978; Lübbert et al., 2013). PEA is the only known odorant that is liquid at room temperature and very low in trigeminal intensity. OS3 (eugenol/cinnamaldehyde) has components that have relatively similar trigeminal profiles; their TRP channel activation profiles overlap, and both have been rated as trigeminal odors in human anosmia research(Bandell et al., 2004; Doty et al., 1978; Kollndorfer et al., 2015). OS2 (eucalyptol/(+)limonene) has components that have possibly close trigeminal intensities; however, limonene is likely to be of lower trigeminal intensity than eucalyptol according to TRP channel activation profiles(Chandorkar et al., 2021; Kaimoto et al., 2016; Nilius & Owsianik, 2011; Takaishi et al., 2012) and human research data(Doty et al., 1978; Kobal & Hummel, 1988). Despite limited data on limonene trigeminal intensity in animal research, given the similarity between the human and rat olfactory systems, we use human data as a guideline. The vendor and CAS numbers for all odorants used are: PEA (Sigma-Aldrich, 60-12-8), eugenol

(Sigma-Aldrich, 97-53-0), citral (Fluka, 5392-40-5), cinnamaldehyde (Sigma-Aldrich, 14371-10-9), (+)limonene (Sigma-Aldrich, 5989-27-5), eucalyptol (Sigma-Aldrich, 470-82-6).

Analysis

Analysis was guided by two goals: 1) characterization of individual odorant recognizability in binary mixtures when component ratio is equalized in the vapor phase (the 50-50 mixtures), and 2) investigation of the effect of trigeminal difference on response frequencies to component odorants of the binary odor mixture. Both of these goals are focused on understanding deviations from symmetry of a psychometric curve around the 50-50 point.

Based on our design, there are four independent variables in the analysis: combination ratios, odor set, sex, and testing day. There are two dependent variables, response and sampling duration. For each trial, sampling duration, response delay, and response side (left/A or right/B) were recorded. Sampling durations and responses are calculated as below.

Response: for each trial, the odor combination ratio and the port that the rat responded to were recorded. The binary values (left or right) for each combination ratio were then calculated into a continuous session parameter with possible values ranging from 0 to 1. The final dependent variable response intensity for each combination ratio is calculated as [n go left/N total] for each odor combination ratio. While the code was written to exclude trials in which rats did not respond, there were no such trials in the data set.

Sampling Duration: the amount of time that the rat had its nose in the odor port (time between nose entry and exit). Although rats were free to nose-poke again, the odorant was on only for the duration of the first nose-poke. Therefore, we used only the time for which the animal could receive odorant.

Univariate and multivariate ANOVAs were conducted in R using the function *aov*. For analysis of response, interaction terms were selected with a focus on combination ratio, because we expected combination ratio to be a significant factor. Hence, to check for latent learning effects based on combination ratios due to 2 days of testing, we included the interaction between combination ratio and test day in the model. To determine whether different mixtures produced different response patterns across the combination ratios, we included interaction between combination ratio and odor set.

Bootstrapping was conducted using a custom function based on the R functions *slice_sample* and *replicate*. Grouping was based on rat, odor set, and combination ratio. Within each group, sampling (n=36, to match approximately the number of our data points) was done with replacement, with 1001 iterations. Bimodality tests were conducted with R using the function *bimodality_coefficient* in the mousetrap package(Wulff et al., 2021 preprint). Logistic regression was conducted with the R *glm* function. T-tests were conducted with the R function *t_test*.

Cohen's d and partial eta-square (η^2_p) statistics were used to evaluate effect sizes. Cohen's d was calculated based on pilot data to determine effect size and subject numbers. Using the mean response intensity from 6 rats on OS1, we simulated data with group mean response intensity as 0.5 at 50A-50B. The standard deviation for the simulated no-effect outcome was assumed to be the same as that of the pilot data. Six subjects produced a large effect size (Cohen's d = 2.1805436), so our 10 subjects are a large enough sample to evaluate our hypothesis. Partial eta squared was calculated with R using the function *partial_eta_squared* based on ANOVA results.

Unless otherwise stated within the text, all analysis was conducted with an alpha value of 0.05. Analyses were done in MATLAB (vR2017a) and R (version 4.0.3). Statistical results are reported in the text.

Results

We hypothesized that the relative trigeminal strengths of the two odorants in each mixture would have differing effects on the perceptual quality of odorants. To test this hypothesis, we trained rats in a TAC task to indicate whether the binary mixture smelled more like one component or the other. We tested rats across four odor sets chosen for their trigeminal differences. There was no difference in phase 3 learning rate across the four test odor sets ($p=0.48$). Rats learned all odor sets in 3.5 +/- 1.1 days.

Perceptual qualities of binary mixtures vary in different manners across combination ratios

We used the Left/Right response ratios for each mixture to determine whether there were significant differences across mixture ratios and odor sets in addition to the influence of sex and test day. We performed a repeated measures multi-way ANOVA on the dependent variable response (proportion of left side responses, where 1=left 100% of the time and 0=right 100% of the time) and the independent variables combination ratio, test day, sex, and odor set. We also tested for interactions between combination ratio and test day, and combination ratio and odor set, assuming there would be differences in how rats respond to ratios that depend on either the odor set or on slow learning of the mixtures. We found a significant main effect of combination

ratio on response ($F(1,440) = 312$, $p < 0.001$) with a large effect size ($\eta^2_p = 0.41$). We also found a significant main effect of odor set on response ($F(1,440) = 11.26$, $p < 0.001$). Both combination ratio and odor set influenced perceptual qualities of the binary odor mixtures, meaning whether the rats responded more to one component or the other depended on the ratio and the odor set. No other variables, test day, sex, interaction between combination ratio and test day, or interaction between combination ratio and odor set showed significant effects. Of the two interaction terms included, the interaction between combination ratio and odor set, contrary to our expectations, does not significantly predict response. It is possible that given the logistic nature of response on all odor sets, the multi-way ANOVA does not offer the sensitivity required to capture the fine differences in response side on the combination ratios around 50A-50B. The main effect of odor set supports our hypothesis that different binary mixtures have different characteristic psychometric curves. The following analysis for response collapses data across test days and sex. Figure 6.1 (A)-(D) shows the mean responses to the left (odor A) operant port for all odor sets plotted against the percentage of odor A in each mixture A and B. For each odor set, the mean go-left frequency for all rats that finished the odor set (n = 6, 10, 7, 8, for the 4 odor sets), at 7 odor combination ratios, is calculated across days and sessions. Variances for combination ratios around 1:1 (45A-55B, 50A-50B, 55A-45B) are higher than at the extremes (0A-100B and 100A-0B) for all odor sets, consistent with the expectation that when the odorants are in equal measure in the mixture, the perceptual quality is more ambiguous and the response more variable.

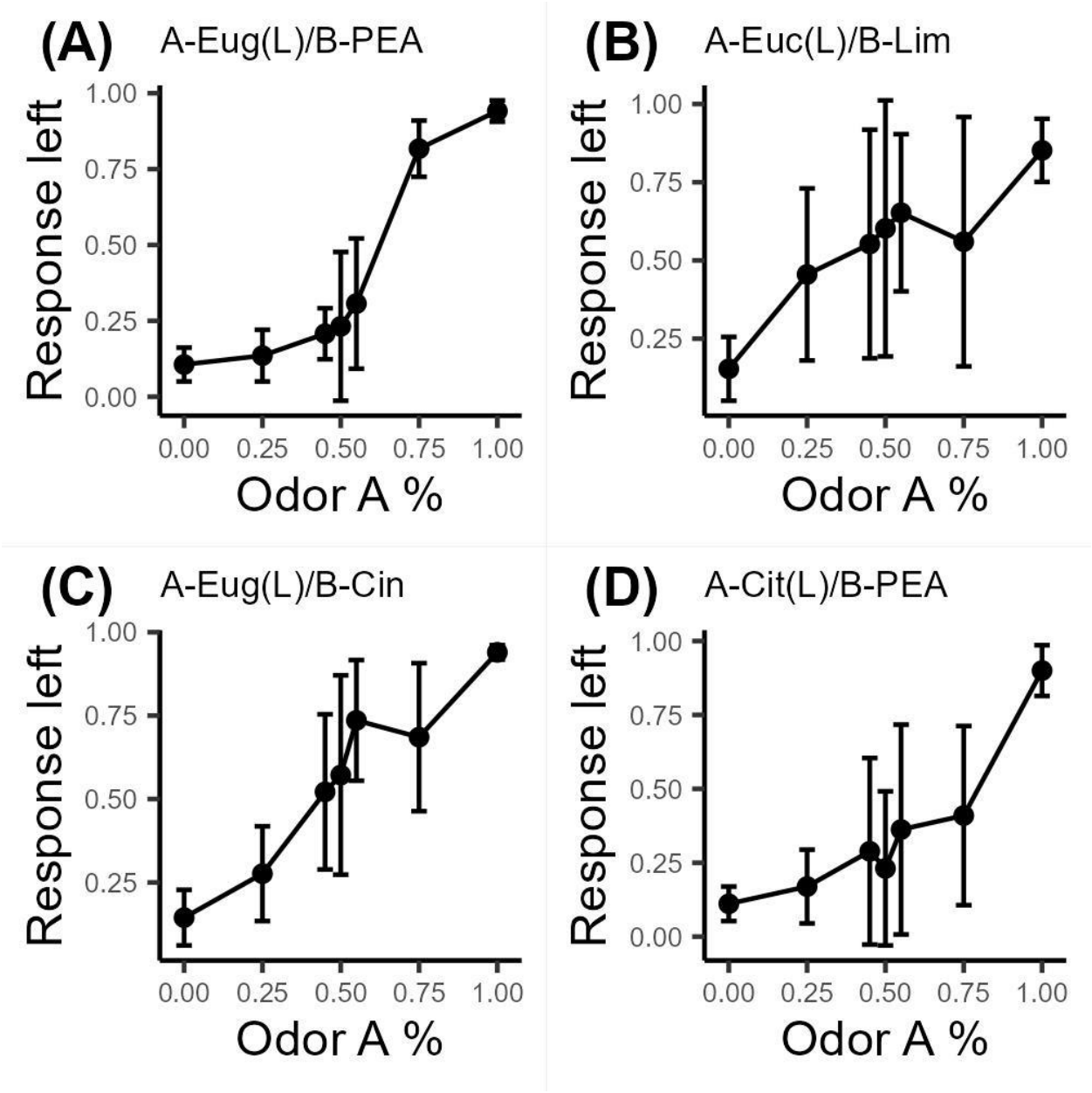

Figure 6.1 Response intensity to the left port of each odor set.
Response intensity is calculated as [n go left/N total] for each odor combination ratio. Odorant A corresponds to the left port. Error bars are based on standard deviation. All odor sets show a logistic trend. Variances at extreme combination ratios (0A and 100A) are smaller than those of other combination ratios for all OS. Figure (A)-(D): (A) n = 6, OS1: Eug/PEA; (B) n = 10, OS2: Euc/Lim; (C) n = 7, OS3: Eug/Cin; (D) n = 8, OS4: Cit/PEA.

Variance within an odor set was large in some cases. The variance for the Eugenol/PEA odor set appeared smaller than that of the other three odor sets. Based on the raw data

distributions, we noted that within some odor sets, rats showed apparent subgroups in response patterns. For instance, odor set 2, Eucalyptol/Limonene shows two possible groups. Therefore, we conducted further variance analysis to determine whether there were subgroups in responding within odor sets.

For each combination ratio, we generated bootstrapped responses from all subjects. We then computed a bimodality coefficient (BC) on the bootstrapped responses for each odor mixture ratio within each odor set using functions in the R package, Mousetrap, to calculate the BCs (Pfister *et al.*, 2013). Our criteria for significant subgroups were based on the BCs value and the number of high BC values in consecutive order in each odor set. The criterion for the distribution of response on each combination ratio to be significantly bimodal is a BC > 0.555. To determine whether the distributions of overall responses were bimodal, we required the BCs of at least four adjacent combination ratios within that odor set to be > 0.555. Furthermore, we required that the bimodality be driven primarily by the same subjects within each mixture ratio. See Figure 6.2(A)-(D) for point by point (combination ratio) mean response to left for each rat (indicated by color identity) based on bootstrapped data. The bimodal distribution can thus be interpreted as the sum of two normal distributions, each representing a group of rats that responded similarly. Using these criteria, we concluded that the response distributions for odor set 2 (Eucalyptol/Limonene) and odor set 4 (Citral/PEA) each have two subgroups of subjects.

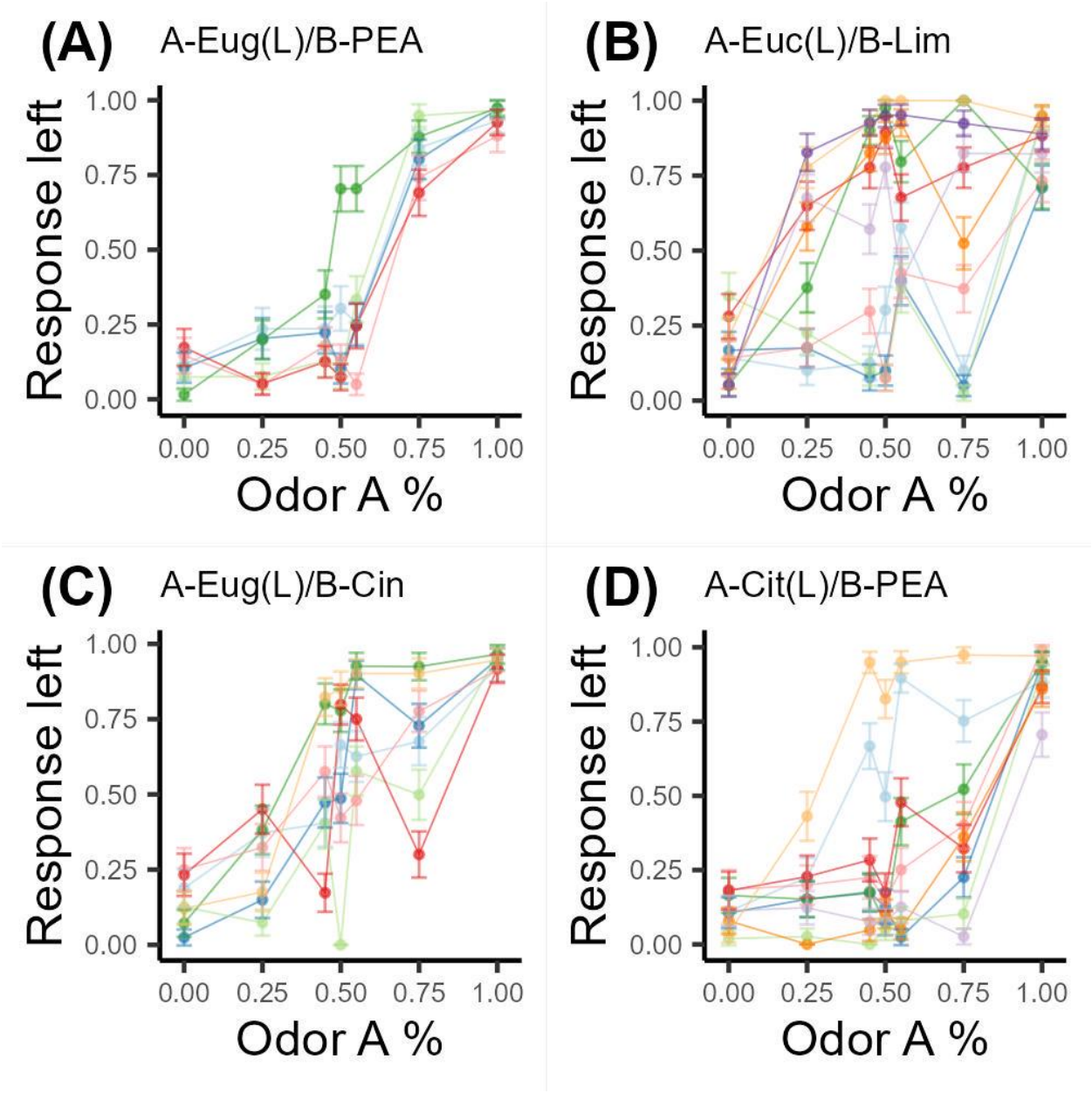

Figure 6.2 Bootstrapped response intensity to the left port for each odor set.
Based on the original binary response, grouping by odor set, rat, combination ratios, we sampled with replacement 36 (to match number of data points in our original data) data points over 1001 iterations. The response ratio to the left port of each rat on each combination ratio for each odor set is again calculated as [n go left/N total] for each odor combination ratio. Error bars are standard deviations. Colors indicated rat identities; same rat has the same color across panels. Figure (A)-(D): (A) n = 6, OS1: Eug/PEA; (B) n = 10, OS2: Euc/Lim, OS2 shows two clear subgroups, one group goes to the left port more than 50% of the time at 50A while the other group goes to the right;(C) n = 7, OS3: Eug/Cin; (D) n = 8, OS4: Cit/PEA.

Asymmetry of psychometric curves

For each odor set, we fit the response to the left to a logistic general linear model with the percentage of odor A as the predictor. Odor sets that passed the bimodality tests were analyzed by subgroup. For all models, the percentage of odor A in the mixture significantly predicts rats' go response (all $p<0.001$). Figure 6.3 shows the predicted response frequency to the left for all percentages of odor A in mixtures. None of the odor sets have a predicted value of 0.5 for response frequency to the left when the composition of components of the binary mixture is 1:1. This argues against the idea that binary mixtures have uniform perceptual qualities across the spectrum of possible combination ratios. Moreover, around component ratio 1:1, different odor sets behave differently. All odor sets falsify the hypothesis that the recognizability of component odorants in a binary mixture is symmetrical about the 50-50 concentration ratio. It appears that each binary odor set is unique.

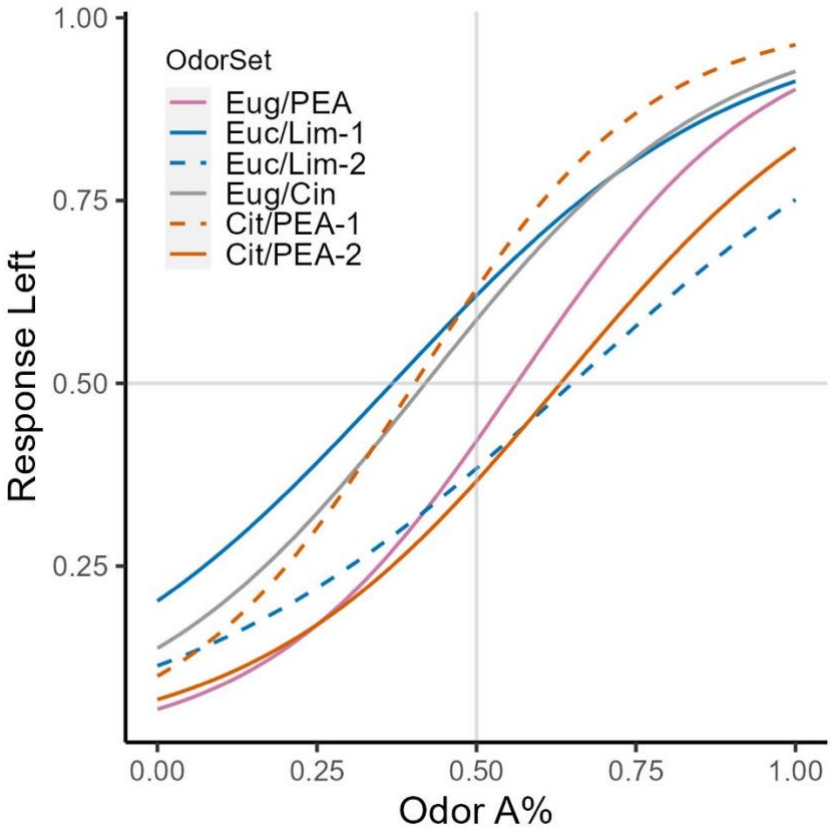

Figure 6.3 Psychometric curve fits for all odor sets
A logistic model was fit to each odor set's response intensities. Subgroups identified for OS2 and OS4 based on bimodality tests are treated as separate groups. For those groups, solid curves indicate the subgroup with more subject numbers (OS2 larger group: n = 6, smaller group n = 4; OS4 larger group n = 6, smaller group n=2). Larger differences in trigeminal profiles do not produce larger overshadowing effects. OS1(Eug/PEA) and OS4(Cit/PEA) do not produce more shifted curves.

There are two ways to test the hypothesis that OS1 and OS4, the odor sets with components of high trigeminal difference, show a more dramatic overshadowing effect. The first way to look at the fitted curves is that, when chemical concentration is controlled to be 1:1 (combination ratio = 50A-50B), response intensity to the left port should not equal 0.5. If response intensity to the left port is lower than 0.5, it means rats go to the right port more when chemical intensity is the same for both components, or odor B (the less trigeminal odorant) overshadows odor A. If response is higher than 0.5, this means that rats go to the left response

port more than the right one at the 50-50 ratio, or odor A (the more trigeminal odorant) overshadows odor B. The second way to look at the fitted models is when response intensity is equal to 0.5 (i.e., when rats report the mixture to smell like either component odor equally), the corresponding mixture ratio should not be 1:1 (50A-50B) if either odor overshadows the other. If the point at which the response intensity to the left port equals 0.5 is to the left of 50A-50B, A overshadows B. If the point at which the response intensity to the left port equals 0.5 is to the right of 50A-50B, then B overshadows A.

OS1 and OS4, with PEA as odorant B, have the best documented high trigeminal difference between components (Doty *et al.*, 1978; Lübbert *et al.*, 2013). OS1 does not show a larger shift of inflection point away from 50-50 than do OS2 and OS3. It is therefore not true that components with larger trigeminal difference show a more dramatic overshadowing effect. However, both OS1 and OS4 curves show that PEA, the nontrigeminal odorant, overshadows the trigeminal odorant.

Sex and odor set differences in sampling duration

Longer sampling duration has been linked to better performance in odor discrimination(Frederick et al., 2017). The distribution of sampling durations within a session is skewed, so the median is a better measure of within-session behavior. Across sessions, the distribution of medians is normal(Frederick et al., 2011). To check the influence of different trial types, or various combination ratios, on rats' decision-making strategies, we performed repeated measures ANOVA on the independent variable median sampling duration and dependent variables test day, combination ratio, sex, and odor set. Combination ratio was not a significant

predictor of sampling duration ($F(1,442) = 1.5$, $p = 0.22$). This supports the effectiveness of our protocol in testing rats' responses to binary mixtures of various ratios. Rats do not employ different sampling strategies in responding to mixtures and pure odorants, meaning that, given the same sampling time across mixtures, the odor quality is well-represented by the response.

We found sex ($F(1,442) = 3.88$, $p = 0.0495$) and odor set ($F(1,442) = 100.99$, $p < 0.001$) to be significant factors in predicting sampling duration. Post hoc t-tests with Bonferroni correction show that only the OS4 average median sampling durations are significantly different between male and female rats. This significance is most likely driven by 1 male rat who consistently sampled longer than 1s for OS4. The mean sampling durations for all rats are shown in Figure 6.5. Similar to previous studies(Frederick et al., 2011, 2017), there is high variance in sampling duration across rats and odor sets. Other studies addressing sex differences in olfaction, including work done in our lab, indicate that male and female rats show differences in sampling time in non-learning tasks(Maheshwar et al., 2025; Perez et al., 2018). In our current study, female rats show a trend to sample longer than males for OS1, but shorter for OS2-4.

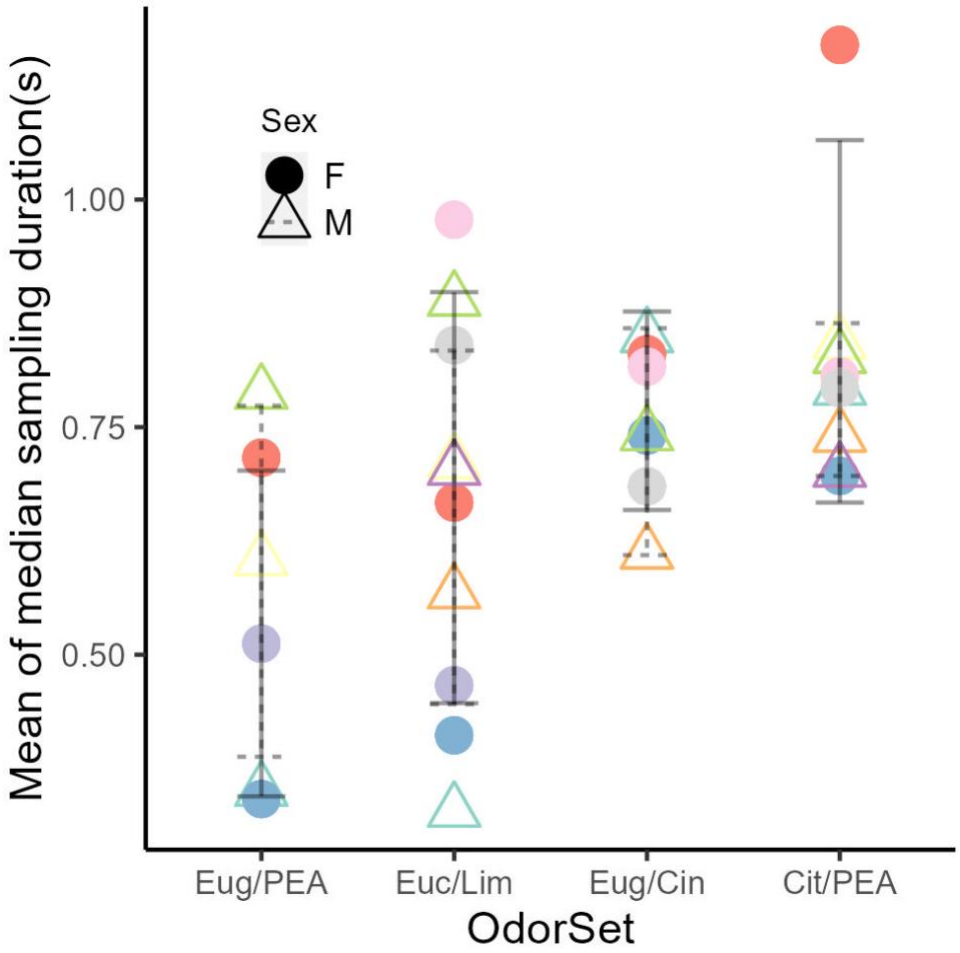

Figure 6.5 Mean of median sampling duration by sex.
Individual rats are identified by shape and color.

Discussion

The majority of binary mixtures are not elemental in perceptual quality, and most show some type of overshadowing effect by one of the odorants over the other. However, we do not know what gives rise to perceptual overshadowing or how to predict the predominance of one odor in a binary mixture. Our hypothesis rested on the expectation that trigeminal profiles of the

components of a binary mixture would reveal information on the direction and size of overshadowing. We recorded rats' responses to mixtures of different ratios to examine the relationship between trigeminal difference and overshadowing in binary odor mixture quality. We used 4 odor sets of varying trigeminal profiles to test the hypothesis that larger trigeminal differences between the two odorants in the binary mixture would predict more overshadowing.

We found that 50-50 mixtures of binary odors did not coincide with equal perceptibility of the two component odorants for all of the odor sets tested (Fig. 3). For both odor sets with large trigeminal differences, the non-trigeminal odorant (PEA) overshadowed the strong trigeminal odorant (eugenol or citral), except for the small subgroup of two rats in the citral/PEA test (Fig. 3). However, trigeminal differences between components did not predict the magnitude of overshadowing effects. These results support our hypothesis that trigeminal activation may drive the directional properties of overshadowing. Our data suggest that the less trigeminal odorant overshadows the more trigeminal one, which could be due to a decrease in perceptual strength of the trigeminal odorant during learning. A caveat is that there are very few known low or non-trigeminal odorants that are liquid and volatile at room temperature, and the only odorant in that category that we tested was PEA. This could be a specific effect of PEA in the binary mixtures we tested.

It is likely that overshadowing dynamics involve a multitude of factors including chemical structure, volatility, sorptiveness, trigeminality, mixture ratio, agonistic and antagonistic interactions with olfactory receptors, and more. To understand overshadowing dynamics, we would benefit from systematizing the trigeminal profiles of commonly used volatile chemicals. Given the progress made in understanding TRP channels, which give rise to chemesthetic properties, there is much work left to be done to characterize the trigeminal profiles

and intensities of commonly used odorants. In selecting more trigeminal odorants, we assumed that chemicals that activate different families of TRP channels elicit generalizable levels of intensities. Future studies comparing the relative intensities of chemicals that activate different subfamilies of TRP channels, for example those that active TRPV1 and TRPM8 when concentrations are controlled to be the inverse ratio of respective vapor pressure, will enable us to characterize perceptual qualities of both monomolecular and mixture odorants more strictly.

None of the mixtures showed a symmetric sigmoid relationship of component perceptibility. We do not yet understand completely what drives the asymmetry, and there appear to be individual differences as well, as exemplified by the subgroups of subjects' response patterns within two of the odor sets. We note that some studies of odor psychophysics and electrophysiology assume that psychophysical curves depend on the liquid or gas phase concentration of odorants, independent of their physical properties or possible interactions at the receptor level either directly through inhibition or indirectly via trigeminal nerve activation (*e.g.*,Uchida & Mainen, 2003). Because all the psychophysical curves we found were asymmetric, our results suggest that training subjects to treat ratios of binary mixtures as perceptually symmetric may add unplanned and unpredictable cognitive load to the animals performing the task. The physiological interpretations or behavioral strategies can then be biased by unknown and unquantified factors. It may be necessary to pretest and/or calibrate mixture ratios so that the curve is perceptually symmetric or of quantified asymmetry.

These data, combined with the overwhelming evidence of inhibition within odor mixtures at the receptor level(Araneda et al., 2000; Kay et al., 2003; Xu et al., 2020), make it clear that understanding mixture quality may not yet be a tractable theoretical problem at the level of neurophysiology. The best way forward for use of mixtures in neurophysiology is to test the

psychophysical properties of each mixture to be used. The methods by which these mixtures are tested may be tuned to address specific qualitative questions. For example, pretraining animals to monomolecular mixture components and then asking them to identify a component favors overshadowing, as we have done here. Training animals to recognize a mixture and asking them to report whether any of the components or decoy odorants smell like the mixture favors discovery of configural or synthetic properties. In most cases, we might simply need to test each mixture individually. The specific odors and their combinations matter.

One limitation of our study is that odor detectability in binary mixtures in our study is used as a measure for odor intensity in the binary mixtures tested. Detectability could be influenced by olfactory intensity, trigeminal intensity and their interactions. Unlike testing human subjects, we cannot measure trigeminal intensity separately, by asking subjects to focus on different aspects of the odor experience. The goal of our study, however, is to examine the binary mixture percept as a whole, to ask rats which odor the mixture smells most like.

Our results align with human research in odor mixture quality. We show that binary mixture psychometric functions are not easily predictable from the components nor generalizable from mixture to mixture(Cometto-Muñiz et al., 1989, 2003; Cometto–Muñiz et al., 1999; Lindqvist et al., 2012). However, it should be noted that human and animal mixture perception studies are not directly comparable due to differences in odor delivery and perceptual testing protocols. In fact, few human studies of binary mixture perception have addressed trigeminality directly. Trigeminal profile may be one of the factors that give rise to odor quality, but odor quality is not directly measurable in animal research.

Chapter 7: Discussion

Overall, chapters 3 to 5 show that the informative and non-informative groups recruit different networks to perform the same four-odor discrimination tasks. Sniffing also drives the network's dynamics differently for these two groups. While most of these differences show up during the block tests, some become more pronounced during the first day of the interleaved test. Our results support our hypothesis that cognitive demand influences OB gamma oscillations. Furthermore, the olfactory and hippocampal network neurodynamics reflect cognitive demand. We provide a brief summary of our results and discuss their implications, future directions, and limitations of our study.

Sampling duration may not be a direct reflection of task difficulty

We trained two groups of rats, one group with an informative cue for the odor stimulus type (one odor from the coarse or fine odor pair) for the upcoming trial of a 4-odor identification task, and one group with a neutral cue. The two groups were equally good at performing the task (reaching similar levels of accuracy), with an overall effect of odor stimulus type. This result conforms with the popular assumption, indicating that fine pairs are harder to discriminate than coarse pairs. Thus, we can conclude that our coarse odors are easier to identify than our fine odors.

However, we found that, contrary to our expectations, the informative group sampled longer to reach the same level of accuracy as the non-informative group. This may seem difficult to interpret. The design of the informative cue was to manipulate cognitive demand in helping

rats to narrow down the potential candidates they need to identify in the four-odor task, hence making the task easier for the informative group. We know that associative cues with information can improve accuracy and shorten reaction time in human research. However, the fact that the informative group sampled 100ms longer than the non-informative group invites us to reexamine the assumption we have taken that sampling duration is a direct reflection of task difficulty. When integrating the whole picture, we can see that it is more likely that this longer sampling duration is not an indicator of how hard the task may be for the informative and the non-informative groups.

The assumption is that the longer the animal samples, the harder the stimulus is to identify. This may lead to the assumption that the harder a decision is, the longer it takes the rats to arrive at the decision. However, generalizing these two assumptions may be questionable. The relationship between sampling duration and task difficulty is not as simple as we thought, especially when cognitive demand other than stimulus complexity comes into the picture.

Since the two groups do not perform differently in response accuracy, this means that both groups are good at telling the odors apart. However, the obvious difference in OB and hippocampal network gamma and beta LFP power and the network coherence between the two groups argues for at least two different strategies and two sets of neural and behavioral states across the two groups (there are also sex differences). The strategy that the informative group of rats choose results in a longer sampling duration, which does not simply map onto how difficult the task may be. In other words, because of the network physiological differences, we have reasons to believe that this manipulation of adding an associative cue to a four-odor discrimination task has changed the nature of the task for the informatively trained rats, making a direct comparison of sampling duration as a cognitive indicator difficult.

We found a block effect on sampling duration and accuracy. Later blocks in a session have higher accuracies compared to the first block, but also shorter sampling durations. This means rats are getting better at the task throughout a session. Within the same session, sampling duration seems to map with accuracy as a reflection how hard rats find the task. Interestingly, day 3 is the day that the informative group has an increased sampling time compared to day 2, not the non-informative group. It is likely that the informative group notices the unpredictability of the interleaved test on day 3 (first day of interleaved test) and develops the strategy of sampling longer to achieve a similar level of success as in the block test. Our interpretation is that informative rats, when ramping up sampling time on day 3, whether they need more time to make a correct choice or they use cue in a way that prolongs the sampling process, pay more attention to the olfactory stimuli than on test day 2 (second day of block test). While on day 3, the informative rats increase sampling duration significantly compared to day 2, on day 4, the difference (in the same direction, higher) on sampling duration is not significant. This supports our interpretation that the increase in sampling duration is driven by strategy emergence to adapt to the increased trial-by-trial variability. On the second day of the interleaved test, rats have become familiar with the interleaved test; hence, we observe a lower sampling duration. The non-informative group does something else to achieve a similar level of performance. Instead of increasing sampling time on day 3, these rats amplify gamma and keep amplifying it into day 4. The informative group rats also amplify gamma on day 3, but it drops precipitously on day 4.

On test day 4, informative rats show lower gamma than on days 1-3. Consistent with our interpretation of the day 3 effect, the dip in OB gamma power on day 4 could be a sign of informative rats paying less attention to the olfactory stimuli, as a result of strengthening the association between cue and odor stimuli on day 3.

We conclude that when using sampling duration as an indicator of difficulty of learning or task, cognitive states should be taken into consideration. When there's a wide net of differences in the neural activities across the informative and the non-informative groups indicating state differences, despite performing a seemingly similar task with a small difference, sampling time differences may be caused by the different network activities underlying the different cognitive process the two groups are using. Lastly, given that we see different dynamics in power and coherence change throughout the four days of training, this provides more reason to compare the two groups of rats carefully.

Interleaved test and block test differences are reflected on a neural level

One of the levels we manipulated for the task is the predictability of a future trial. Over four testing days, both the informative and the non-informative rats perform two tests, the block and interleaved tests, for two days consecutively, first two days of block test and then two days of interleaved test. We refer to them as test days 1-4 generally. Our results show that OB gamma power difference between the two cue groups, the informative and the non-informative, starts to be significant on day 3, or on the first day of the interleaved test.

We see that for the non-informative group, OB gamma power increased during interleaved test compared to block test. Moreover, for non-informative rats OB gamma power on the second day of the interleaved test is higher than on the first day of the interleaved test. Given that the non-informative rats have similar behaviors throughout the four test days, the increasing trend in OB gamma power associated with task type (virtually test day) is interesting. The non-informative rats sample similarly for all test days. However, OB gamma increases for the more

unpredictable interleaved test, continuing to increase on the second interleaved test. This could be explained by increasing attention to the olfactory input. Since they don't have other cues to help them reach the correct decision, paying attention to the sensory cue is the best strategy. This idea supports that OB gamma power is reflective of the weight of sensory input in the OB and a decrease in top-down input (Martin et al., 2006). If the weight is strengthened by more attention to olfactory stimuli, the OB circuit is primed to increase gamma; if the weight is weakened by more attention to other factors, such as the light cue conveying predicative information of the coming trial, the OB circuit is primed for less gamma. This means in our case, when non-informative rats learned to pay more attention to the details of the olfactory stimuli, informative rats learned to pay less attention to the olfactory stimuli or more attention to the light cue, likely engaging the hippocampus and other top-down inputs more strongly.

Moreover, for the informative group, OB-PC beta coherence during sampling goes up on day 3, compared to the block test days, which reflects higher weight of PC inhibitory input on the first day of interleaved testing. For the informative group, OB-PC beta coherence during the period of post odor off (400ms after withdrawing nose from the odor port) increases on day 3 and then drops to a lower level (even compared to the block test days) on day 4, not for the non-informative group. There is also an overall OB-PC beta coherence difference in the informative and non-informative rats, with the informative rats having higher OB-PC beta coherence starting with the onset of sampling to 400ms after response. The higher OB-PC beta coherence for the informative compared to the non-informative group indicates more inhibitory tone in the OB due to input from PC to OB granule cells. We see two instances of higher OB inhibition due to PC input to OB for the informative group, one on day 3 compared to day 1 and 2, one in comparison to the non-informative overall. However, the exact mechanism moderating this increase of input

from PC to OB is yet to be determined and is possibly different for the two scenarios. Regardless, this evidence suggests that informative rats are in a different state compared to non-informative rats.

The fact that the interleaved test increases the difference between the non-informative and the informative group and that the two groups also have different neurodynamical patterns on the 2nd day of the block test and 2nd day of the interleaved test, we conclude that the non-informative and informative groups use different cognitive process to learn, perform and adapt to the same task with or without an informative cue.

We found that during sampling, OB gamma power on day 4 and day 2 for the non-informative group is respectively higher than that on day 3 and day 1. However, for the informative group, while there's no difference in OB gamma power during sampling between day 2 and day 1, day 4 is lower than day 3. To our surprise, these changes in gamma power are largely accompanied by the same direction in OB beta changes. For the non-informative group, OB beta power across events on day 2 is higher than on day 1, and on day 4 is higher than on day 3. For the informative group, OB beta power across events on day 2 is lower than on day 1, on day 4 is lower than on day 3. In the OB, previous studies have shown gamma and beta power interchange within a trial and that when gamma is elevated in fine odor discrimination, beta is also lower (Frederick et al., 2016). That pattern is repeated here in the difference between fine and coarse odors, but not as a general pattern that increase in gamma always means decrease in beta. During a trial, there is a defined sequence of peak oscillation powers. We see gamma during the down cycle of respiration during sampling, and start seeing beta as rats anticipate withdrawing their nose and go to a response port, lasting till after they respond. This makes sense since in the OB, the same dendrodendritic reciprocal circuits make gamma and beta oscillations

depending on the excitability of the interneurons, granule cells (Osinski and Kay, 2016). However, now we see a case where when gamma oscillations go up, beta oscillations also go up. In the next section, we discuss more how to interpret this phenomenon.

These changes in OB gamma and beta power are also coupled with OB-PC effects on task type/day interactions. OB-PC beta coherence during sampling for the informative group on day 4 is lower than on day 3, while for the non-informative, OB-PC beta coherence is the same across the 4 test days. OB-PC beta coherence post odor off (400ms after nose withdraw, which includes the period of response and some time after the response, as the interval between response and nose withdraw is largely within 100ms, median ~50ms) for the non-informative group on day 4 is lower than on day 1, while for the informative group OB-PC beta power during post odor off is lower than on day 3, and days 1 and 2. Moreover, during the pre light baseline period, the informative group also shows elevated OB-PC beta coherence. The elevation in beta coherence during pre-light baseline and post odor off period between OB and PC is highest on the first day of the interleaved test and is reminiscent of a beta band preafferent signal seen in an earlier study arising in the entorhinal cortex (Kay & Freeman, 1998). The neural activity changes during the pre-light baseline for the informative group on day 3 is another supporting argument for the overall state change between rats in different cue groups.

Interpreting the power shift in the gamma and beta bands

Since beta oscillations have been shown to be associated with many factors, such as movement initiation(Hermer-Vazquez et al., 2007) odor volatility(Lowry & Kay, 2007), learning(Martin et al., 2004, 2007), decisions(Fries, 2023; Khanna & Carmena, 2017; Symanski et al., 2020), it's unclear what exactly is the behavioral or cognitive driver for this phenomenon. We didn't find an effect of odor stimulus type on OB gamma power, but did find an effect on OB

beta power. It requires less beta oscillations to discriminate the fine odor pairs compared to the coarse odor pairs, while rats have a similar level of gamma oscillations for both coarse and fine pairs. This result has happened in Frederick et al. 2016, where extremely similar odor pairs induced minimal level of beta but high amplitude gamma. Given that our task is presumed to be even harder than the TAC task because rats are required to discriminate between four stimuli, it's possible that the higher beta during coarse discrimination is due to a similar reason compared to Frederick et al. 2016, but our odors were less similar than in that study. The OB requires top-down input to make beta oscillations. When centrifugal input is severed, the OB shows robust gamma but not beta(Gray & Skinner, 1988; Martin et al., 2006). Hence, when beta is inhibited, it could be a sign of network adaptation to amplify sensory signals. Less beta during fine trials in our study may be due to beta inhibition, a sign of expertise for the coarse trials, as they require less beta inhibition. How does this help in interpreting higher gamma at the same time as higher beta power in the OB?

Higher beta power in the OB can be the result of either low need for gamma oscillations (local network having dominant beta) or high need of beta oscillations (network state as a result of higher top-down input and local activities). Both are possible indicators of cognitive demand; however, likely driven by different aspects of cognitive demand. High gamma power reflects high demand to process sensory input, while high beta could reflect more involvement from higher cortical areas to adjust the brain for more functions than sensory disambiguation, or even further facilitation of sensory disambiguation. The answer to this interesting question may be out of the scope of the study. Based on Osinski et al. 2016, the state of high beta and high gamma is possible, and may be a result of a change in the overall gain threshold of the OB.

Overall, the OB beta results support our hypothesis that learned associations modulate the OB LFP. The added association changes rats' brain states while performing a discrimination task of varying cognitive demand. It also results in different adaptation behaviors in the interleaved test we designed, which requires higher cognitive demand, discriminating four odors on a trial-by-trial basis, without any predictable pattern (as opposed to an intermediate demand of discriminating four odors in a block-by-block manner, with alternating blocks of coarse and fine pairs).

The olfactory-limbic network neurodynamic reflects cognitive demand

The hippocampus has been shown to play an important role in context-specific associative learning(Good & Honey, 1991; Holland & Bouton, 1999; Ji & Maren, 2007; Niv, 2019), and it's connected with the olfactory system through EC and directly via CA1 inputs to the OB(Gulyás et al., 1998). We've shown that OB neurodynamics are modulated by task demand, and this effect also varies depending on whether a given odor set is learned as the first set or the second set. Olfactory-limbic coherence and network respiratory coherence reflect cognitive load during phase 3 training period and phase 4 testing period.

During phase 4, the informative group beta coherence is higher for PC-DG for the post odor-off period, but the non-informative group shows stronger PC-CA1 beta coherence. On the same day, the OB-DG gamma coherence during sampling is also elevated for the informative cue group, which is not the case for the non-informative group. This conforms with previous research that different parts of the hippocampus(Aqrabawi & Kim, 2018; Biane et al., 2023), such as DG and CA1 may play different roles in associative tasks(McHugh et al., 2024). In odor based associative tasks, blocking CA1 and EC pathway slows down olfactory cue association(Li et al.,

2017); while DG LFP is associated with meaningful cue learning and expectation of rewards when encountering cues(Rangel et al., 2015), and offline memory consolidation(McHugh et al., 2024). While it is puzzling to see that the non-informative group shows stronger PC-CA1 coherence, contrary to our expectation, our result provides further evidence of the differentiated roles different parts of hippocampus play in associative learning. Our interpretation of the higher coherence of beta band between PC-CA1 in the non-informative group points to the different roles CA1 plays in a pure odor associative cues vs an odor-based context associative task. CA1 involvement is required in odor cue associative learning(Kesner et al., 2005). The non-informative group, performing a pure odor associative task, enlists the CA1 differently than the informative group. Though still performing an odor cue-based associative task, by virtue of the associated context cues, the informative group may have changed the involvement of CA1 and DG. In other words, the informative group is not performing a simple odor cue associative task, which changes hippocampus involvement. Such differences could be achieved through PC, EC and AON pathways(Aqrabawi & Kim, 2018; Li et al., 2017; Strauch & Manahan-Vaughan, 2018). Notice that the onset of increase in PC-CA1 beta coherence for the non-informative group is later in the trial compared to the onset of increase in PC-DG beta coherence for the informative group. Consistent with the theory that DG may play more a role in the expectation of rewards as a result of meaningful cues and that CA1 may play more a role in associated memory retrieval.

We saw effects of learning with the changes in the network when we examined coherence across the network (OB, PC, DG, CA1, and TC) on the last day of training (TD or day -1), and day 3 of testing (first day of interleaved test). For both the informative and the non-informative group, we found a pattern of higher coherence in theta, beta and gamma bands for the second

relative to the first learned odor set. The difference between the two groups lies in the different connections between the olfactory (OB, PC) and the hippocampal (DG, CA1) areas. The informative group effects are for OB-DG, and PC-DG connections, while the non-informative group effects center around OB-PC and PC-CA1 coherence.

Respiratory coherence also differs between cue groups. The theta band signal from the thermocouple we implanted into the left nostril, which tracks sniffing cycles by detecting the temperature change in the nostril due to air flow, is more coherent with the hippocampal areas we recorded from for the non-informative group, compared to the informative group. This suggests heavier sniffing modulation to the hippocampus for the non-informative group, and supports our interpretation that the non-informative group weighs the sensory input to the olfactory system more than the non-informative group. However, this cue effect is in the opposite direction for OB-respiratory coherence. OB-TC theta is more coherent for the informative group compared to the non-informative group. This suggests that for the informative group, the network of sniffing and OB may be more separate from the rest of the network. Moreover, while respiratory coherence with olfactory areas is elevated for the first odor set, respiratory coherence with CA1 is elevated for the second one. This also suggests that sniffing modulates CA1 activity as part of learning.

Overall, these results show that task demand modulates not only OB gamma, but also OB beta and network connections that make these oscillations. Neural oscillations are dynamic indicators of system states and maps onto the cognitive and behavioral level.

Future directions

We see a sampling duration difference between the two cue groups even during the first odor set learned for testing. The last day of training, for the first odor set rats are tested on, informative rats sample longer than the non-informative rats. It would be interesting to further investigate at what point of training/learning this behavioral difference emerges.

It would also be valuable to conduct more experiments designed to identify the source of the difference of the network and how the brain achieves it. The scope to which our data can answer this question is limited. However, I plan on performing coherence phase analysis to identify phase relations between the areas recorded. We know the connections between the areas recorded well enough for the phase difference estimation and direction to give us an estimate of who is initiating the conversation between two areas. Also, following our current efforts in characterizing the relationship between cognitive demand and network oscillations in the OB and hippocampus, it would also be informative to include other areas such as EC, AON, OT, and the reward-related areas in future experiments.

Last but not least, we found robust sex effects. The work on sex differences is invaluable, especially because females have traditionally been excluded in medical research. We insist the inclusion of female subjects is crucial for the soundness of science. We plan to investigate more fully the sex effects we have found in this experiment, which is consistent with a few other experiments in the lab.

Limitations

Given the complexity of the four-odor task, the time it takes for a rat to arrive at the lab till she or he finishes testing for two sets of odors is significantly longer than a traditional TAC

test. This limited the number of animals we were able to include in this experiment. Hence, we may lack the power to investigate the sex effect robustly. We still report the differences we saw, and this can provide a starting point for further research.

We disproved our null hypothesis concerning the cognitive load influence on OB oscillations. However, the large number of significant effects we found among the three-way interaction of cue, day and coarse versus fine in our design may be a sign to further investigate the exact relationship between these variables. It is important to tease their relationship apart and ensure that future studies are sufficiently powered. In our study, to ensure power, we conducted two types of tests twice, with each session of around 300 trials. For rat neurophysiology, 4 subjects in each group is a general rule. Because we had sex differences embedded in the results, double the number of animals would have been necessary to fully address this added variance.

Reference

Abraham, N. M., Guerin, D., Bhaukaurally, K., & Carleton, A. (2012). Similar Odor Discrimination Behavior in Head-Restrained and Freely Moving Mice. *PLOS ONE*, *7*(12), e51789. https://doi.org/10.1371/journal.pone.0051789

Abraham, N. M., Spors, H., Carleton, A., Margrie, T. W., Kuner, T., & Schaefer, A. T. (2004). Maintaining accuracy at the expense of speed: Stimulus similarity defines odor discrimination time in mice. *Neuron*, *44*(5), 865–876. https://doi.org/10.1016/j.neuron.2004.11.017

Aqrabawi, A. J., & Kim, J. C. (2018). Hippocampal projections to the anterior olfactory nucleus differentially convey spatiotemporal information during episodic odour memory. *Nature Communications*, *9*(1), 2735. https://doi.org/10.1038/s41467-018-05131-6

Araneda, R. C., Kini, A. D., & Firestein, S. (2000). The molecular receptive range of an odorant receptor. *Nature Neuroscience*, *3*(12), 1248–1255. https://doi.org/10.1038/81774

Aylwin, M. L., Aguilar, G. A., Flores, F. J., & Maldonado, P. E. (2009). Odorant modulation of neuronal activity and local field potential in sensory-deprived olfactory bulb. *Neuroscience*, *162*(4), 1265–1278. https://doi.org/10.1016/j.neuroscience.2009.05.051

Bandell, M., Story, G. M., Hwang, S. W., Viswanath, V., Eid, S. R., Petrus, M. J., Earley, T. J., & Patapoutian, A. (2004). Noxious Cold Ion Channel TRPA1 Is Activated by Pungent Compounds and Bradykinin. *Neuron*, *41*(6), 849–857. https://doi.org/10.1016/S0896-6273(04)00150-3

Baxter, B. D., Larson, E. D., Merle, L., Feinstein, P., Polese, A. G., Bubak, A. N., Niemeyer, C. S., Hassell, J., Shepherd, D., Ramakrishnan, V. R., Nagel, M. A., & Restrepo, D. (2021). Transcriptional profiling reveals potential involvement of microvillous TRPM5-expressing cells in viral infection of the olfactory epithelium. *BMC Genomics*, *22*(1), 224. https://doi.org/10.1186/s12864-021-07528-y

Becker, J. B., Prendergast, B. J., & Liang, J. W. (2016). Female rats are not more variable than male rats: A meta-analysis of neuroscience studies. *Biology of Sex Differences*, *7*, 34. https://doi.org/10.1186/s13293-016-0087-5

Bedrosian, T. A., Vaughn, C. A., Galan, A., Daye, G., Weil, Z. M., & Nelson, R. J. (2013). Nocturnal Light Exposure Impairs Affective Responses in a Wavelength-Dependent Manner. *Journal of Neuroscience*, *33*(32), 13081–13087. https://doi.org/10.1523/JNEUROSCI.5734-12.2013

Beshel, J., Kopell, N., & Kay, L. M. (2007). Olfactory Bulb Gamma Oscillations Are Enhanced with Task Demands. *Journal of Neuroscience*, *27*(31), 8358–8365. https://doi.org/10.1523/JNEUROSCI.1199-07.2007

Biane, J. S., Ladow, M. A., Stefanini, F., Boddu, S. P., Fan, A., Hassan, S., Dundar, N., Apodaca-Montano, D. L., Zhou, L. Z., Fayner, V., Woods, N. I., & Kheirbek, M. A. (2023). Neural dynamics underlying associative learning in the dorsal and ventral

hippocampus. *Nature Neuroscience*, *26*(5), 798–809. https://doi.org/10.1038/s41593-023-01296-6

Biskamp, J., Bartos, M., & Sauer, J.-F. (2017). Organization of prefrontal network activity by respiration-related oscillations. *Scientific Reports*, *7*(1), 45508. https://doi.org/10.1038/srep45508

Buron, G., Hacquemand, R., Pourié, G., & Brand, G. (2009). Carbon dioxide effects on olfactory functioning: Behavioral, histological and immunohistochemical measurements. *Toxicology Letters*, *188*(3), 251–257. https://doi.org/10.1016/j.toxlet.2009.04.018

Carneiro, B. T. S., & Araujo, J. F. (2012). Food entrainment: Major and recent findings. *Frontiers in Behavioral Neuroscience*, *6*. https://doi.org/10.3389/fnbeh.2012.00083

Chandorkar, N., Tambe, S., Amin, P., & Madankar, C. (2021). A systematic and comprehensive review on current understanding of the pharmacological actions, molecular mechanisms, and clinical implications of the genus *Eucalyptus*. *Phytomedicine Plus*, *1*(4), 100089. https://doi.org/10.1016/j.phyplu.2021.100089

Chen, W. R., Xiong, W., & Shepherd, G. M. (2000). Analysis of relations between NMDA receptors and GABA release at olfactory bulb reciprocal synapses. *Neuron*, *25*(3), 625–633. https://doi.org/10.1016/s0896-6273(00)81065-x

Cometto-Muñiz, J. E., Cain, W. S., & Abraham, M. H. (2003). Dose-addition of individual odorants in the odor detection of binary mixtures. *Behavioural Brain Research*, *138*(1), 95–105. https://doi.org/10.1016/S0166-4328(02)00234-6

Cometto–Muñiz, J. E., Cain, W. S., Abraham, M. H., & Gola, J. M. R. (1999). Chemosensory Detectability of 1-Butanol and 2-Heptanone Singly and in Binary Mixtures. *Physiology & Behavior*, *67*(2), 269–276. https://doi.org/10.1016/S0031-9384(99)00074-8

Cometto-Muñiz, J. E., García-Medina, M. R., & Calviño, A. M. (1989). Perception of pungent odorants alone and in binary mixtures. *Chemical Senses*, *14*(1), 163–173. https://doi.org/10.1093/chemse/14.1.163

Coureaud, G., Languille, S., Schaal, B., & Hars, B. (2009). Pheromone-induced olfactory memory in newborn rabbits: Involvement of consolidation and reconsolidation processes. *Learning & Memory*, *16*(8), 470–473. https://doi.org/10.1101/lm.1434009

Coureaud, G., Letagneaux, C., Thomas-Danguin, T., & Romagny, S. (2020). Developmental changes in elemental and configural perception of odor mixtures in young rabbits. *Developmental Psychobiology*, *62*(4), 471–483. https://doi.org/10.1002/dev.21929

de Olmos, J., Hardy, H., & Heimer, L. (1978). The afferent connections of the main and the accessory olfactory bulb formations in the rat: An experimental HRP-study. *Journal of Comparative Neurology*, *181*(2), 213–244. https://doi.org/10.1002/cne.901810202

Djordjevic, J., Jones-Gotman, M., De Sousa, K., & Chertkow, H. (2008a). Olfaction in patients with mild cognitive impairment and Alzheimer's disease. *Neurobiology of Aging*, *29*(5), 693–706. https://doi.org/10.1016/j.neurobiolaging.2006.11.014

Djordjevic, J., Jones-Gotman, M., De Sousa, K., & Chertkow, H. (2008b). Olfaction in patients with mild cognitive impairment and Alzheimer's disease. *Neurobiology of Aging*, *29*(5), 693–706. https://doi.org/10.1016/j.neurobiolaging.2006.11.014

Doty, R. L., Brugger, W. E., Jurs, P. C., Orndorff, M. A., Snyder, P. J., & Lowry, L. D. (1978). Intranasal trigeminal stimulation from odorous volatiles: Psychometric responses from anosmic and normal humans. *Physiology & Behavior*, *20*(2), 175–185. https://doi.org/10.1016/0031-9384(78)90070-7

Eeckman, F. H., & Freeman, W. J. (1990). Correlations between unit firing and EEG in the rat olfactory system. *Brain Research*, *528*(2), 238–244. https://doi.org/10.1016/0006-8993(90)91663-2

Finger, T. E., & Böttger, B. (1993). Peripheral peptidergic fibers of the trigeminal nerve in the olfactory bulb of the rat. *The Journal of Comparative Neurology*, *334*(1), 117–124. https://doi.org/10.1002/cne.903340110

Frasnelli, J., Albrecht, J., Bryant, B., & Lundström, J. N. (2011). Perception of specific trigeminal chemosensory agonists. *Neuroscience*, *189*, 377–383. https://doi.org/10.1016/j.neuroscience.2011.04.065

Frederick, D. E., Brown, A., Brim, E., Mehta, N., Vujovic, M., & Kay, L. M. (2016). Gamma and Beta Oscillations Define a Sequence of Neurocognitive Modes Present in Odor Processing. *Journal of Neuroscience*, *36*(29), 7750–7767. https://doi.org/10.1523/JNEUROSCI.0569-16.2016

Frederick, D. E., Brown, A., Tacopina, S., Mehta, N., Vujovic, M., Brim, E., Amina, T., Fixsen, B., & Kay, L. M. (2017). Task-Dependent Behavioral Dynamics Make the Case for Temporal Integration in Multiple Strategies during Odor Processing. *The Journal of Neuroscience*, *37*(16), 4416–4426. https://doi.org/10.1523/JNEUROSCI.1797-16.2017

Frederick, D. E., Rojas-Líbano, D., Scott, M., & Kay, L. M. (2011). Rat behavior in go/no-go and two-alternative choice odor discrimination: Differences and similarities. *Behavioral Neuroscience*, *125*(4), 588–603. https://doi.org/10.1037/a0024371

Freeman, W. J. (n.d.). *Consciousness, Intentionality and Causality*.

Freeman, W. J. (1972). Measurement of oscillatory responses to electrical stimulation in olfactory bulb of cat. *Journal of Neurophysiology*, *35*(6), 762–779. https://doi.org/10.1152/jn.1972.35.6.762

Fries, P. (2023). Rhythmic attentional scanning. *Neuron*, *111*(7), 954–970. Scopus. https://doi.org/10.1016/j.neuron.2023.02.015

Galliot, E., Laurent, L., Hacquemand, R., Pourié, G., & Millot, J.-L. (2012). Fear-like behavioral responses in mice in different odorant environments: Trigeminal versus olfactory mediation under low doses. *Behavioural Processes*, *90*(2), 161–166. https://doi.org/10.1016/j.beproc.2012.01.002

Genovese, F., Bauersachs, H. G., Gräßer, I., Kupke, J., Magin, L., Daiber, P., Sertel-Nakajima, Möhrlen, F., Messlinger, K., & Frings, S. (2017). Possible role of calcitonin gene-related

peptide in trigeminal modulation of glomerular microcircuits of the rodent olfactory bulb. *European Journal of Neuroscience*, *45*(4), 587–600. https://doi.org/10.1111/ejn.13490

Good, M., & Honey, R. C. (1991). Conditioning and contextual retrieval in hippocampal rats. *Behavioral Neuroscience*, *105*, 499–509. https://doi.org/10.1037/0735-7044.105.4.499

Gourévitch, B., Kay, L. M., & Martin, C. (2010). Directional coupling from the olfactory bulb to the hippocampus during a go/no-go odor discrimination task. *Journal of Neurophysiology*, *103*(5), 2633–2641. https://doi.org/10.1152/jn.01075.2009

Gray, C. M., & Skinner, J. E. (1988). Centrifugal regulation of neuronal activity in the olfactory bulb of the waking rabbit as revealed by reversible cryogenic blockade. *Experimental Brain Research*, *69*(2), 378–386. https://doi.org/10.1007/BF00247583

Grossman, K. J., Mallik, A. K., Ross, J., Kay, L. M., & Issa, N. P. (2008). Glomerular activation patterns and the perception of odor mixtures. *The European Journal of Neuroscience*, *27*(10), 2676–2685. https://doi.org/10.1111/j.1460-9568.2008.06213.x

Gschwend, O., Abraham, N. M., Lagier, S., Begnaud, F., Rodriguez, I., & Carleton, A. (2015). Neuronal pattern separation in the olfactory bulb improves odor discrimination learning. *Nature Neuroscience*, *18*(10), 1474–1482. https://doi.org/10.1038/nn.4089

Gulyás, A. I., Tóth, K., McBain, C. J., & Freund, T. F. (1998). Stratum radiatum giant cells: A type of principal cell in the rat hippocampus. *European Journal of Neuroscience*, *10*(12), 3813–3822. https://doi.org/10.1046/j.1460-9568.1998.00402.x

Han, P., Mann, S., Raue, C., Warr, J., & Hummel, T. (2018). Pepper with and without a sting: Brain processing of intranasal trigeminal and olfactory stimuli from the same source. *Brain Research*, *1700*, 41–46. https://doi.org/10.1016/j.brainres.2018.07.010

Hansen, A., & Finger, T. E. (2008). Is TrpM5 a reliable marker for chemosensory cells? Multiple types of microvillous cells in the main olfactory epithelium of mice. *BMC Neuroscience*, *9*(1), 115. https://doi.org/10.1186/1471-2202-9-115

Heck, D. H., Kozma, R., & Kay, L. M. (2019). The rhythm of memory: How breathing shapes memory function. *Journal of Neurophysiology*, *122*(2), 563–571. https://doi.org/10.1152/jn.00200.2019

Hermer-Vazquez, R., Hermer-Vazquez, L., Srinivasan, S., & Chapin, J. K. (2007). Beta- and gamma-frequency coupling between olfactory and motor brain regions prior to skilled, olfactory-driven reaching. *Experimental Brain Research. Experimentelle Hirnforschung. Experimentation Cerebrale*, *180*(2), 217–235. https://doi.org/10.1007/s00221-007-0850-2

Holland, P. C., & Bouton, M. E. (1999). Hippocampus and context in classical conditioning. *Current Opinion in Neurobiology*, *9*(2), 195–202. https://doi.org/10.1016/S0959-4388(99)80027-0

Hummel, T., & Livermore, A. (2002). Intranasal chemosensory function of the trigeminal nerve and aspects of its relation to olfaction. *International Archives of Occupational and Environmental Health*, *75*(5), 305–313. https://doi.org/10.1007/s00420-002-0315-7

Igarashi, K. M., Ieki, N., An, M., Yamaguchi, Y., Nagayama, S., Kobayakawa, K., Kobayakawa, R., Tanifuji, M., Sakano, H., Chen, W. R., & Mori, K. (2012). Parallel mitral and tufted

cell pathways route distinct odor information to different targets in the olfactory cortex. *The Journal of Neuroscience: The Official Journal of the Society for Neuroscience*, *32*(23), 7970–7985. https://doi.org/10.1523/JNEUROSCI.0154-12.2012

Imamura, F., Ito, A., & LaFever, B. J. (2020). Subpopulations of Projection Neurons in the Olfactory Bulb. *Frontiers in Neural Circuits*, *14*, 561822. https://doi.org/10.3389/fncir.2020.561822

Iravani, B., Arshamian, A., Ohla, K., Wilson, D. A., & Lundström, J. N. (2020). Non-invasive recording from the human olfactory bulb. *Nature Communications*, *11*(1), 648. https://doi.org/10.1038/s41467-020-14520-9

Isaacson, J. S., & Strowbridge, B. W. (1998). Olfactory reciprocal synapses: Dendritic signaling in the CNS. *Neuron*, *20*(4), 749–761. https://doi.org/10.1016/s0896-6273(00)81013-2

Jacquot, L., Hidalgo, J., & Brand, G. (2010). Just noticeable difference in olfaction is related to trigeminal component of odorants. *Rhinology*, *48*(3), 281–284. https://doi.org/10.4193/Rhino09.200

Jacquot, L., Monnin, J., & Brand, G. (2004). Unconscious odor detection could not be due to odor itself. *Brain Research*, *1002*(1–2), 51–54. https://doi.org/10.1016/j.brainres.2003.12.011

Ji, J., & Maren, S. (2007). Hippocampal involvement in contextual modulation of fear extinction. *Hippocampus*, *17*(9), 749–758. https://doi.org/10.1002/hipo.20331

Kaimoto, T., Hatakeyama, Y., Takahashi, K., Imagawa, T., Tominaga, M., & Ohta, T. (2016). Involvement of transient receptor potential A1 channel in algesic and analgesic actions of the organic compound limonene. *European Journal of Pain (London, England)*, *20*(7), 1155–1165. https://doi.org/10.1002/ejp.840

Kay, L. M. (2003). TWO SPECIES OF GAMMA OSCILLATIONS IN THE OLFACTORY BULB: DEPENDENCE ON BEHAVIORAL STATE AND SYNAPTIC INTERACTIONS. *Journal of Integrative Neuroscience*, *02*(01), 31–44. https://doi.org/10.1142/S0219635203000196

Kay, L. M. (2005). Theta oscillations and sensorimotor performance. *Proceedings of the National Academy of Sciences*, *102*(10), 3863–3868. https://doi.org/10.1073/pnas.0407920102

Kay, L. M. (2015). Olfactory system oscillations across phyla. *Current Opinion in Neurobiology*, *31*, 141–147. https://doi.org/10.1016/j.conb.2014.10.004

Kay, L. M. (2022). COVID-19 and olfactory dysfunction: A looming wave of dementia? *Journal of Neurophysiology*, *128*(2), 436–444. https://doi.org/10.1152/jn.00255.2022

Kay, L. M. (2025). *Sex Differences In Rats' Olfactory Behavior Depend On Behavioral Context* [Poster]. AChemS 2025.

Kay, L. M., & Beshel, J. (2010). A Beta Oscillation Network in the Rat Olfactory System During a 2-Alternative Choice Odor Discrimination Task. *Journal of Neurophysiology*, *104*(2), 829–839. https://doi.org/10.1152/jn.00166.2010

Kay, L. M., Crk, T., & Thorngate, J. (2005). A redefinition of odor mixture quality. *Behavioral Neuroscience*, *119*(3), 726–733. https://doi.org/10.1037/0735-7044.119.3.726

Kay, L. M., Lowry, C. A., & Jacobs, H. A. (2003). Receptor contributions to configural and elemental odor mixture perception. *Behavioral Neuroscience*, *117*(5), 1108–1114. https://doi.org/10.1037/0735-7044.117.5.1108

Kesner, R. P., Hunsaker, M. R., & Gilbert, P. E. (2005). The Role of CA1 in the Acquisition of an Object-Trace-Odor Paired Associate Task. *Behavioral Neuroscience*, *119*(3), 781–786. https://doi.org/10.1037/0735-7044.119.3.781

Khan, R. M., & Sobel, N. (2004). Neural processing at the speed of smell. *Neuron*, *44*(5), 744–747. https://doi.org/10.1016/j.neuron.2004.11.024

Khanna, P., & Carmena, J. M. (2017). Beta band oscillations in motor cortex reflect neural population signals that delay movement onset. *eLife*, *6*, e24573. https://doi.org/10.7554/eLife.24573

Kobal, G., & Hummel, C. (1988). Cerebral chemosensory evoked potentials elicited by chemical stimulation of the human olfactory and respiratory nasal mucosa. *Electroencephalography and Clinical Neurophysiology*, *71*(4), 241–250. https://doi.org/10.1016/0168-5597(88)90023-8

Kohli, P., Soler, Z. M., Nguyen, S. A., Muus, J. S., & Schlosser, R. J. (2016). The Association Between Olfaction and Depression: A Systematic Review. *Chemical Senses*, *41*(6), 479–486. https://doi.org/10.1093/chemse/bjw061

Kollndorfer, K., Kowalczyk, K., Frasnelli, J., Hoche, E., Unger, E., Mueller, C. A., Krajnik, J., Trattnig, S., & Schöpf, V. (2015). Same Same but Different. Different Trigeminal Chemoreceptors Share the Same Central Pathway. *PLOS ONE*, *10*(3), e0121091. https://doi.org/10.1371/journal.pone.0121091

Lagier, S., Carleton, A., & Lledo, P.-M. (2004). Interplay between Local GABAergic Interneurons and Relay Neurons Generates γ Oscillations in the Rat Olfactory Bulb. *The Journal of Neuroscience*, *24*(18), 4382–4392. https://doi.org/10.1523/JNEUROSCI.5570-03.2004

Lane, G., Zhou, G., Noto, T., & Zelano, C. (2020). Assessment of direct knowledge of the human olfactory system. *Experimental Neurology*, *329*, 113304. https://doi.org/10.1016/j.expneurol.2020.113304

Laska, M., & Teubner, P. (1999). Olfactory Discrimination Ability for Homologous Series of Aliphatic Alcohols and Aldehydes. *Chemical Senses*, *24*(3), 263–270. https://doi.org/10.1093/chemse/24.3.263

Lepousez, G., & Lledo, P.-M. (2013). Odor discrimination requires proper olfactory fast oscillations in awake mice. *Neuron*, *80*(4), 1010–1024. https://doi.org/10.1016/j.neuron.2013.07.025

Leung, L. S., Gill, R. S., Shen, B., & Chu, L. (2024). Cholinergic and behavior-dependent beta and gamma waves are coupled between olfactory bulb and hippocampus. *Hippocampus*, *34*(9), 464–490. https://doi.org/10.1002/hipo.23622

Levin, R. A., McDade, L. A., & Raguso, R. A. (2003). The Systematic Utility of Floral and Vegetative Fragrance in Two Genera of Nyctaginaceae. *Systematic Biology*, *52*(3), 334–351. https://doi.org/10.1080/10635150390196975

Li, Y., Xu, J., Liu, Y., Zhu, J., Liu, N., Zeng, W., Huang, N., Rasch, M. J., Jiang, H., Gu, X., Li, X., Luo, M., Li, C., Teng, J., Chen, J., Zeng, S., Lin, L., & Zhang, X. (2017). A distinct entorhinal cortex to hippocampal CA1 direct circuit for olfactory associative learning. *Nature Neuroscience*, *20*(4), 559–570. https://doi.org/10.1038/nn.4517

Lindqvist, A., Höglund, A., & Berglund, B. (2012). The Role of Odour Quality in the Perception of Binary and Higher-Order Mixtures. *Perception*, *41*(11), 1373–1391. https://doi.org/10.1068/p7267

Linster, C., & Smith, B. H. (1999). Generalization Between Binary Odor Mixtures and Their Components in the Rat. *Physiology & Behavior*, *66*(4), 701–707. https://doi.org/10.1016/S0031-9384(99)00007-4

Livermore, A., Hummel, T., & Kobal, G. (1992). Chemosensory event-related potentials in the investigation of interactions between the olfactory and the somatosensory (trigeminal) systems. *Electroencephalography and Clinical Neurophysiology*, *83*(3), 201–210. https://doi.org/10.1016/0013-4694(92)90145-8

Lowry, C. A., & Kay, L. M. (2007). Chemical Factors Determine Olfactory System Beta Oscillations in Waking Rats. *Journal of Neurophysiology*, *98*(1), 394–404. https://doi.org/10.1152/jn.00124.2007

Lübbert, M., Kyereme, J., Schöbel, N., Beltrán, L., Wetzel, C. H., & Hatt, H. (2013). Transient Receptor Potential Channels Encode Volatile Chemicals Sensed by Rat Trigeminal Ganglion Neurons. *PLOS ONE*, *8*(10), e77998. https://doi.org/10.1371/journal.pone.0077998

Maheshwar, K. V., Stuart, A. E., & Kay, L. M. (2025). Sex differences in olfactory behavior and neurophysiology in Long Evans rats. *Journal of Neurophysiology*, *133*(1), 257–267. https://doi.org/10.1152/jn.00222.2024

Manabe, H., & Mori, K. (2013). Sniff rhythm-paced fast and slow gamma-oscillations in the olfactory bulb: Relation to tufted and mitral cells and behavioral states. *Journal of Neurophysiology*, *110*(7), 1593–1599. https://doi.org/10.1152/jn.00379.2013

Martin, C., Beshel, J., & Kay, L. M. (2007). An Olfacto-Hippocampal Network Is Dynamically Involved in Odor-Discrimination Learning. *Journal of Neurophysiology*, *98*(4), 2196–2205. https://doi.org/10.1152/jn.00524.2007

Martin, C., Gervais, R., Hugues, E., Messaoudi, B., & Ravel, N. (2004). Learning Modulation of Odor-Induced Oscillatory Responses in the Rat Olfactory Bulb: A Correlate of Odor Recognition? *Journal of Neuroscience*, *24*(2), 389–397. https://doi.org/10.1523/JNEUROSCI.3433-03.2004

Martin, C., Gervais, R., Messaoudi, B., & Ravel, N. (2006). Learning-induced oscillatory activities correlated to odour recognition: A network activity. *European Journal of Neuroscience*, *23*(7), 1801–1810. https://doi.org/10.1111/j.1460-9568.2006.04711.x

Martin, C., & Ravel, N. (2014). Beta and gamma oscillatory activities associated with olfactory memory tasks: Different rhythms for different functional networks? *Frontiers in Behavioral Neuroscience*, *8*. https://www.frontiersin.org/articles/10.3389/fnbeh.2014.00218

McHugh, S. B., Lopes-dos-Santos, V., Castelli, M., Gava, G. P., Thompson, S. E., Tam, S. K. E., Hartwich, K., Perry, B., Toth, R., Denison, T., Sharott, A., & Dupret, D. (2024). Offline hippocampal reactivation during dentate spikes supports flexible memory. *Neuron*, *112*(22), 3768-3781.e8. https://doi.org/10.1016/j.neuron.2024.08.022

Messlinger, K., Balcziak, L. K., & Russo, A. F. (2020). Cross-talk signaling in the trigeminal ganglion: Role of neuropeptides and other mediators. *Journal of Neural Transmission (Vienna, Austria: 1996)*, *127*(4), 431–444. https://doi.org/10.1007/s00702-020-02161-7

Mitra, P., & Bokil, H. (2008). *Observed Brain Dynamics*. Oxford University Press.

Mori, K., & Takagi, S. F. (1978). An intracellular study of dendrodendritic inhibitory synapses on mitral cells in the rabbit olfactory bulb. *The Journal of Physiology*, *279*, 569–588.

Murphy, C., & Cain, W. S. (1980). Taste and olfaction: Independence vs interaction. *Physiology & Behavior*, *24*(3), 601–605. https://doi.org/10.1016/0031-9384(80)90257-7

Nagayama, S., Homma, R., & Imamura, F. (2014). Neuronal organization of olfactory bulb circuits. *Frontiers in Neural Circuits*, *8*, 98. https://doi.org/10.3389/fncir.2014.00098

Neville, K. R., & Haberly, L. B. (2003). Beta and Gamma Oscillations in the Olfactory System of the Urethane-Anesthetized Rat. *Journal of Neurophysiology*, *90*(6), 3921–3930. https://doi.org/10.1152/jn.00475.2003

Nilius, B., & Owsianik, G. (2011). The transient receptor potential family of ion channels. *Genome Biology*, *12*(3), 218. https://doi.org/10.1186/gb-2011-12-3-218

Niv, Y. (2019). Learning task-state representations. *Nature Neuroscience*, *22*(10), Article 10. https://doi.org/10.1038/s41593-019-0470-8

Nunez-Parra, A., Maurer, R. K., Krahe, K., Smith, R. S., & Araneda, R. C. (2013). Disruption of centrifugal inhibition to olfactory bulb granule cells impairs olfactory discrimination. *Proceedings of the National Academy of Sciences*, *110*(36), 14777–14782. https://doi.org/10.1073/pnas.1310686110

Nusser, Z., Kay, L. M., Laurent, G., Homanics, G. E., & Mody, I. (2001). Disruption of GABAA Receptors on GABAergic Interneurons Leads to Increased Oscillatory Power in the Olfactory Bulb Network. *Journal of Neurophysiology*, *86*(6), 2823–2833. https://doi.org/10.1152/jn.2001.86.6.2823

Okuyama, T., Kitamura, T., Roy, D. S., Itohara, S., & Tonegawa, S. (2016). Ventral CA1 neurons store social memory. *Science (New York, N.Y.)*, *353*(6307), 1536–1541. https://doi.org/10.1126/science.aaf7003

Osinski, B. L., & Kay, L. M. (2016). Granule cell excitability regulates gamma and beta oscillations in a model of the olfactory bulb dendrodendritic microcircuit. *Journal of Neurophysiology*, *116*(2), 522–539. https://doi.org/10.1152/jn.00988.2015

Osinski, B. L., Kim, A., Xiao, W., Mehta, N. M., & Kay, L. M. (2018). Pharmacological manipulation of the olfactory bulb modulates beta oscillations: Testing model predictions. *Journal of Neurophysiology*, *120*(3), 1090–1106. https://doi.org/10.1152/jn.00090.2018

Padmanabhan, K., Osakada, F., Tarabrina, A., Kizer, E., Callaway, E. M., Gage, F. H., & Sejnowski, T. J. (2019). Centrifugal Inputs to the Main Olfactory Bulb Revealed Through Whole Brain Circuit-Mapping. *Frontiers in Neuroanatomy*, *12*. https://www.frontiersin.org/articles/10.3389/fnana.2018.00115

Panhuber, H., Laing, D. G., Willcox, M. E., Eagleson, G. K., & Pittman, E. A. (1985). The distribution of the size and number of mitral cells in the olfactory bulb of the rat. *Journal of Anatomy*, *140*(Pt 2), 297–308.

Perez, E. C., Rodgers, S. P., Inoue, T., Pedersen, S. E., Leasure, J. L., & Gaber, M. W. (2018). Olfactory Memory Impairment Differs by Sex in a Rodent Model of Pediatric Radiotherapy. *Frontiers in Behavioral Neuroscience*, *12*. https://doi.org/10.3389/fnbeh.2018.00158

Prendergast, B. J., Onishi, K. G., & Zucker, I. (2014). Female mice liberated for inclusion in neuroscience and biomedical research. *Neuroscience and Biobehavioral Reviews*, *40*, 1–5. https://doi.org/10.1016/j.neubiorev.2014.01.001

Rall, W., & Shepherd, G. M. (1968). Theoretical reconstruction of field potentials and dendrodendritic synaptic interactions in olfactory bulb. *Journal of Neurophysiology*, *31*(6), 884–915. https://doi.org/10.1152/jn.1968.31.6.884

Rangel, L. M., Chiba, A. A., & Quinn, L. K. (2015). Theta and beta oscillatory dynamics in the dentate gyrus reveal a shift in network processing state during cue encounters. *Frontiers in Systems Neuroscience*, *9*. https://doi.org/10.3389/fnsys.2015.00096

Ravel, N., Chabaud, P., Martin, C., Gaveau, V., Hugues, E., Tallon-Baudry, C., Bertrand, O., & Gervais, R. (2003). Olfactory learning modifies the expression of odour-induced oscillatory responses in the gamma (60–90 Hz) and beta (15–40 Hz) bands in the rat olfactory bulb. *European Journal of Neuroscience*, *17*(2), 350–358. https://doi.org/10.1046/j.1460-9568.2003.02445.x

Ravia, A., Snitz, K., Honigstein, D., Finkel, M., Zirler, R., Perl, O., Secundo, L., Laudamiel, C., Harel, D., & Sobel, N. (2020). A measure of smell enables the creation of olfactory metamers. *Nature*, *588*(7836), 118–123. https://doi.org/10.1038/s41586-020-2891-7

Rojas-Líbano, D., Frederick, D. E., Egaña, J. I., & Kay, L. M. (2014). The olfactory bulb theta rhythm follows all frequencies of diaphragmatic respiration in the freely behaving rat. *Frontiers in Behavioral Neuroscience*, *8*, 214. https://doi.org/10.3389/fnbeh.2014.00214

Rojas-Líbano, D., & Kay, L. M. (2012). Interplay between sniffing and odorant sorptive properties in the rat. *The Journal of Neuroscience: The Official Journal of the Society for Neuroscience*, *32*(44), 15577–15589. https://doi.org/10.1523/JNEUROSCI.1464-12.2012

Rozin, P. (1982). "Taste-smell confusions" and the duality of the olfactory sense. *Perception & Psychophysics*, *31*(4), 397–401. https://doi.org/10.3758/BF03202667

Schaefer, M. L., Böttger, B., Silver, W. L., & Finger, T. E. (2002). Trigeminal collaterals in the nasal epithelium and olfactory bulb: A potential route for direct modulation of olfactory information by trigeminal stimuli. *Journal of Comparative Neurology*, *444*(3), 221–226. https://doi.org/10.1002/cne.10143

Schoppa, N. E., Kinzie, J. M., Sahara, Y., Segerson, T. P., & Westbrook, G. L. (1998). Dendrodendritic Inhibition in the Olfactory Bulb Is Driven by NMDA Receptors. *The Journal of Neuroscience*, *18*(17), 6790–6802. https://doi.org/10.1523/JNEUROSCI.18-17-06790.1998

Semin, G. R., Scandurra, A., Baragli, P., Lanatà, A., & D'Aniello, B. (2019). Inter- and Intra-Species Communication of Emotion: Chemosignals as the Neglected Medium. *Animals*, *9*(11), Article 11. https://doi.org/10.3390/ani9110887

Sheriff, A., Pandolfi, G., Nguyen, V. S., & Kay, L. M. (2021). Long-Range Respiratory and Theta Oscillation Networks Depend on Spatial Sensory Context. *The Journal of Neuroscience*, *41*(48), 9957–9970. https://doi.org/10.1523/JNEUROSCI.0719-21.2021

Silver, W. L., Clapp, T. R., Stone, L. M., & Kinnamon, S. C. (2006). TRPV1 Receptors and Nasal Trigeminal Chemesthesis. *Chemical Senses*, *31*(9), 807–812. https://doi.org/10.1093/chemse/bjl022

Stanić, D., Kuteeva, E., Nylander, I., & Hökfelt, T. (2010). Characterization of CGRP protein expression in "satellite-like" cells and dendritic arbours of the mouse olfactory bulb. *Journal of Comparative Neurology*, *518*(6), 770–784. https://doi.org/10.1002/cne.22226

Stopfer, M., Bhagavan, S., Smith, B. H., & Laurent, G. (1997). Impaired odour discrimination on desynchronization of odour-encoding neural assemblies. *Nature*, *390*(6655), Article 6655. https://doi.org/10.1038/36335

Strauch, C., & Manahan-Vaughan, D. (2018). In the Piriform Cortex, the Primary Impetus for Information Encoding through Synaptic Plasticity Is Provided by Descending Rather than Ascending Olfactory Inputs. *Cerebral Cortex*, *28*(2), 764–776. https://doi.org/10.1093/cercor/bhx315

Symanski, C. A., Bladon, J. H., Kullberg, E. T., Miller, P., & Jadhav, S. P. (2020). *Rhythmic coordination of hippocampal-prefrontal ensembles for odor-place associative memory and decision making*. https://doi.org/10.1101/2020.06.08.140939

Takaishi, M., Fujita, F., Uchida, K., Yamamoto, S., Sawada (Shimizu), M., Hatai (Uotsu), C., Shimizu, M., & Tominaga, M. (2012). 1,8-Cineole, a TRPM8 Agonist, is a Novel Natural Antagonist of Human TRPA1. *Molecular Pain*, *8*, 1744-8069-8–86. https://doi.org/10.1186/1744-8069-8-86

Travlos, G. S., Wilson, R. E., Murrell, J. A., Chignell, C. F., & Boorman, G. A. (2001). The Effect of Short Intermittent Light Exposures on the Melatonin Circadian Rhythm and NMU-Induced Breast Cancer in Female F344/N Rats. *Toxicologic Pathology*, *29*(1), 126–136. https://doi.org/10.1080/019262301301418937

Uchida, N., & Mainen, Z. F. (2003). Speed and accuracy of olfactory discrimination in the rat. *Nature Neuroscience*, *6*(11), 1224–1229. https://doi.org/10.1038/nn1142

Watson, D. L. B., Campbell, M., Hopkins, C., Smith, B., Kelly, C., & Deary, V. (2021). Altered smell and taste: Anosmia, parosmia and the impact of long Covid-19. *PLOS ONE*, *16*(9), e0256998. https://doi.org/10.1371/journal.pone.0256998

Wiltrout, C., Dogra, S., & Linster, C. (2003). Configurational and nonconfigurational interactions between odorants in binary mixtures. *Behavioral Neuroscience*, *117*(2), 236–245. https://doi.org/10.1037/0735-7044.117.2.236

Wulff, D. U., Kieslich, P. J., Henninger, F., & Haslbeck, J. M. (n.d.). *Movement tracking of cognitive processes: A tutorial using mousetrap*.

Xu, L., Li, W., Voleti, V., Zou, D.-J., Hillman, E. M. C., & Firestein, S. (2020). Widespread receptor-driven modulation in peripheral olfactory coding. *Science (New York, N.Y.)*, *368*(6487), eaaz5390. https://doi.org/10.1126/science.aaz5390

Zelano, C., Bensafi, M., Porter, J., Mainland, J., Johnson, B., Bremner, E., Telles, C., Khan, R., & Sobel, N. (2005). Attentional modulation in human primary olfactory cortex. *Nature Neuroscience*, *8*(1), 114–120. https://doi.org/10.1038/nn1368